UNIVERSIDADE FEDERAL DA PARAÍBA

Programa de Pós-Graduação em Física

# Quantum Dynamics Beyond Lorentz Invariance

Gislaine Varão da Silva

Tese de Doutorado



João Pessoa – 2026

UNIVERSIDADE FEDERAL DA PARAÍBA

Programa de Pós-Graduação em Física

# Quantum Dynamics Beyond Lorentz Invariance

Gislaine Varão da Silva

Tese de Doutorado apresentada ao Programa de Pós-Graduação em Física da Universidade Federal da Paraíba, como requisito para obtenção do título de Doutora em Física.

**Orientador:** Prof. Dr. Valdir Barbosa Bezerra
**Coorientador:** Prof. Dr. Iarley Pereira Lobo

João Pessoa – 2026

**Catalogação na publicação**
**Seção de Catalogação e Classificação**

S586q Silva, Gislaine Varão da.
Quantum dynamics beyond lorentz invariance / Gislaine Varão da Silva. - João Pessoa, 2026.
115 f. : il.

Orientação: Valdir Barbosa Bezerra.
Coorientação: Iarley Pereira Lobo.
Tese (Doutorado) - UFPB/CCEN.

1. Gravidade quântica - fenomenologia. 2. Escala de Planck. 3. Simetria de Lorentz. 4. Regime não relativístico. 5. Relação de Dispersão Modificada. I. Bezerra, Valdir Barbosa. II. Lobo, Iarley Pereira. III. Título.

UFPB/BC CDU 531.5(043)

Elaborado por RUSTON SAMMEVILLE ALEXANDRE MARQUES DA SILVA - CRB-15/0386

Universidade Federal da Paraíba
Centro de Ciências Exatas e da Natureza
**Programa de Pós-Graduação *Stricto Sensu* em Física**

Ata da Sessão Pública da Defesa de tese de Doutorado da aluna **Gislaine Varão da Silva**, candidata ao Título de Doutora em Física na Área de Concentração Gravitação e Cosmologia.

Aos vinte e três dias do mês de fevereiro do ano de dois mil e vinte e seis, às 09h00, na sala virtual meet.google.com/rjp-ocvi-fkz, reuniram-se os membros da Banca Examinadora constituída para avaliar a tese de Doutorado, na área de Gravitação e Cosmologia, de **Gislaine Varão da Silva**. A banca foi composta pelos(as) professores(as) doutores(as): Valdir Barbosa Bezerra (PPGF/UFPB), orientador e presidente da banca examinadora, Iarley Pereira Lobo (UFPB), coorientador, Albert Petrov (PPGF/UFPB), Fábio Leal de Melo Dahia (PPGF/UFPB), Francisco de Assis de Brito (UFCG) e Nelson de Oliveira Yokomizo (UFMG). Dando início aos trabalhos, o Prof. Valdir Barbosa Bezerra comunicou aos presentes a finalidade da reunião. A seguir, passou a palavra para a candidata, para que a mesma fizesse, oralmente, a exposição da pesquisa de tese intitulada "*Dinâmica Quântica além da Invariância de Lorentz*" (Quantum Dynamics Beyond Lorentz Invariance). Concluída a exposição, a candidata foi arguida pela Banca Examinadora, que emitiu o parecer **"aprovada"**. Assim sendo, deve a Universidade Federal da Paraíba expedir o respectivo diploma de Doutora em Física na forma da lei. E para constar, Ana Beatriz Cândido Vieira, Assistente em Administração, redigiu a presente ata que vai assinada pelos membros da Banca Examinadora. João Pessoa, Paraíba, **23 de fevereiro de 2026**.

Documento assinado digitalmente
gov.br
VALDIR BARBOSA BEZERRA
Data: 26/02/2026 08:37:46-0300
Verifique em https://validar.iti.gov.br

Prof. Dr. Valdir Barbosa Bezerra
Orientador - PPGF/UFPB

Documento assinado digitalmente
gov.br
IARLEY PEREIRA LOBO
Data: 25/02/2026 10:07:36-0300
Verifique em https://validar.iti.gov.br

Prof. Dr. Iarley Pereira Lobo
Coorientador - UFPB

Documento assinado digitalmente
gov.br
ALBERT PETROV
Data: 25/02/2026 09:00:30-0300
Verifique em https://validar.iti.gov.br

Prof. Dr. Albert Petrov
PPGF/UFPB

Documento assinado digitalmente
gov.br
FABIO LEAL DE MELO DAHIA
Data: 25/02/2026 05:41:57-0300
Verifique em https://validar.iti.gov.br

Prof. Dr. Fábio Leal de Melo Dahia
PPGF/UFPB

Documento assinado digitalmente
gov.br
FRANCISCO DE ASSIS DE BRITO
Data: 24/02/2026 20:40:18-0300
Verifique em https://validar.iti.gov.br

Prof. Dr. Francisco de Assis de Brito
UFCG

Documento assinado digitalmente
gov.br
NELSON DE OLIVEIRA YOKOMIZO
Data: 23/02/2026 16:44:14-0300
Verifique em https://validar.iti.gov.br

Prof. Dr. Nelson de Oliveira Yokomizo
UFMG

# Acknowledgements

Agradeço ao professor Valdir Barbosa Bezerra pela orientação, pela generosidade e pela paciência, bem como pelo privilégio de trabalhar com um pesquisador com mais de meio século de trajetória acadêmica.

Agradeço ao professor Iarley Pereira Lobo pela coorientação deste trabalho, pelo caráter desbravador, pelas discussões, pelas oportunidades proporcionadas e, sobretudo, pela amizade.

Agradeço também à professora Giulia Gubitosi pela hospitalidade e pela supervisão durante meu período como estudante visitante na *Università degli Studi di Napoli Federico II*, no âmbito do Programa de Doutorado Sanduíche da CAPES.

Aos meus amigos Pedro Morais, Saulo Soares e Matheus Paganelly, meu agradecimento pelo apoio e pelas trocas intelectuais ao longo deste período, e a João Paulo Morais Graça, Thiago Nascimento e Artur Pinheiro, pela amizade que antecede esta tese e que tornou possível a sua realização.

Agradeço à Universidade Federal da Paraíba e ao seu Programa de Pós-Graduação em Física pelo suporte acadêmico e institucional. Agradeço igualmente à *Università degli Studi di Napoli Federico II*, por me receber como estudante visitante. Agradeço às agências de fomento CAPES e CNPq, pelo suporte financeiro.

Agradeço aos colaboradores dos trabalhos que compõem esta tese pelas discussões e contribuições pontuais ao longo de seu desenvolvimento.

Por fim, agradeço à minha família, pelo essencial.

# Abstract

Many approaches to quantum gravity predict the existence of a minimal length associated with the Planck scale, leading to modifications in the relations between energy, momentum, and position, which may in turn affect Lorentz symmetry. In this thesis, we investigate these effects in both systematic and stochastic scenarios, with particular emphasis on their low-energy manifestations. In the first part, we analyze systematic effects derived from modified dispersion relations (MDRs) motivated by quantum gravity. We show that the nonrelativistic limit of general MDRs leads to a deformed nonrelativistic Schrödinger equation containing fractional and nonlocal terms in the Hamiltonian. These terms modify quantum kinematics and allow the establishment of experimental bounds on MDR parameters using low-energy systems. We further demonstrate that certain MDRs with fractional powers give rise to a dynamics described by fractional quantum mechanics at low energies, associated with an effectively fractal geometry in the infrared. We also study stochastic effects associated with Planck-scale fluctuations in MDRs, modeling a stochastic violation of Lorentz symmetry. Performing the stochastic average leads to a Lindblad equation that describes a mechanism of gravitational decoherence in the nonrelativistic regime. We apply this formalism to gravitational Schrödinger cat states (gravcats), revealing the competition between gravitationally induced entanglement and decoherence driven by Planckian fluctuations, and allowing us to estimate the scales at which such effects become relevant. In the second part, we analyze an additional scenario based on noncommutative spacetimes, showing that the deformation of the energy composition rule characteristic of the $\kappa$-Minkowski spacetime induces quantum correlations between two systems, even in the nonrelativistic limit. These results demonstrate that low-energy quantum systems provide a novel avenue to test Lorentz symmetry, either through systematic deformations or stochastic violations. The infrared regime has the potential to amplify Planck-suppressed corrections, thereby providing new opportunities to test effective quantum gravity models in tabletop experiments.

**Keywords:** Planck-Scale; Quantum Gravity Phenomenology; Lorentz Symmetry; Nonrelativistic Regime; Modified Dispersion Relations.

# Resumo

Muitas abordagens da gravidade quântica preveem a existência de um comprimento mínimo associado à escala de Planck, o que leva a modificações nas relações entre energia, momento e posição, que, por sua vez, podem afetar a simetria de Lorentz. Nesta tese, investigamos esses efeitos em cenários tanto sistemáticos quanto estocásticos, com ênfase particular em suas manifestações de baixa energia. Na primeira parte, analisamos efeitos sistemáticos derivados de relações de dispersão modificadas (MDRs, na sigla em inglês) motivadas pela gravidade quântica. Mostramos que o limite não relativístico de MDRs gerais leva a uma equação de Schrödinger não relativística deformada, contendo termos fracionais e não locais no Hamiltoniano. Esses termos modificam a cinemática quântica e permitem estabelecer limites experimentais para os parâmetros das MDRs usando sistemas de baixa energia. Ademais, demonstramos que certas MDRs com potências fracionárias dão origem a uma dinâmica descrita pela mecânica quântica fracional em baixas energias, associada a uma geometria efetivamente fractal no infravermelho. Também estudamos efeitos estocásticos associados a flutuações na escala de Planck nas MDRs, modelando uma violação estocástica da simetria de Lorentz. A realização da média estocástica resulta em uma equação de Lindblad que descreve um mecanismo de decoerência gravitacional no regime não relativístico. Aplicamos esse formalismo a estados gato de Schrödinger gravitacionais (*gravcats*), revelando a competição entre o emaranhamento induzido gravitacionalmente e a decoerência impulsionada por flutuações planckianas, permitindo-nos estimar as escalas nas quais tais efeitos se tornam relevantes. Na segunda parte, analisamos um cenário adicional baseado em espaços-tempos não comutativos, mostrando que a deformação da regra de composição de energias característica do espaço-tempo $\kappa$-Minkowski induz correlações quânticas entre dois sistemas, mesmo no limite não relativístico. Esses resultados demonstram que sistemas quânticos de baixa energia oferecem um novo caminho para testar a simetria de Lorentz, seja por meio de deformações sistemáticas ou violações estocásticas. O regime infravermelho tem o potencial de amplificar correções suprimidas pela escala de Planck, fornecendo assim novas oportunidades para testar modelos efetivos de gravidade quântica em experimentos de bancada.

**Palavras-chave:** Escala de Planck; Fenomenologia de Gravidade Quântica; Simetria de Lorentz; Regime Não Relativístico; Relação de Dispersão Modificada.

# List of publications

1. WAGNER, F.; **VARÃO, G.**; LOBO, I. P.; BEZERRA, V. B. Quantum-spacetime effects on nonrelativistic Schrödinger evolution. Physical Review D, v. 108, n. 6, p. 065012, 2023. DOI: 10.1103/PhysRevD.108.065012. (arxiv: 2306.05205)

   The contents of this article are presented in Chapters 2 and 3.

2. ALBUQUERQUE, S.; BEZERRA, V. B.; LOBO, I. P.; MACEDO, G.; MORAIS, P. H.; RODRIGUES, E.; SANTOS, L. C. N.; **VARÃO, G**. Quantum Configuration and Phase Spaces: Finsler and Hamilton Geometries. Physics, v. 5, n. 1, p. 90-115, 2023. DOI: 10.3390/physics5010007. (arxiv: 2301.09448)

   The contents of this article are partially presented in Chapter 2.

3. **VARÃO, G.**; LOBO, I. P.; BEZERRA, V. B. Fractional quantum mechanics meets quantum gravity phenomenology. EPL, v. 148, n. 3, p. 30001, 2024. DOI: 10.1209/0295-5075/ad8b65. (arXiv: 2405.13544).

   The contents of this article are presented in Chapter 4.

4. LOBO, I. P.; SAMPAIO, K.; **VARÃO, G.**; ROJAS, M.; BEZERRA, V. B. LIV-decoherence on gravitational cat states. Physics Letters B, v. 870, p. 139923, 2025. DOI: 10.1016/j.physletb.2025.139923. (arXiv: 2510.08828).

   The contents of this article are presented in Chapter 5.

5. LOBO, I. P.; **VARÃO, G.**; GUBITOSI, G.; ROJAS, M.; BEZERRA, V. B. Coherence and entanglement in a non-commutative spacetime. Classical and Quantum Gravity, v. 42, n. 22, p. 225010, 2025. DOI: 10.1088/1361-6382/ae1ac5. (arXiv: 2506.03282).

   The contents of this article are presented in Chapter 6.

# Contents

# CHAPTER 1

# Introduction

Since Bronstein's pioneering work in the 1930s [1], it has been understood that the quantum gravity problem should be solved by a reformulation of our understanding of gravity and quantum mechanics. This is because probing progressively smaller distance scales requires increasingly high energies. As these energies approach the Planck scale [2], gravitational effects governed by General Relativity (GR) become sufficiently pronounced that the classical geometric description of spacetime is expected to break down. In this context, semiclassical reasoning indicates that confining a particle to a region of the order of the Planck length would result in the formation of an event horizon, thereby precluding direct local observation. This limitation constitutes one of the motivations for the search for a theory of quantum gravity [3]. Over the past decades, the inherent tension between the continuous and deterministic spacetime of GR and the probabilistic nature of quantum mechanics has motivated extensive theoretical efforts, giving rise to several approaches to quantum gravity, including String Theory [4] and Loop Quantum Gravity [5].

Although probing the Planck scale directly requires extreme energies, its physical relevance can extend beyond this regime [6]. In certain effective models, Planck-scale physics may induce small yet structured modifications of relativistic kinematics, for instance, through deformations of dispersion relations [7]. While such effects are typically suppressed at low energies, they can nonetheless influence the quantum dynamics of physical systems in specific regimes. Under suitable conditions, these modifications may become detectable, enabling tests of potential deviations from standard quantum behavior [8, 9].

To address this challenge, increasing attention has been devoted to the phenomenology of quantum gravity. This research program aims to identify indirect signatures of quantum spacetime at energy scales much lower than the Planck regime. The guiding idea is that any fundamental theory should leave residual imprints that may still be accessible through sufficiently precise experiments. This shift in perspective, from the ultraviolet (UV) to the infrared (IR), redirects attention to regimes where experimental accuracy can partially compensate for the large separation of energy scales.

In this context, significant attention has been directed toward deformations of relativistic kinematics, particularly in the form of Modified Dispersion Relations (MDRs). These approaches are not mutually exclusive. MDRs can emerge as effective descriptions of field-theoretic models, and some dynamical frameworks can be described with modified kinematics. These deformations, which are frequently linked to modifications of Lorentz symmetry as in Doubly Special Relativity (DSR) or to explicit Lorentz Invariance Violation (LIV), modify the energy-momentum relation for test particles. While these developments are primarily motivated by high-energy physics, certain classes of MDRs can, under specific conditions, produce effective low-energy modifications of quantum dynamics.

A natural extension of this line of inquiry has emerged in the connection between MDRs and fractional quantum mechanics [10, 11]. Incorporating non-integer powers of momentum into dispersion relations can lead to modified Schrödinger equations involving fractional derivative operators, which are inherently nonlocal. This perspective suggests that quantum spacetime, particularly in a deep infrared regime, may exhibit effective fractal-like structures [12]. Interestingly, this behavior resonates with the anomalous dimensional flow predicted in the ultraviolet domain by several approaches to quantum gravity [13, 14].

Beyond single-particle dynamics and kinematical modifications, this thesis also examines the role of quantum spacetime as an effective environment for quantum systems. From this perspective, spacetime deformations may induce decoherence and mediate interactions that generate and modulate quantum correlations in bipartite systems [15].

This thesis investigates the impact of violations and deformations of Lorentz symmetry on nonrelativistic quantum systems, and delineates the specific conditions in which typically suppressed Planck-scale corrections become significant in the infrared regime.

This work is guided by the following questions concerning how Planck-scale modifications affect low-energy quantum dynamics:

(i) In what way do MDRs appear in the nonrelativistic Schrödinger equation, and under what conditions do the associated corrections shift from a perturbative to a non-perturbative regime?

(ii) In which momentum and energy regimes do fractional terms from MDRs become more significant than the standard quadratic kinetic term, giving rise to effective fractional quantum dynamics in the infrared?

(iii) In stochastic scenarios, how do Planck-scale fluctuations affect coherence and entanglement in mesoscopic quantum systems?

(iv) Can deformations of spacetime symmetries induce quantum correlations between distinct systems, even in the absence of direct interactions?

It starts by outlining the kinematical foundations of quantum gravity phenomenology and then analyzes the resulting dynamical and stochastic effects.

In Chapter 2, we introduce the kinematical framework underlying Planck-scale deformations, including Modified Dispersion Relations and scenarios with Lorentz invariance violation. This chapter establishes the physical assumptions and shared language employed throughout the thesis.

In Chapter 3, we examine deformed nonrelativistic quantum dynamics. The subtleties of taking the nonrelativistic limit of relativistic theories with Planck-scale corrections are analyzed using both canonical quantization and the nonrelativistic limit of modified Klein-Gordon equations. These approaches lead to a deformed Schrödinger equation, whose phenomenological implications in the infrared regime are discussed.

Chapter 4 is devoted to the emergence of fractional infrared dynamics. It shows how certain classes of modified dispersion relations lead to fractional operators in the effective quantum dynamics and discusses their connection to quantum gravity phenomenology, as well as possible experimental analogues.

Chapter 5 addresses stochastic Planck-scale effects and their implications for gravitational Schrödinger cat states. The corresponding Lindblad master equations are derived and applied to study the interplay between gravitationally induced entanglement and decoherence in mesoscopic quantum systems.

Finally, Chapter 6 investigates how deformations of spacetime symmetries, particularly in noncommutative geometries, can induce quantum correlations in bipartite systems. Several information theoretic measures are employed to analyze the competition between Planck-scale interactions and decoherence. Chapter 7 summarizes the main results of the thesis and discusses their broader implications.

# CHAPTER 2

## Planck-Scale Phenomenology in the Infrared

This chapter presents the conceptual and kinematic framework that underpins the original results of this thesis. Rather than reviewing existing approaches to quantum gravity, it introduces a minimal operational set of principles for modeling possible Planck-scale effects in low-energy quantum systems. The discussion focuses on the infrared regime, where the high experimental precision enables probing phenomena ordinarily suppressed by the Planck energy.

In particular, this framework does not represent a modification of gravity, does not introduce gravitational dynamics, and does not employ Einstein's field equations. The analysis remains confined to kinematic and operational aspects pertinent to quantum systems, independent of any particular gravitational theory. The main argument is that modified dispersion relations (MDRs) provide a kinematic and phenomenological framework for studying Planck-scale effects [7, 16].

## 2.1 Low-Energy Phenomenology

Quantum gravity phenomenology faces a fundamental obstacle: direct experimental access to the Planck scale is beyond current technological capabilities [17, 2]. Energies of order of Planck energy $E_P \sim 10^{19}$GeV and lengths of order of Planck length $\ell_P \sim 10^{-35}$m are inaccessible in terrestrial experiments and in most astrophysical observations. As a result, empirical searches for quantum spacetime effects cannot rely exclusively on probing the ultraviolet regime, where quantum-gravitational phenomena are traditionally expected to dominate. This limitation necessitates innovative approaches that look for subtle, amplified signatures in lower-energy regimes [16].

This motivates the adoption of a complementary, low-energy strategy. Rather than directly probing Planck-scale physics, this approach seeks its most pronounced amplified imprints within low-energy quantum systems. The central assumption is that any fundamental description of spacetime necessarily induces small yet systematic corrections to standard relativistic kinematics [18]. Although these corrections are generally suppressed by ratios such as $E/E_P$ or $p/p_P$, they may become observable through specific infrared amplification mechanisms. Such mechanisms include mass enhancement (large mass $M$), coherence-time accumulation (over long evolution times $T$), macroscopic quantum superpositions, and collective effects in many-body systems [8, 9]. The combined operation of these mechanisms provides a feasible approach for converting an otherwise undetectable Planck-scale effect into a measurable "smoking gun" signature in a controlled laboratory environment.

The challenge is therefore not merely quantitative, but conceptual. A viable low-energy phenomenology requires a framework in which Planck-scale corrections can be parametrized in a controlled and experimentally meaningful way. Naive extrapolations of relativistic deformations to the nonrelativistic regime often fail in this respect, as they neglect the role of external structures introduced by the choice of reference frame, temporal foliation, or low-velocity limit. Such issues lead to ambiguities in the definition of observables and apparent violations of covariance. Addressing these conceptual obstacles is a prerequisite for a consistent infrared phenomenology of quantum gravity.

## 2.2 Modified Dispersion Relations

Insights from effective field theories (EFT) prompt the question of whether an intrinsic mass or energy scale governs both classical and quantum gravity [19]. In quantum gravity, the Planck units (the energy $E_P$, length $\ell_P$, mass $M_P$, and time $t_P$) are natural candidates for this scale. Various *gedankenexperiments* that combine quantum mechanics and general relativity support these units [20, 21, 22, 23, 24]. If these scales are fundamental, they require modifications to standard relativistic kinematics.

### 2.2.1 Geometric Interpretation in Momentum Space

Relativistic kinematics is encoded in the dispersion relation, defined by the mass Casimir operator of the underlying spacetime symmetry algebra,

$$\mathcal{C}(E, \mathbf{k}, M) = M^2 c^2 = \mathcal{C}_\ell = \mathcal{C}_0 + \delta\mathcal{C}, \tag{2.1}$$

where $\mathcal{C}_0 = (E/c)^2 - \mathbf{k}^2$ is the standard Lorentz-invariant Casimir, $E$ the particle energy, $\mathbf{k}$ its spatial momentum, $M$ its rest mass, $c$ the speed of light, and $\delta\mathcal{C}$ encodes Planck-scale corrections.

In relativistic theories, the dispersion relation corresponds to the Casimir invariant of the spacetime symmetry algebra, ensuring invariance under symmetry transformations. In the standard case, this invariant reduces to a quadratic form $P^\mu P_\mu$, reflecting the flat geometry of momentum space.

However, in deformed scenarios, this structure is modified. If the spacetime symmetry algebra or the phase space structure is altered, the quadratic Casimir is no longer preserved and is replaced by a generalized invariant function $\mathcal{C}(P)$, encoding modified kinematics.

Geometrically, this modification can be understood as arising from a nontrivial momentum-space structure [25, 26], in which the dispersion relation is associated with a geodesic distance rather than a quadratic form. In this sense, the correction term $\delta\mathcal{C}$ captures deviations from flat momentum space and provides a model-independent parametrization of Planck-scale effects.

More generally, the Casimir operator can be interpreted as the momentum-space analog of the world function of Synge [27], with the mass measuring the geodesic distance from the origin. This distance can be written as [28, 29, 30]

$$\mathcal{C} = \left( \int_{\mathcal{O}}^{P} \sqrt{G^{\mu\nu}(x,k)\,\mathrm{d}k_\mu\,\mathrm{d}k_\nu} \right)^2, \tag{2.2}$$

where $G^{\mu\nu}$ denotes a possibly momentum-dependent metric on the cotangent bundle. This geometric viewpoint naturally frames MDRs as arising from curved momentum space and establishes connections to Finsler and Hamilton geometries [30, 31].

The momentum-space curvature interpretation provides a unifying framework for several quantum gravity phenomenology approaches. In this picture:

- **Deformed Special Relativity** corresponds to a maximally symmetric curved momentum space with constant curvature proportional to $\ell_P^{-2}$ [32, 33, 34].
- **Lorentz Invariance Violation** emerges from momentum-space geometries with preferred directions or anisotropies [35, 7].
- **Generalized Uncertainty Principles** can be derived from the non-trivial symplectic structure associated with curved momentum space [36, 37, 38].

### 2.2.2 Parametrizing Planck-Scale Deformations

To parametrize Planck-scale corrections in a minimal and model-agnostic manner, it is convenient to consider small deformations of the relativistic Casimir. Restricting attention to flat spacetime for simplicity, one may write

$$M^2c^2 = \mathcal{C}_0 + \delta\mathcal{C}(E,\mathbf{k},M) = \left(\frac{E}{c}\right)^2 - \mathbf{k}^2 + \delta\mathcal{C}(E,\mathbf{k},M), \tag{2.3}$$

where $\mathcal{C}_0$ denotes the standard Lorentz-invariant Casimir and $\delta\mathcal{C}$ encodes Planck-scale suppressed corrections governed by a microscopic length scale $\ell \sim \ell_P$. Although Lorentz symmetry need not be preserved, the dispersion relation may still be interpreted as a

Casimir invariant if the underlying momentum space remains maximally symmetric, as in deformed relativistic symmetry frameworks.

At first order in $\ell$, and excluding inverse powers of energy, momentum, or mass, the most general modified dispersion relation can be written as

$$M^2c^4 = E^2 - \mathbf{k}^2c^2 + \ell \sum_{n=0}^{2} \sum_{m=0}^{3-n} a_{n,m,3-n-m}(Mc)^n \mathbf{k}^m \left(\frac{E}{c}\right)^{3-n-m}, \tag{2.4}$$

where $\mathbf{k}$ represents the spatial momentum, $E$ denotes the energy, and $M$ is the rest mass of the particle. The indices $n$ and $m$ indicate the powers of mass and spatial momentum, respectively, in each correction term, while the power of energy is fixed by dimensional consistency as $(3-n-m)$. The dimensionless coefficients $a_{n,m,3-n-m}$ characterize distinct deformation channels and are generally expected to be of order unity if the deformation is natural.

This expression encompasses:

- **Energy-dependent corrections** ($m = 0$): These modify photon time-of-flight and are constrained by gamma-ray bursts [39, 40].
- **Momentum-dependent corrections** ($n = 0$): These affect particle thresholds in astrophysical processes [41, 42, 43].
- **Mixed terms**: These can induce novel effects in composite systems [44, 45].

Specific choices reproduce familiar models, including Lorentz-invariance-violating scenarios and deformed symmetry algebras such as $\kappa$-Poincaré, but no particular realization will be assumed here. The advantage of this general parametrization lies in its ability to capture model-independent features while remaining testable.

### 2.2.3 Timelike Preferred Structures

To define energy and spatial momentum in a covariant manner and to generalize the construction to curved spacetime, introduce a normalized timelike vector field $d^\mu$, which selects a preferred temporal direction at each spacetime point. It satisfies

$$d^\mu d^\nu g_{\mu\nu} = -1. \tag{2.5}$$

This vector defines a preferred temporal direction and induces a foliation of spacetime into hypersurfaces orthogonal to $d^\mu$. The associated spatial projector,

$$g_{\perp}{}^{\mu}{}_{\nu} = \delta^\mu_\nu + d^\mu d_\nu, \tag{2.6}$$

allows for a covariant decomposition of the four-momentum into temporal and spatial components,

$$E = c\, d^\mu k_\mu, \qquad k_{\perp\mu} = g_{\perp\mu}^{\ \ \nu} k_\nu, \tag{2.7}$$

with spatial norm

$$k_\perp = \sqrt{g_\perp^{\mu\nu} k_\mu k_\nu}. \tag{2.8}$$

In terms of these quantities, the modified dispersion relation extends straightforwardly to curved spacetime,

$$M^2c^2 = g^{\mu\nu} k_\mu k_\nu + \ell \sum_{n=0}^{2} \sum_{m=0}^{3-n} a_{n,m,3-n-m} (Mc)^n k_d^m k_\perp^{3-n-m}, \tag{2.9}$$

where $g^{\mu\nu}$ is the spacetime metric, $k_\mu$ is the four-momentum, $k_d = d^\mu k_\mu$ is the projection along the preferred direction $d^\mu$, and $k_\perp$ is the spatial norm defined via the projector above.

The introduction of the vector $d^\mu$ signals a tension with local Lorentz invariance. If treated as a fixed background structure, it corresponds to Lorentz invariance violation; if instead it transforms under deformed symmetry transformations, it is compatible with doubly special relativity [46]. This ambiguity has significant phenomenological implications:

- **LIV interpretation**: $d^\mu$ selects a preferred frame, often identified with the cosmic microwave background rest frame [47].
- **DSR interpretation**: $d^\mu$ transforms non-linearly under local boosts, preserving relativity of simultaneity at the cost of locality [48].
- **Observational consequences**: The two interpretations lead to different predictions for time-of-flight measurements and threshold effects [35].

In either case, such a timelike structure is unavoidable once a nonrelativistic regime is to be defined. This necessity highlights a fundamental insight: *the infrared amplification of Planck-scale effects inherently breaks Lorentz covariance at the level of effective descriptions.*

### 2.2.4 High-Energy vs Low-Energy

Modified dispersion relations of this type give rise to energy and momentum dependent corrections to particle propagation, leading to phenomena such as in-vacuo dispersion (energy-dependent propagation speeds even in vacuum) and threshold effects, which have been extensively constrained in high-energy astrophysical observations [18]. The most stringent bounds come from [49]:

- **Gamma-ray bursts**: Time delays between photons of different energies provide constraints at the level of $|\ell/\ell_P| \lesssim 1$ for linear corrections [50, 41, 51].

- **Ultra-high-energy cosmic rays**: Absence of GZK cutoff modifications constrains certain deformation patterns [43, 42]. This cutoff represents the Greisen–Zatsepin–Kuzmin limit, the theoretical upper bound on the energy of cosmic rays imposed by their interaction with the cosmic microwave background.
- **Neutrino oscillations**: Possible energy-dependent effects remain unobserved [52, 53, 54].

At the same time, the presence of a preferred temporal structure opens the possibility for amplified Planck-scale effects in the infrared, where high-precision quantum experiments provide a complementary testing ground. The amplification mechanisms include:

- **Mass enhancement**: Corrections proportional to $M^n$ can become significant for massive systems [8, 45].
- **Coherence time accumulation**: Small phase shifts accumulate over long evolution times [8, 55].
- **Collective effects**: Many-body systems can enhance sensitivity through entanglement or squeezing [56, 57].

With the kinematic scenario established, the next step is to derive the dynamical consequences in the nonrelativistic regime. Chapter 3 is dedicated precisely to this by starting from the general MDRs introduced earlier, systematically deriving the nonrelativistic limit, and obtaining the deformed Schrödinger equation.

# CHAPTER 3

## Deformed Nonrelativistic Dynamics

Having established in the previous chapter a kinematic framework in which Planck-scale corrections are encoded through MDRs, this chapter examines the resulting dynamical implications at low energies. The objective is to implement the nonrelativistic limit of these deformed relativistic relations and to determine their impact on the effective quantum dynamics of individual particles. This approach yields a deformed Schrödinger equation.

## 3.1 The Nonrelativistic Limit

The derivation of the nonrelativistic limit of relativistic theories constitutes a traditional and well-established line of research in physics [58, 59, 60, 61]. These analyses seek not only to recover classical descriptions, such as the transition from general relativity to Newtonian gravity or from the Klein–Gordon equation to the Schrödinger equation in the limit $c \to \infty$, but also to identify post-Newtonian corrections, which are higher-order terms that systematically represent relativistic effects.

Although expanding a theory in powers of $1/c$ may initially seem straightforward, this procedure involves significant conceptual and mathematical subtleties. The primary challenge arises because $c$ is a dimensionful parameter. Therefore, any expansion in $1/c$ requires a precise specification of the physical quantities being compared to the speed of light.

To illustrate this point, consider that energy $E$ and mass $m$ have different dimensions. In such an expansion, it is therefore crucial to specify whether one is comparing $E$ to $mc^2$ or momentum $p$ to $mc$. In the absence of such a specification, the resulting series lacks a clear physical meaning. In particle theories, the low-velocity limit, $v/c \ll 1$, is typically adopted to justify the nonrelativistic approximation. On the other hand, in field theories, criteria such as $p/mc \ll 1$ or $|E - mc^2|/mc^2 \ll 1$ are often employed. Establishing this scale of reference is thus a fundamental step to ensure both dimensional consistency and a coherent physical interpretation of the nonrelativistic limit.

In practice, implementing the nonrelativistic limit requires selecting a preferred temporal direction for measuring velocities and energies. Making this structure explicit is not simply a technical convenience. It is a fundamental step toward establishing a consistent Hamiltonian description. The following section constructs this formalism using geometric methods.

### 3.1.1 Breaking Covariance

In the nonrelativistic regime, particle velocities are assumed to be small compared to the speed of light. Similarly, in the Hamiltonian formulation, spatial momenta must be small relative to the rest-mass scale. However, Einstein's principle of relativity implies that neither velocity nor momentum possesses an absolute meaning: both are inherently frame dependent. Consequently, any statement that a given velocity is "small" depends on the choice of coordinates.

It follows that truncating an expansion in powers of $1/c$ at finite order necessarily breaks Lorentz covariance. In the present context, this is not a shortcoming, but an intrinsic aspect of the nonrelativistic approximation. Whereas Newtonian mechanics assumes an absolute time, relativity does not. Therefore, implementing the nonrelativistic limit requires introducing a preferred temporal structure that effectively defines a notion of Newtonian time and specifies which observers are approximately at rest.

Operationally, this is achieved by selecting a timelike curve $\gamma$ relative to which the expansion is performed. Along this curve, we define the tangent vector $\dot{\gamma}^\mu = \mathrm{d}\gamma^\mu/\mathrm{d}\lambda$, where $\lambda$ is a parameter with dimensions of length, and impose the normalization condition $\gamma^\mu\gamma^\nu g_{\mu\nu} = -1$. Given this vector, the background spacetime can be foliated as

$$g_{\mu\nu} = h_{\mu\nu} - \dot{\gamma}_\mu\dot{\gamma}_\nu, \tag{3.1}$$

where $h_{\mu\nu}$ describes the induced metric on spacelike hypersurfaces to which $\dot{\gamma}^\mu$ is normal, i.e. $\dot{\gamma}^\mu h_{\mu\nu} = 0$. To wit, the form $\dot{\gamma}_\mu \mathrm{d}x^\mu$ defines the direction of time which is supposed to become global in the expansion.

While the four-dimensional notation is appropriate at the relativistic level, when considering nonrelativistic physics, it is helpful to revert to adapted coordinates $(ct, x^i)$ which are defined by

$$\dot{\gamma}_\mu \mathrm{d}x^\mu \equiv -N\mathrm{d}t, \tag{3.2}$$

with the normalisation factor $N$, namely the lapse function. Then, the adapted-coordinate time $t$ can also be understood as a curve parameter along $\gamma$, defined up to time-reparameterisation invariance (which we will take advantage of in Secs. 3.2 and 3.3). Given a general background geometry, it can be shown that the line element can be expressed in terms of ADM-variables [62, 63] (see chapter 12 of [64] for a recent introduction), i.e. $N$ as well as the shift vector $N^i$ and the induced metric $h_{ij}$, as

$$\mathrm{d}s^2 = -N^2c^2\mathrm{d}t^2 + h_{ij}(N^i c\mathrm{d}t + \mathrm{d}x^i)(N^j c\mathrm{d}t + \mathrm{d}x^j). \tag{3.3}$$

Here the lapse function and the shift vector are pure gauge degrees of freedom. They are fixed by the choice of curve $\gamma$. It is in these adapted coordinates that the overall dependence on $1/c$ is manifest, thus significantly simplifying the expansion.

We are now in the position to understand the meaning of the term "small velocities". In adapted coordinates, we may use the soon-to-be global time as curve parameter such that

$$U^\mu \equiv \frac{\mathrm{d}x^\mu}{\mathrm{d}(ct)} = \left(1, c^{-1}\frac{\mathrm{d}x^i}{\mathrm{d}t}\right) \equiv \left(1, \frac{\dot{x}^i}{c}\right). \tag{3.4}$$

It is the quantity $\dot{x}^i/c$ that we have to expand in. Similarly, on the level of momenta $p_i/Mc \ll 1$, with the mass of the considered object $M$.

A closer look at Eq. (3.4) tells us that an analogous expansion has to affect vector and tensor fields. Throughout this work, we will indicate this series as

$$\mathcal{T} = \sum_{n=0}^{\infty} c^{-n}\mathcal{T}^{(n)}, \tag{3.5}$$

where the symbol $\mathcal{T}$ stands for any general tensor field content.[1]

The analogue of Eq. (3.4) for general vectors $V^\mu$ has particular consequences at lowest order, i.e. in the limit $c \to \infty$. In adapted coordinates such a vector may be written as

$$V^\mu_{(0)} \equiv \lim_{c\to\infty} \frac{\mathrm{d}\gamma^\mu_V}{\mathrm{d}t} = \lim_{c\to\infty}\left(1, c^{-1}\frac{\mathrm{d}\gamma^i_V}{\mathrm{d}t}\right) = (1,0)\,, \tag{3.6}$$

where $\gamma_V$ denotes the curve to which $V^\mu$ is tangent, and we used the reparametrisation invariance of the curve to set $\mathrm{d}\gamma^0_V/\mathrm{d}t = 1$. As a result, in this limit every vector is either timelike, and possesses vanishing spacelike components or it vanishes altogether. Thus, in adapted coordinates, every spatial vector such as, for example, $N^i$ is vanishing at lowest order, i.e. $N^i_{(0)} = 0$ such that $\dot{\gamma}^\mu_{(0)} = N^{-1}_{(0)}\delta^\mu_0$. On the level of scalar quantities, we may formulate this fact as

$$\lim_{c\to\infty} V^\mu V^\nu g_{\mu\nu} = \lim_{c\to\infty}\left[g_{00} + c^{-1}\frac{\mathrm{d}\gamma^i_V}{\mathrm{d}t}g_{0i} + c^{-2}\frac{\mathrm{d}\gamma^i_V}{\mathrm{d}t}\frac{\mathrm{d}\gamma^j_V}{\mathrm{d}t}g_{ij}\right] = -N^2_{(0)}, \tag{3.7}$$

which is negative, implying that the vector is either timelike or equal to zero. Geometrically, this can be understood as the light-cones making out the entire manifold as $1/c$ approaches 0 – spacelike-separated events are an infinite distance apart.

[1]For example, this includes the metric either in its covariant formulation $g_{\mu\nu}$ or the canonical one in terms of $N$, $N^i$ and $h_{ij}$, but also additional (quantum-gravity inspired or electromagnetic) fields.

For normalised timelike vectors $v^\mu$, we may go even further. In this case, we obtain

$$v^\mu v^\nu g_{\mu\nu} \simeq -\left(v^0_{(0)}\right)^2 N^2_{(0)} - 2c^{-1}\left(v^0_{(1)}v^0_{(0)}N^2_{(0)} + (v^0_{(0)})^2 N_{(0)}N_{(1)}\right) = -1, \tag{3.8}$$

which can only be solved by $v^\mu_{(0)} = \pm\dot{\gamma}^\mu_{(0)}$ and $v^0_{(1)} = \mp N_{(1)}/N^2_{(0)}$. Thus, to lowest order, any normalised timelike vector is either aligned or antialigned with the global time and the absolute value of the time-component of any timelike unit vector is equal up to second-order corrections. In particular, this observation applies to the Lorentz-violating vector $d^\mu$ introduced in the preceding section.

In a nutshell, there is a lot of information that can be derived from the necessity of breaking covariance alone. This, however, is not the only subtlety of the nonrelativistic limit in curved geometries.

All background tensor fields are expanded in $1/c$. This approach indicates that, in general, the analysis involves more than a comparison of velocities to the speed of light. External fields may introduce additional characteristic scales. For instance, the speed of light appears explicitly in the coupling of Einstein's field equations,

$$G_{\mu\nu} = \frac{8\pi G}{c^4}T_{\mu\nu}. \tag{3.9}$$

In an expansion involving the Einstein tensor $G_{\mu\nu}$, Newton's constant $G$, and the stress-energy tensor $T_{\mu\nu}$ (see [65] for details), a series in powers of $1/c$ implicitly assumes a weak-gravity regime. It is crucial to distinguish, however, that the nonrelativistic limit, defined by $v/c \ll 1$, does not necessarily preclude strong gravitational fields. This kind of ambiguity is to be expected when expanding in dimensionful parameters like $1/c$.

Because this work focuses on low-energy phenomenology, we neglect gravitational corrections at lowest order and set $N_{(0)} = 1$.

### 3.1.2 Quantum-Gravity Inspired Corrections

External scales cannot only arise when coupling to classical gravity or other forces. The quantum-gravity inspired corrections to relativistic particle dynamics we introduce in sections 3.2.2 and 3.3.2 themselves depend on the Planck length $\ell$. The Planck length, in turn, is defined as

$$\ell \equiv \sqrt{\frac{\hbar G}{c^3}} \sim 10^{-35}m, \tag{3.10}$$

which clearly depends on $c$. Similarly, in the $1/c$-expansion of the correction term, there will be terms behaving like positive powers of $c$. In the strict limit of $c \to \infty$ these would become infinitely large.[2] In the phenomenological context, however, this is irrelevant

[2]Similar issues have been encountered when taking the classical limit of minimal-length quantum mechanics [66]. They have been elaborated upon and discussed further in [67].

because the Planck length itself is exceedingly small and, independently of the appearance of the speed of light, serves as perturbative parameter when compared to other length (or inverse-energy) scales. Bear in mind that it is not required to apply the strict limit of $c \to \infty$. In reality, in the nonrelativistic regime, the speed of light is not infinite, it is just very large. In particular it can be compensated for by other scales.

Henceforth, we refrain from expanding the phenomenological corrections to the same degree in $1/c$ as we do with other terms. Instead, we solely focus on their leading contribution in $1/c$, coupled with the Planck length $\ell$, an independent expansion in powers of which is understood. By adopting this approach, we recognise the importance of singling out the leading effects that manifest within the interplay of these distinct factors.

### Time-dependent backgrounds in quantum mechanics

Now, let us obtain nonrelativistic quantum dynamics in two different ways – by virtue of canonical quantisation of classical dynamics and as a limit of the covariant Klein-Gordon equation (and its generalisations). When confronted with a background geometry that lacks a timelike Killing vector field, both of these approaches encounter their respective limitations.

In short, the issue lies in the fact that the natural Hilbert-space scalar product on surfaces of constant time (i.e. normal to $\mathrm{d}t$), be it derived from the Klein-Gordon scalar product [68]

$$\langle\Psi|\Phi\rangle_{\mathrm{KG}} = \int \mathrm{d}\Sigma^{\mu}_{t_0}\left[\Psi^*\nabla_\mu\Phi - (\nabla_\mu\Psi)^*\Phi\right], \tag{3.11}$$

or created by canonical quantization according to geometric calculus [69], contains the volume form on these hypersurfaces $\Sigma_t$ [70, 71, 72], i.e.

$$\langle\psi|\phi\rangle = \int_{\Sigma_t} \mathrm{d}^d x\sqrt{h}\psi^*\phi, \tag{3.12}$$

where $h = \det h_{ij}$ in adapted coordinates. If the volume measure $\sqrt{h}$ appearing in this integral changes with time, the unitarity of the resulting quantum theory ceases to be obvious [73] just because Hilbert-space elements at infinitesimally different times cannot be identified anymore [61]. In a similar vein, the very notion of single-particle quantum theory becomes slightly problematic in evolving backgrounds due to particle creation.

In the main body of the thesis, we will assume that the spatial part of the metric is constant, i.e. in adapted coordinates $\partial_0 h_{ij} = 0$.

## 3.2 Canonical quantisation of nonrelativistic dynamics

This section focuses on the first of two methods employed to derive the deformed Schrödinger equation from an MDR. We begin by considering the nonrelativistic limit at the classical level. Next, we quantise the resulting classical theory using canonical techniques, following the established approach to quantisation on curved spaces originally proposed by deWitt [70].

In general, starting at a dispersion relation of the kind given in Eq. (2.1), we have to choose a slicing along which we define the Hamiltonian which governs single-particle dynamics. Conveniently, for the nonrelativistic limit, we employ the adapted coordinate system $x^\mu = (ct, x^i)$ introduced in Sec. 3.1.1. Provided the ADM-decomposition of the metric (3.3), Eq. (2.1) can be solved for $k_0$. Then, the dynamics of a particle along the worldline $\gamma$ is governed by the Hamiltonian

$$H = ck_0(k_i, M, \Phi), \tag{3.13}$$

where $\Phi$ stands for general external field content (like the metric or an electromagnetic field). In other words, the Hamiltonian provides the energy as measured along $\gamma$. This function is to be expanded in $1/c$, first for Riemannian backgrounds, and subsequently for a deformations thereof corresponding to the MDR in Eq. (2.9).

### 3.2.1 Riemannian spacetime

In order to describe motion in curved spacetime, the special relativistic dispersion relation has to be enhanced. As a result, the dynamics of a relativistic particle on a curved spacetime of four-momentum $k_\mu$ must satisfy the constraint

$$\mathcal{C}_0 = -g^{\mu\nu}(x)k_\mu k_\nu = M^2c^2. \tag{3.14}$$

Demanding that the energy of the particle be positive and using Eq. (3.3), we find the Hamiltonian

$$H_0 = NMc^2\sqrt{1 + \frac{h^{ij}k_ik_j}{(Mc)^2}} + N^ik_ic. \tag{3.15}$$

We expand this function in velocities, thus assuming that $h^{ij}k_ik_j \ll M^2c^2$, as well as the background fields as required by Eq. (3.5).

The nonrelativistic limit in and of itself consists in letting the speed of light tend to infinity. This is only a well-defined procedure if the terms in the Hamiltonian proportional to positive powers of $c$ do not contribute to the equations of motion, i.e. amount to constants. In order for this condition to be satisfied, the quantity $N_{(1)}$ has to be constant such that it can be set equal to zero by a constant reparameterisation of the time-coordinate.

As a result, the unperturbed three-dimensional tensor $h_{ij}^{(0)}$ becomes the effective metric on the resulting hypersurfaces. In the following, the induced metric and its inverse $h_{(0)}^{ij}$ are used to raise and lower spatial indices. Neglecting the trivial constant part, the nonrelativistic Hamiltonian amounts to

$$H_{0,\mathrm{NR}} = \frac{h_{(0)}^{ij}}{2M} \left(k_i - MA_i^{\mathrm{g}}\right) \left(k_j - MA_j^{\mathrm{g}}\right) + \phi_{\mathrm{g}} M, \tag{3.16}$$

with the gravitomagnetic vector potential $A_i^{\mathrm{g}} = -N_i^{(1)}$ and the gravitoelectrostatic potential $\phi_{\mathrm{g}} = (N_{(2)} - N_{(1)}^i N_i^{(1)}/2)$ (for further details, refer to [74]). The resemblance of this Hamiltonian to the one describing a charged particle in the presence of an electromagnetic field is evident. Here, the role of the charge is assumed by $M$.

Following deWitt's approach, the quantisation of the dynamics of single particle on a curved background is preferably obtained by choosing the Hilbert-space measure to be provided by the invariant volume-form $h\mathrm{d}^d x$, where $h = \det h_{ij}$ [70, 71, 72]. Correspondingly, the wave functions $\psi \in \mathcal{H}$ are scalars and so is the representation of the Hamiltonian. Following the principles of geometric calculus [69], this representation is most straight-forwardly provided in terms of covariant derivatives $\nabla_i$ compatible with the induced metric. Including the minimal coupling of an external magnetic field obtained by enforcing local $U(1)$ invariance of the wave function (i.e. $\hat{k}_i \to \hat{k}_i - eA_i$, $\hat{H} \to \hat{H} + e\phi$), we obtain the operator-equivalent of the Hamiltonian

$$\hat{H}_{0,\mathrm{NR,EM}}\psi = \left[-\frac{h^{ij}}{2M} \left(\nabla_i - ieA_i - iMA_i^{\mathrm{g}}\right) \left(\nabla_j - ieA_j - iMA_j^{\mathrm{g}}\right) + e\phi_e + M\phi_{\mathrm{g}}\right] \psi. \tag{3.17}$$

Thus, in the nonrelativistic limit we observe a particle moving on a curved $d$-dimensional geometry which is charged under a $U(1)_e \times U(1)_M$-symmetry with charges $e$ and $M$.

This finding is in line with [61], nevertheless corresponding to a generalisation thereof because in this study the spatial metric is not assumed to be flat. Equation (3.17) is to be extended to MDRs in the subsequent subsection.

### 3.2.2 Modified dispersion relations

In contrast to the Riemannian case, solving Eq. (2.1) for $k_0$ is highly nontrivial. However, we are only interested in solutions to order $\ell$. Therefore, we can approximately reduce Eq. (2.1) such that

$$\begin{aligned} \mathcal{C}_0 &= M^2c^2 - \ell \sum_{n=0}^{2} \sum_{m=0}^{3-n} a_{n,m,3-n-m} (Mc)^n k_\perp^m k_d^{3-n-m} \Bigg|_{k_0 = H_0/c} \\ &= (Mc)^2 - \delta\bar{\mathcal{C}}, \end{aligned} \tag{3.18}$$

where we abbreviated $\delta\bar{\mathcal{C}} \equiv \delta\mathcal{C}|_{k_0=H_0/c}$. Consequently, we obtain the deformed Hamiltonian

$$H_\ell = NMc^2\sqrt{1+\frac{h^{ij}k_ik_j-\delta\bar{\mathcal{C}}}{(Mc)^2}}+N^ik_ic \simeq H_0-\frac{N\delta\bar{\mathcal{C}}}{2M}\left(1+\frac{h^{ij}k_ik_j}{(Mc)^2}\right)^{-1/2}. \tag{3.19}$$

As argued in Sec. 3.1.2, only the leading-order correction in $1/c$ is of interest to us. Bear in mind, however, that relevant contributions are not allowed to amount to a total derivative so as to contribute nontrivially to the dynamics. In particular, it has to be dependent on positions and/or momenta.

In order to evaluate the leading contribution of $\delta\bar{C}$, we have to study the projections of the four-momenta respective to the slicing carved out by $d^\mu$, i.e. $k_d$ and $k_\perp$ under the replacement $k_0 \to H_0/c$. This is most effectively done by expressing the Lorentz-violating vector in terms of its deviation from the global time such that

$$d^\mu = \dot{\gamma}^\mu - \mathcal{A}^\mu, \tag{3.20}$$

where we may normalise in accordance with Eq. (3.8) such that

$$\mathcal{A}^\mu_{(0)} = \mathcal{A}^0_{(1)} = 0, \qquad\qquad \mathcal{A}^0_{(2)} = \frac{\mathcal{A}^i_{(1)}\mathcal{A}^j_{(1)}h^{(0)}_{ij}}{2N_{(0)}}. \tag{3.21}$$

Applying these conditions and expanding to second order, we obtain the momentum projected to the hypersurfaces

$$k_\perp|_{k_0=H_0/c} \simeq \sqrt{h^{ij}_{(0)}\left(k_i - M\mathcal{A}^{(1)}_i\right)\left(k_j - M\mathcal{A}^{(1)}_j\right)}. \tag{3.22}$$

This quantity deviates from the magnitude of the momentum inasmuch as it contains the quantity $\mathcal{A}^{(1)}_i$. Having units of velocity, this vector quantifies the relative velocity between the reference system for the nonrelativistic limit and the deformation vector.

Defining $k^{\mathcal{A}}_i \equiv k_i - M\mathcal{A}_i$ and $k^2_{\mathcal{A}} \equiv h^{ij}_{(0)}k^{\mathcal{A}}_ik^{\mathcal{A}}_j$, we can finally express the corrected nonrelativistic Hamiltonian as

$$H_{\ell,\mathrm{NR}} \simeq H_{\mathrm{NR}} - \frac{\ell}{2M}\sum_{n=0}^{2}\sum_{m=0}^{3-n} a_{n,m,3-n-m}(Mc)^{3-m}k^m_{\mathcal{A}}\left[1+\frac{3-n-m}{2Mc}k^2_{\mathcal{A}}\right]. \tag{3.23}$$

While it appears that we display not only the leading but also the next-to-leading order in $1/c$ here, this is rooted in the fact that the leading contribution in models with $m=0$ is constant. A constant addition to a Hamiltonian, however, has no influence on the equations of motion.

To make this manifest, we parameterise the deformed nonrelativistic Hamiltonian differently such that it becomes

$$H_{\ell,\mathrm{NR}} \simeq H_{\mathrm{NR}} - \frac{\ell}{2M} \sum_{n=1}^{3} \xi_n (Mc)^{3-n} k_{\mathcal{A}}^n. \tag{3.24}$$

The newly introduced dimensionless parameters $\xi_n$ are clearly more suited to the nonrelativistic dynamics. They are related to the original parameterisation as

$$\begin{aligned} \xi_1 &= a_{1,1,1} + a_{2,1,0} + a_{0,1,2}, \\ \xi_2 &= a_{1,2,0} + a_{0,2,1} + \frac{1}{2} a_{2,0,1} + a_{1,0,2} + \frac{3}{2} a_{0,0,3}, \\ \xi_3 &= a_{0,3,0}. \end{aligned} \tag{3.25}$$

We are left with the task of canonically quantising the corrections. By analogy with Sec. 3.2, this can be done by representing momenta as gauge-covariant derivatives when acting on position eigenstates. The Hamiltonian thus acts on wave functions $\psi$ as

$$\begin{aligned} \hat{H}_{\ell,\mathrm{NR,EM}} \psi = \hat{H}_{0,\mathrm{NR,EM}} \psi &- \frac{\ell}{2M} \sum_{n=1}^{3} \xi_n (Mc)^{3-n} \\ &\times \left[ -h_{(0)}^{ij} \Big( \nabla_i - iM\mathcal{A}_i - ieA_i \Big) \Big( \nabla_j - iM\mathcal{A}_j - ieA_j \Big) \right]^{n/2} \psi. \end{aligned} \tag{3.26}$$

As the corrections are functions of one operator only, namely the Laplacian with an insertion of the field $\mathcal{A}_i$, they are automatically symmetric with respect to the ordinary volume measure $h\mathrm{d}^d x$. Notice that the gravitomagnetic potential $A_i^{\mathrm{g}}$ only contributes to the unperturbed Hamiltonian, and does not appear in the correction term. In the subsequent section, this result is complemented with the deformed Schrödinger equation derived from relativistic field theory.

## 3.3 Nonrelativistic limit of modified Klein-Gordon equation

An alternative avenue to derive nonrelativistic quantum dynamics from its relativistic counterpart is by applying the nonrelativistic limit to the single-particle sector of quantum field theory. This approach relies on a somewhat heuristic methodology, as it necessitates the division of modes into positive and negative frequencies, a task that generally eludes perturbative treatment within the $1/c$ expansion, refer to [61] for more details. As discussed in Sec. 3.1.2, due to particle creation this is certainly an issue in time-dependent backgrounds.

In order to describe the dynamics of a single spinless particle, charged with respect to $U(1)$ gauge field, we consider the covariant Klein-Gordon equation as well as generalisations thereof, i.e. in adapted coordinates

$$\left[\hat{\mathcal{C}}(-iD_0, -iD_i, M) - M^2\right]\varphi = 0. \tag{3.27}$$

Here, $\varphi$ is the scalar field, and $D_\mu$ stands for the gauge-covariant derivative including the $U(1)$-gauge field $A_\mu$ and the charge $e$, i.e.

$$D_\mu = \nabla_\mu - ieA_\mu. \tag{3.28}$$

The covariant derivative $\nabla_\mu$ is based on the Levi-Civita connection $\Gamma^\rho_{\mu\nu}$ compatible with the background metric $g_{\mu\nu}$.

Inspired by an approach developed in [73, 59, 75, 61], we apply a WKB-like expansion to Eq. (3.27). In this vein, we assume the scalar field to be given as

$$\varphi = e^{-iMc\lambda}\psi = e^{-iMc\lambda}\sum_{n=0}^{\infty}\frac{\psi_n}{c^n}, \tag{3.29}$$

with some scalar function with units of length $\lambda$, assumed to be uncharged under $U(1)$, while the field $\psi = \sum_{n=0}^{\infty} c^{-n}\psi_n$ carries the charge $e$. From the field equation, it is possible to derive the effective equation of motion for the Schrödinger field $\psi_0$. First, this procedure will be followed for general Riemannian geometries, to be subsequently generalised to deformed Casimir operators.

### 3.3.1 Riemannian spacetime

On a curved spacetime characterised by the metric $g^{\mu\nu}(x)$ and considering a $U(1)$-gauge field, the mass Casimir operator equals the covariant d'Alembertian

$$\hat{\mathcal{C}}_0(-i\nabla_\mu, A_\mu) = g^{\mu\nu}D_\mu D_\nu. \tag{3.30}$$

Plugging in the ansatz given by Eq. (3.29), the corresponding Klein-Gordon equation reads

$$\left[-M^2c^2(g^{\mu\nu}\nabla_\mu\lambda\nabla_\nu\lambda + 1) - iMc\left(\Box\lambda + 2g^{\mu\nu}\nabla_\mu\lambda D_\nu\right) + g^{\mu\nu}D_\mu D_\nu\right]\psi = 0, \tag{3.31}$$

with the d'Alembertian $\Box = g^{\mu\nu}\nabla_\mu\nabla_\nu$. This equation is to be expanded in powers of $1/c$. In accordance with Eq. (3.5), the involved background fields, i.e. the metric $g_{\mu\nu}$ and the gauge field $A_\mu$, necessarily have to be expanded as well.

At order $c^2$, the covariant Klein-Gordon equation yields the condition

$$-g^{\mu\nu}_{(0)}\partial_\mu\lambda\partial_\nu\lambda = 1. \tag{3.32}$$

This equation implies two points.

- First, it characterises $\lambda$ as the proper distance (or rescaled proper time) covered along a timelike curve on the geometry compatible with the metric $g^{(0)}_{\mu\nu}$, i.e. $\lambda = c\tau_{(0)}$. Thus, the solution (3.29) indeed corresponds to a single particle moving along this curve.

- Second, the timelike form $\partial_\mu\lambda$ is normalised at zeroth order. Thus, by Eq. (3.8), it is aligned with the global time, i.e. $\dot{\gamma}^{(0)}\mathrm{d}x^\mu = \mathrm{d}\lambda$. In adapted coordinates, we may express this condition as $\mathrm{d}\lambda = -N_{(0)}c\mathrm{d}t$, which suffices to foliate the background spacetime into evolving hypersurfaces of constant time as in Eq. (3.1).

When further expanding Eq. (3.31) in powers of $1/c$, it is important to bear in mind that $g^{\mu\nu}_{(0)}\dot{\gamma}^{(0)}_\nu\nabla^{(0)}_\mu$ in adapted coordinates is to become a derivative with respect to the time coordinate, thus being accompanied by a factor of $1/c$. This will cease to be the case at higher order, where the vector $g^{\mu\nu}\dot{\gamma}^{(0)}_\mu$ gains spacelike components. Similarly, the timelike component of the electromagnetic potential $\dot{\gamma}^{(0)}_\mu A^\mu$, in general, goes at most as $1/c$. At order $c$ Eq. (3.31) then reduces to a complex constraint on the background metric. Thus, we obtain two consistency conditions for the existence of solutions of the form (3.29), i.e.

$$g^{\mu\nu}_{(1)}\dot{\gamma}^{(0)}_\mu\dot{\gamma}^{(0)}_\nu = K_{(0)} = 0, \tag{3.33}$$

with the trace of the extrinsic curvature of the spacelike hypersurfaces $K \equiv -h^{\mu\nu}\nabla_\mu\dot{\gamma}_\nu$. Consequently, similarly to the classical case $N_{(1)} = 0$ (c. f. the reasoning below Eq. (3.15)), and the extrinsic curvature vanishes at lowest order. This is the logical consequence of there only being timelike vectors at that level. In adapted coordinates, the extrinsic curvature reads [64]

$$K = \frac{h^{ij}}{2N}\left(2\nabla_i N_j - c^{-1}\partial_0 h_{ij}\right). \tag{3.34}$$

Hence, $K_{(0)} = 0$ is trivially satisfied. Finally, at order $(1/c)^0$, we obtain the effective Schrödinger equation

$$i\partial_0\psi = \left[-\frac{h^{ij}}{2M}\left(\nabla_i - ieA_i - iMA^{\mathrm{g}}_i\right)\left(\nabla_j - ieA_j - iMA^{\mathrm{g}}_j\right) + M\phi_{\mathrm{g}} + e\phi_e\right]\psi, \tag{3.35}$$

where the gravitational and magnetic potentials are defined as below Eq. (3.16), and where we removed the sub- and superscripts indicating the orders to avoid unnecessary cluttering.

As $N_{(0)} = 1$ and $N^i_{(0)} = 1$, the spatial part of the covariant derivatives $\nabla^{(0)}_i$ is compatible with the induced metric $h^{ij}_{(0)}$. Therefore, the vector operator $-i\nabla_i$ is Hermitian with respect to the effective Klein-Gordon measure given in Eq. (3.11). Following straightforwardly what is done in Sec. 3.2.2, Eq. (3.35) will now be generalised to MDRs.

### 3.3.2 Modified dispersion relations

Modifications of the mass Casimir as in Eq. (2.3) imply deformations to the Klein-Gordon equations in accordance with Eq. (3.27). In this sense, we may interpret the four-momentum as a gauge-covariant derivative. Define the operator-valued counterparts of $k_\perp$ and $k_d$ as

$$\hat{k}_\perp^2\varphi = - D_\mu g_\perp^{\mu\nu} D_\nu\varphi, \tag{3.36}$$

$$\hat{k}_d\varphi = \frac{i}{2}\{d^\mu, D_\mu\}\varphi = \sqrt{M^2c^2 + \hat{k}_\perp^2}\psi + \mathcal{O}(\ell), \tag{3.37}$$

the anticommutator $\{,\}$ was introduced to render the operator $\hat{k}_d$ symmetric with respect to the Klein-Gordon measure (provided in (3.11)). Consequently, $[\hat{k}_d, \hat{k}_\perp] = 0$ at order $\ell^0$. This implies that the pseudo-Riemannian Casimir is modified as (c. f. [76, 77, 78, 79])

$$\begin{aligned}\hat{\mathcal{C}}_\ell &= \hat{\mathcal{C}}_0 + \frac{\ell}{2}\sum_{n=0}^{2}\sum_{m=0}^{3-n} a_{n,m,3-n-m}(Mc)^n \hat{k}_\perp^m \hat{k}_d^{3-n-m} \\ &= \hat{C}_0 + \delta\hat{C}.\end{aligned} \tag{3.38}$$

The model coefficients $a_{n,m,3-m-n}$ are in one-to-one correspondence to the ones in Eq. (2.4).

In the following, we aspire to obtain the leading corrections to the action of $\delta\hat{C}$ on the scalar. In this vein, it is crucial to recognize that the phase factor satisfies $D_i^{(0)}\lambda = 0$ and $D_0^{(0)}\lambda = -c$. Thus, to lowest order the phase is an eigenfunction of the covariant time-derivative operator

$$iD_0^{(0)}e^{iMc\lambda} = Mc^2 e^{iMc\lambda}. \tag{3.39}$$

As a result, the combination $D_0^{(0)}\varphi$ is of order $c^2$, while $D_i^{(0)}\varphi$ is of order one. Furthermore, at order $\ell$ the time-derivative of the wave function can be approximated by applying Eq. (3.35) to it. Then, using Eq. (3.21) and parameterising the deviation of the Lorentz-violating vector from the tangent vector of the curve $\gamma$ in accordance with Eq. (3.20), we obtain the leading-order representations

$$e^{-Mc\lambda}\hat{k}_\perp^2\varphi \simeq - h_{(0)}^{ij}\left(D_i^{(0)} - iM\mathcal{A}_i^{(1)}\right)\left(D_j^{(0)} - iM\mathcal{A}_j^{(1)}\right)\psi \equiv \hat{k}_{\mathcal{A}}^2\psi, \tag{3.40}$$

$$e^{-Mc\lambda}\hat{k}_d\varphi \simeq \left(Mc + \frac{\hat{k}_{\mathcal{A}}^2}{2Mc}\right)\psi. \tag{3.41}$$

With these expressions in mind, we can obtain the corrections to the Schrödinger equation

$$i\partial_0\psi = \hat{H}_{0,\mathrm{NR,EM}}\psi - \frac{\ell}{2M}\sum_{n=1}^{3}\xi_n(Mc)^{3-n}\hat{k}_{\mathcal{A}}^n\psi, \tag{3.42}$$

where the dimensionless numbers $\xi_n$ parameterise the result in accordance with Eq. (3.25). Thus, the nonrelativistic evolution exactly equals Eq. (3.26).

## 3.4 Phenomenological implications in the infrared

Summarising the above, we have derived nonrelativistic quantum dynamics in two complementary ways, as presented in Eqs. (3.26) and (3.42), converging to the nonrelativistic Hamiltonian operator

$$\begin{aligned}\hat{H}_{\ell,\mathrm{NR,EM}}\psi = \Bigg[ & -\frac{h^{ij}}{2M}\left(\nabla_i - ieA_i^e - iMA_i^g\right)\left(\nabla_j - ieA_j^e - iMA_j^g\right) + e\phi_e + M\phi_{\mathrm{g}} \\ & -\frac{\ell}{2M}\sum_{n=1}^{3}\xi_n (Mc)^{3-n}\left[-h^{ij}\left(\nabla_i - ieA_i^e - iM\mathcal{A}_i\right)\left(\nabla_j - ieA_j^e - iM\mathcal{A}_j\right)\right]^{\frac{n}{2}}\Bigg]\psi. \end{aligned} \tag{3.43}$$

Equation (3.43) constitutes the central result of this chapter. We emphasise that this Hamiltonian encompasses the nonrelativistic dynamics of all analytic MDRs up to order $\ell$.

Before proceeding to specific applications, a conceptual point must be addressed regarding the applicability of Eq. 3.43 to composite systems. A naive extrapolation of single-particle deformations to a macroscopic body composed of $\mathcal{N}$ constituents would suggest an unphysical accumulation of Planck-scale corrections, scaling with the total mass $M_{mac} = \mathcal{N}m$. This is the essence of the so-called **soccer-ball problem** [80, 44, 81, 82]. However, as explicitly derived in Appendix A from the classical Lagrangian of a multi-particle system, the effective deformation parameter for the center-of-mass dynamics is rescaled according to $\ell \to \ell/\mathcal{N}$. Consequently, when analyzing macroscopic objects, the relevant comparison is not between the macroscopic mass and the Planck mass, but rather between the mass of the fundamental constituents (e.g., protons) and the Planck mass. This dilution mechanism ensures the suppression of quantum-gravity effects in the classical limit while preserving the possibility of amplified signatures in the infrared regime of individual or few-particle quantum systems.

The focus of this section is on analysing this unified Schrödinger equation as to report which kinds of models serve as a reliable foundation for low-energy quantum gravity phenomenology. Indeed, there are some conclusions that can be drawn from Eq. (3.43) at the general level, without specifying the considered MDR. Amongst these are the results depicted in Fig. 3.1.

- Being dependent on fractional powers of the second-order differential operator $\hat{k}^2_{\mathcal{A}}$, the corrections to the Hamiltonian are generally nonanalytic and therefore nonlocal. The appearance of such nonanalyticities is not a novelty in linearly deformed

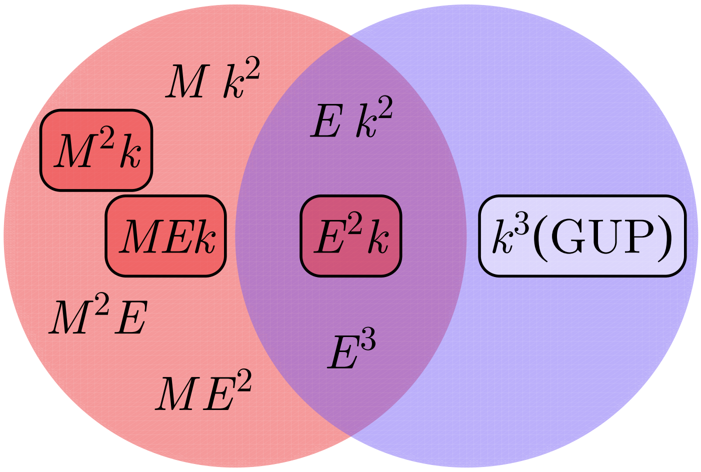


Figure 3.1: Dependence of correction terms to the relativistic dispersion relation on momentum $k$, mass $M$, and energy $E$ for all models at order $\ell$. The violet (right) and red (left) circles indicate those which are amenable to relativistic (UV) and nonrelativistic (IR) measurements, respectively. Those which are particularly suitable for nonrelativistic reasoning are framed and have an additional red background. The GUP is indicated by a frame and with a white background.

nonrelativistic quantum dynamics and generally expected at the nonperturbative level. For instance, they have been encountered in the context of the linear and quadratic GUP (see e. g. [83]).

- As in the nonrelativistic regime by construction $\langle h^{ij}\hat{k}_i\hat{k}_j\rangle \ll (Mc)^2$, those MDRs which lead to linear corrections in $\hat{k}_\mathcal{A}$, in Eq. (2.4) the ones linear in $k$, i.e. deformations of the form $E^2k$, $MEk$ or $M^2k$, have the largest effects. Therefore, they are displayed in frames in Fig. 3.1. The corresponding Hamiltonians have the form

$$\hat{H}_{\ell,\mathrm{NR,EM}} \simeq \hat{H}_{0,\mathrm{NR,EM}} - \frac{\xi_1\ell Mc^2}{2}\hat{k}_\mathcal{A}, \tag{3.44}$$

such that the ensuing quantum-gravity contribution to the dynamics has the advantage of being amplified by a factor of $c^2$. However, this also implies that the corrections become large in the far IR. If, for simplicity, $\mathcal{A}_i = 0$, this is the case once $\langle\hat{k}\rangle \lesssim \xi_1\ell(Mc)^2$. In fact, this property is shared with the underlying MDR which at small momenta becomes

$$M^2c^4 \simeq E^2 - k^2c^2 - \xi_1\ell M^2c^4k \simeq E^2 - \xi_1\ell M^2c^4k. \tag{3.45}$$

This finding entails an entirely new string of IR-phenomenology which has already been emphasised in [84, 6].

- Corrections quadratic in $\hat{k}_\mathcal{A}$, stemming from the models $Mk^2$, $Ek^2$ (corresponding to the bicrossproduct basis of the $\kappa$-Poincaré algebra [85]), $M^2E$, $ME^2$ and $E^3$, lead to a modification akin to the kinetic term. The underlying Hamiltonian is of the form

$$\hat{H}_{\ell,\mathrm{NR,EM}} \simeq \hat{H}_{0,\mathrm{NR,EM}} - \frac{\xi_2 \ell M c^2}{2} \hat{k}^2_{\mathcal{A}}. \tag{3.46}$$

In comparison to the ordinary kinetic term, here the mass is amended by a term comparing $M$ to $c/\ell$ (i.e. the Planck mass), and the particle is minimally coupled to the vector potential $\mathcal{A}^i$. If $\mathcal{A}^i$ and $N^i$ vanish, this comes down to a modification of the inertial mass, thus leading to a violation of the equivalence principle. We will come back to this point in section 3.6.2.

- Corrections proportional to $k^3_{\mathcal{A}}$, i.e. MDRs of the form $k^3$ occurring in LIV-models [86] and a lesser-known basis of the $\kappa$-Poincaré algebra [87, 88], are special in their own right. Indeed, for isotropic backgrounds ($\mathcal{A}_i = 0$), they exactly correspond to the kind of correction induced by the linear GUP [89, 90], i.e.

$$\hat{H}_{\ell,\mathrm{NR,EM}} \simeq \hat{H}_{0,\mathrm{NR,EM}} - \frac{\xi_3 \ell}{2M} \hat{k}^3_{\mathcal{A}}. \tag{3.47}$$

In other words, this class of models predicts the customary minimal-length contribution at lowest order. Remarkably, those are the models which are least amenable to nonrelativistic tests, roughly going like $v^2/c^2$ (with the speed of the object at hand $v$) with respect to those which are linear in $\hat{k}_{\mathcal{A}}$. Therefore, they are the only ones on the violet side of Fig. 3.1.

- The relative velocity between the reference system and the deformation vector $\mathcal{A}^i$ is a central characteristic of the deformation-induced contributions to the evolution. This is where LIV and DSR diverge in interpretation. While the application of DSR avoids the presence of a preferred frame such that the vector $\mathcal{A}_i$ is probably unobservable,[3] LIV requires a preferred frame. For the moment, we concentrate on the latter. Considering planet earth as the reference as, for example, required to describe table-top experiments, barring cosmic conspiracies, this dependency implies universal seasonal changes to most of the existing observables. Indeed, it is well-known not only that the earth moves relative to the rest frame of the cosmic microwave background at a speed of $\sim 10^{-3}c$ but also that this speed undergoes changes of order 1 along the earth's trajectory. Hence, if the deformation vector $d^\mu$ does not vary along the way exactly such that this effect is continuously cancelled out, amounting to the above-mentioned cosmic conspiracy, we can generally estimate that

$$\mathcal{A} \equiv \sqrt{h^{ij}\mathcal{A}_i\mathcal{A}_j} \geq 10^{-3}c \tag{3.48}$$

[3] While vectors of this kind do arise in DSR, they transform in a special way under the deformed Lorentz transformations such that their orientation with respect to the observer does not change [91]. If the preferred direction, for instance, is to the observer's right, it will be so in every reference frame.

for considerable time-spans during the year. While this speed is nonrelativistic, it results comparably large with respect to the dynamics of ordinary nonrelativistic systems. Therefore, in many relevant cases for phenomenology we can approximate $\hat{k}_{\mathcal{A}} \simeq M\mathcal{A}$. This is particularly interesting because, then, in terms of the kinetic term $\hat{H}_{\text{kin}} = \hat{k}^2/2M$, the correction terms $\hat{H}_n$ assume the form

$$\hat{H}_n = -\xi_n \ell (Mc)^{3-n} \frac{\hat{k}_{\mathcal{A}}^n}{\hat{k}^2} \hat{H}_{\text{kin}} \simeq -\xi_n \ell M^3 c^{3-n} \frac{\mathcal{A}^n}{\hat{k}^2} \hat{H}_{\text{kin}}. \tag{3.49}$$

In comparison to the ordinary kinetic term their contribution becomes larger, the smaller the velocities of the involved particles relative to the given reference system are. This introduces a strong amplifier for macroscopic quantum objects which generally move more slowly. Indeed, on the classical level, we obtain

$$H_n \geq -\xi_n 10^{-3n} \ell M c \left(\frac{c}{v}\right)^2 \hat{H}_{\text{kin}}, \tag{3.50}$$

with the velocity $v$. If $10^{-3n}\ell Mc \sim 10^{-19-3n}$ as, for example for the proton (whose mass is generally compared to the Planck mass also for macroscopic objects, c. f. Appendix A), this factor may soon be overcome by precise experimentation involving small velocities.

In a nutshell, with Eq. (3.43) we have a unifying description of MDRs in the nonrelativistic regime at our disposal, and ranked the underlying MDRs by amenability to nonrelativistic experiments leading up to Fig. 3.1. Furthermore, we have already found a connection to minimal-length models. In the subsequent section, we deepen this connection by translating the corrections into the language of GUPs.

## 3.5 Relation to minimal-length models

As expressed in Eq. (3.43), the nonrelativistic limit of MDRs harbours quantum-gravity inspired deformations of the single-particle Hamiltonian. The kinematics, in turn, is undeformed. Schematically, this structure can be outlined as

$$[\hat{x}^i, \hat{k}_j] = i\delta^i_j, \qquad \hat{H} = \frac{\hat{k}^2}{2M} + V(\hat{x}) + \delta H(\hat{k}). \tag{3.51}$$

In the context of minimal-length theories, this way of displaying the corrections is known as the wave-number representation [92], owing to the fact that the wave number $\hat{k}$ is *defined* to be the conjugate variable to the position. The momentum $\hat{p}$, in turn, is understood to be a function of the wave number. The customary starting point then lies in deforming the Heisenberg algebra (between $\hat{x}^i$ and $\hat{p}_j$), while assuming the Hamiltonian to appear undeformed in the phase-space coordinates underlying that algebra, i.e.

$$[\hat{x}^i, \hat{p}_j] = if^i_j(\hat{p}), \qquad \hat{H} = \frac{\hat{p}^2}{2M} + V(\hat{x}), \tag{3.52}$$

for some tensor-valued function $f^i_j$. As long as the coordinates $\hat{x}^i$ commute,[4] the schemes in Eqs. (3.51) and (3.52) are related by the noncanonical transformation $\hat{k}_i \to \hat{p}_i$, $\hat{x}^i \to \hat{x}^i$. Therefore, as long as the Jacobian $J^i_j = \partial\hat{p}_i/\partial\hat{k}_j = f^i_j$, is nondegenerate, models of the kind given in Eq. (3.51) can be reexpressed as a minimal-length deformation of the Heisenberg algebra with commuting coordinates. Note that this transformation essentially corresponds to a relabelling of momenta. The pair of phase-space variables $(\hat{x}, \hat{p})$, not being of Darboux-type, does not satisfy Hamilton's equations but a generalisation thereof derived from the Heisenberg equation (for the position operator for example $\dot{\hat{x}} = -i[\hat{x}, \hat{H}] \neq \mathrm{d}\hat{H}/\mathrm{d}\hat{p}$). Time-dependent canonical transformations require a modification of the Hamiltonian in order to preserve the structure of Hamilton's equations. As Hamilton's equations can *a priori* not be preserved in the present case, the Hamiltonian stays unmodified under the change $(\hat{x}, \hat{k}) \to (\hat{x}, \hat{p})$ even if the vector field $\mathcal{A}_i$ is time-dependent.

For the deformations we obtained in Eqs. (3.26) and (3.42) (ignoring for the moment the unrelated issues with time-dependent backgrounds), and to first order in $\ell$, we can express the momentum operator as

$$\hat{p}_i = \hat{k}_i - \frac{\ell}{4}\left\{\hat{k}_i - 2M\mathcal{A}_i + \frac{M^2}{2}\left\{\mathcal{A}^2, \frac{\hat{k}_i}{\hat{k}^2}\right\}, \frac{\xi_1(Mc)^2}{\hat{k}_\mathcal{A}} + \xi_2 Mc + \xi_3\hat{k}_\mathcal{A}\right\}, \tag{3.53}$$

where $\mathcal{A}^2 = h^{ij}\mathcal{A}_i\mathcal{A}_j$, to obtain a structure of the kind given in Eq. (3.52). This implies that the canonical commutation relations are deformed as

$$\begin{aligned}
[\hat{x}^i, \hat{p}_j] =& i\delta^i_j\left[1 - \frac{\ell}{4}\left\{1 + \frac{M^2}{2}\left\{\mathcal{A}^2, \hat{p}^{-2}\right\}, \frac{\xi_1(Mc)^2}{\hat{p}_\mathcal{A}} + \xi_2 Mc + \xi_3\hat{p}_\mathcal{A}\right\}\right] \\
&+ \frac{i\ell M^2}{4}\left\{\left\{\frac{\hat{p}^i\hat{p}_j}{\hat{p}^3}, \mathcal{A}^2\right\}, \frac{\xi_1(Mc)^2}{\hat{p}_\mathcal{A}} + \xi_2 Mc + \xi_3\hat{p}_\mathcal{A}\right\} \\
&- \frac{i\ell}{4}\left\{\hat{p}^i_\mathcal{A}\left(-\frac{\xi_1(Mc)^2}{\hat{p}^3_\mathcal{A}} + \frac{\xi_3}{\hat{p}_\mathcal{A}}\right), \hat{p}_j - 2M\mathcal{A}_j + \frac{M^2}{2}\left\{\mathcal{A}^2, \frac{\hat{p}_j}{\hat{p}^2}\right\}\right\},
\end{aligned} \tag{3.54}$$

where we introduced the operator $\hat{p}^\mathcal{A}_i = \hat{p}_i - M\mathcal{A}_i$. As Eq. (3.54) is, admittedly, involved, it is instructive to revert to the isotropic case $\mathcal{A}_i = 0$. As a result, the momentum operator $\hat{p}_i$ can be expressed as

$$\hat{p}_i|_{\mathcal{A}_i=0} = \hat{k}_i\left[1 - \frac{\ell}{2}\left(\frac{\xi_1(Mc)^2}{\hat{k}} + \xi_2 Mc + \xi_3\hat{k}\right)\right]. \tag{3.55}$$

[4]The commutator of the coordinates is exactly specified by a Jacobi identity given a function $f^i_j$, see [71] for more details.

By analogy with Eq. (3.54), the Heisenberg algebra is deformed as

$$[\hat{x}^i, \hat{p}_j] = i\left[1 - \frac{\ell}{2}\left(\frac{\xi_1(Mc)^2}{\hat{p}} + \xi_2 Mc + \xi_3\hat{p}\right)\right]\delta^i_j - \frac{i\ell}{2}\left(\frac{\xi_1(Mc)^2}{\hat{p}^3} + \frac{\xi_3}{\hat{p}}\right)\hat{p}^i\hat{p}_j. \tag{3.56}$$

In the context of the literature on minimal-length models the deformed Heisenberg algebra given in Eq. (3.54) as well as its simplified version (Eq. (3.56)) are unusual in several aspects. A number of comments are in order.

- The appearance of $\mathcal{A}_i$ in Eq. (3.54) indicates a degree of anisotropy in the model induced by the external vector $d^\mu$. Anisotropic minimal-length models, while having been considered recently [93, 94], are rather uncommon. As highlighted in in the reasoning leading up to Eq. (3.91), in LIV the vector $\mathcal{A}_i$ is expected to undergo seasonal changes (and therefore be time-dependent) by a magnitude of the order $10^{-3}c$ which amounts to a large velocity in comparison to conventional nonrelativistic dynamics. Yet, if the model is complemented by deformed Lorentz-transformations under which it is symmetric, the nonrelativistic model is expected to inherit a symmetry under a deformation of rotations so that the anisotropy may only be apparent, see e. g. [95].

- For nonvanishing $\mathcal{A}_i$, but also for isotropic models with nonvanishing $\xi_1$, the deformed Heisenberg algebra contains inverse powers of the momentum operator. Considering, for simplicity, $\mathcal{A}_i = \xi_2 = \xi_3 = 0$, we have

$$[\hat{x}^i, \hat{p}_j] = i\left[1 - \frac{\xi_1\ell(Mc)^2}{2\hat{p}}\right]\delta^i_j + \frac{i\ell\xi_1(Mc)^2}{2\hat{p}}\frac{\hat{p}^i\hat{p}_j}{p^2}. \tag{3.57}$$

  Both correction terms in this case go like $\hat{p}^{-1}$. This implies that the models do not reduce to ordinary quantum mechanics in the small-momentum limit, i.e. $\lim_{\hat{p}_i\to 0}[\hat{x}^i, \hat{p}_j] \neq i\delta^i_j$. As the commutator of positions and momenta exactly equals the Jacobi matrix, this implies that the noncanonical transformation $\hat{x}^i \to \hat{x}^i$, $\hat{k}_i \to \hat{p}_i$ is degenerate at this point. In other words, our perturbative expansion in $\ell$ breaks down because the correction to the nonrelativistic Hamiltonian, Eq. (3.43), becomes larger than the kinetic term – note that this is not an issue at the relativistic level where the dispersion relation additionally contains the rest mass (c. f. Eq. (3.45)). In minimal-length model building the appearance of inverse powers of $\hat{p}$ is usually avoided due to the technical and conceptual issues nontrivial IR effects entail. However, these problems do not indicate that the model is wrong *per se*. As mentioned in the preceding section, this effect may just be the result of UV/IR-mixing (see [96, 97]) in low-energy quantum gravity phenomenology (c. f. Sec. of [6] and [84]).

- Customary minimal-length models correspond to the sector $\mathcal{A}_i = \xi_1 = \xi_2 = 0$ of the full parameter space, thus deriving from MDRs of the kind

$$M^2c^4 = E^2 - k^2c^2 - \xi_3\ell c^2k^3, \tag{3.58}$$

and can be turned into the deformed Heisenberg algebra

$$[\hat{x}^i, \hat{p}_j] = i\left[1 - \frac{\xi_3\ell\hat{p}}{2}\right]\delta^i_j - \frac{i\ell\xi_3\hat{p}}{2}\frac{\hat{p}^i\hat{p}_j}{p^2}, \tag{3.59}$$

which is equivalent to the first-order approximation of the linear and quadratic GUP [89] with model parameter $\alpha = 2\xi_3$. Similarly, the quadratic GUP, involving commutative coordinates, at second order in $\ell$ assumes the form

$$[\hat{x}^i, \hat{p}_j] \simeq i\left[(1 + \beta\ell^2\hat{p}^2)\delta^i_j + 2\beta\hat{p}^i\hat{p}_j\right], \tag{3.60}$$

with the dimensionless quadratic GUP-parameter $\beta$. These results have two consequences.

First, it is noteworthy that all existing constraints on minimal-length models can be readily employed to constrain the parameter $\xi_3 = a_{0,0,3}$ and vice versa. The reciprocal transfer of information between minimal-length models and MDRs imposes rather stringent limitations on the linear GUP-parameter $\alpha$ (and, by extension, on its quadratic counterpart $\beta$). Notably, time-delay measurements, for instance of the gamma-ray burst GRB 190114C [98], the blazar PKS 2155-304 [99], and the Crab pulsar [100] yield constraints on the order of magnitude

$$\alpha < \mathcal{O}(1) \quad \text{and} \quad \beta < \mathcal{O}(10^{16}). \tag{3.61}$$

Consequently, these findings establish stringent bounds on the linear GUP reaching up to the Planck scale, while also improving upon previous constraints for the quadratic GUP by approximately 17 orders of magnitude.[5]

Second, there is a clear sense in which the MDRs given in Eq. (2.3) are more general than conventional minimal-length models.

- As the relation to minimal-length models is instantiated by a redefinition of the momentum phase-space variable, the underlying coordinates are forced to commute. This continues to be the case on the nonperturbative level. General isotropic[6] minimal-length models encompass noncommutative geometries. Hence, in a certain sense, minimal-length models are also more general than MDRs.

[5]Previously, scanning tunnelling microscope experiments [8, 101] had provided the most stringent constraints of $\beta < 10^{33}$ in this context (see [67] for an up-to-date collection of bounds).

[6]Here we only consider isotropic models for clarity. The underlying reasoning could be straightforwardly generalised to anisotropic ones.

The link between minimal-length models and MDRs offers notable advantages by enabling the transfer of constraints from the latter to the former. However, it is worth emphasising that nonrelativistic considerations can also contribute to enhancing the constraints on MDRs. This aspect is exemplified in the subsequent subsection.

## 3.6 Applications

A phenomenological model is considered incomplete if it does not yield reasonably testable predictions concerning observable phenomena. The following analysis examines the implications of the deformations proposed in Eq. (3.43).

### 3.6.1 Harmonic Oscillator

In flat spacetime, there exists a foliation where $N = 1$, $N^i = 0$, and $h_{ij} = \delta_{ij}$. Therefore, we straightforwardly obtain the deformed flat-space Schrödinger equation

$$i\partial_0\psi = \left[-\frac{\Delta_0}{2M} + e\phi_e - \frac{\ell}{2M}\sum_{n=1}^{3}\xi_n(Mc)^{3-n}(-\Delta_{\mathcal{A}})^{n/2}\right]\psi, \tag{3.62}$$

with the $\mathcal{A}$-deformed gauge-covariant flat-space Laplacian $\Delta_{0,\mathcal{A}}$[7]. In Cartesian coordinates, this differential operator can be expressed as

$$\Delta_{0,\mathcal{A}} = \delta^{ij}\left(\partial_i - ieA_i^e - iM\mathcal{A}_i\right)\left(\partial_j - ieA_i^e - iM\mathcal{A}_j\right). \tag{3.63}$$

The ordinary gauge-covariant Laplacian $\Delta_0$ can be derived using the following relation as $\Delta_0 = \Delta_{0,\mathcal{A}}|_{\mathcal{A}_i=0}$. Furthermore, in flat space, we can translate the deformed Schrödinger equation into the momentum representation

$$i\partial_0\tilde{\psi} = \left[-\frac{k^2}{2M} + e\phi_e(i\dot{\partial}^i) - \frac{\ell}{2M}\sum_{n=1}^{3}\xi_n(Mc)^{3-n}k_{\mathcal{A}}^n\right]\tilde{\psi}, \tag{3.64}$$

with the momentum-derivative $\dot{\partial}^i = \partial/\partial k_i$. The shift to the momentum-representation removes the intricacies of fractional powers of differential operators. The ensuing corrections are universal in the same way that GUP-corrections are [101]. This allows for a plethora of different applications to table-top experiments.

Among others, in the context of minimal-length models, for example, there have been constraints from implementations of Planck-scale corrections to the harmonic oscillator [102, 103, 104, 90], the hydrogen atom [105, 106, 107, 108, 109], the scanning tunnelling microscope [8, 101], the $\mu$ anomalous magnetic moment [110, 101], the Landau levels

[7]We decompose the operator as $\Delta_{0,\mathcal{A}} = \Delta_0 + \Delta_{\mathcal{A}}$, where $\Delta_0$ denotes the ordinary gauge-covariant Laplacian and $\Delta_{\mathcal{A}}$ encodes the contributions proportional to $\mathcal{A}_i$.

[90, 101, 111] (c. f. Sec. 3.6.3), the lamb shift [101, 90], $^{87}$Rb interferometry [112, 113], the Kratzer potential [114], stimulated emission [115], quantum noise [116] and the Tsirel'son bound [117]. A wide range of examples, including those mentioned above and many others, can be explored within the broader framework of MDR-induced deformations.

Here, we will content ourselves with corrections to energy eigenvalues of the isotropic harmonic oscillator under the assumption that $\mathcal{A}_i = 0$, thus outlining a procedure for general analyses into central potentials for isotropic Lorentz-violation. At the unperturbed level, and in spherical coordinates, the isotropic harmonic oscillator allows for the stationary states [118]

$$\tilde{\psi}_{nlm} = R_{nl}(k) Y_l^m(\theta, \phi), \tag{3.65}$$

with the spherical harmonics $Y_l^m$ and the radial component

$$R_{nl}(k) = N_{nl} k^l L_{\frac{n-l}{2}}^{l+\frac{1}{2}} \left(\frac{k^2}{M\omega}\right) e^{-\frac{k^2}{2M\omega}}. \tag{3.66}$$

Here, we introduced the normalisation factor

$$N_{nl} = 2\sqrt{\frac{2^{\frac{n+l}{2}} (M\omega)^{-\frac{3}{2}-l} (\frac{n-l}{2})!}{\sqrt{\pi}(n+l+1)!!}}. \tag{3.67}$$

Moreover, $\omega$ and $L_n^a(x)$ stand for the oscillation frequency and the generalised Laguerre polynomials, respectively. The integers $(n, l, m)$, where $n \geq 0$, $l = \mod (n, 2), \mod (n, 2) + 2, \dots n$, $-l \leq m \leq l$, denote the quantum numbers, in terms of which the unperturbed eigenenergies read

$$E_n = \omega \left(n + \frac{3}{2}\right). \tag{3.68}$$

Applying time-independent perturbation theory [119], the corrections to the eigenvalues can be obtained as

$$\Delta E_{nl} = -\frac{\ell}{2M} \sum_{o=1}^{3} \xi_o (Mc)^{3-o} \langle \psi_{nlm} | \hat{k}^o \psi_{nlm} \rangle. \tag{3.69}$$

Thus, we have to calculate the expectation value of powers of $\hat{k}$, which effectively comes down to evaluating a momentum-space integral in spherical coordinates. The angular integration is trivial, such that the expectation value simplifies to

$$\langle \hat{k}^o \rangle = N_{nl}^2 \int_0^\infty \mathrm{d}k k^{o+2} R_{nl}^2(k). \tag{3.70}$$

Indeed, this kind of expression for corrections to the spectrum of the Hamiltonian is generic for every central potential. In this specific case, the integral is over polynomials multiplying a Gaussian akin to moments of a normal distribution. Thus, introducing the dimensionless $\bar{k} = k/\sqrt{M\omega}$, we can solve the integral in all generality with the help of an analogue to a source $J$ such that

$$\langle \hat{k}^o \rangle = (M\omega)^{\frac{3+2l+o}{2}} N_{nl}^2 \lim_{J\to 0} \frac{\partial^{o+2l+2}}{\partial J^{o+2l+2}} \left[ L_{\frac{n-l}{2}}^{\frac{1}{2}+l}\left(\frac{\partial^2}{\partial J^2}\right)\right]^2 \int_0^\infty \mathrm{d}\bar{k} e^{-\bar{k}^2+J\bar{k}}, \tag{3.71}$$

$$= (M\omega)^{\frac{o}{2}} \frac{2^{\frac{2+n+l}{2}}\left(\frac{n-l}{2}\right)!}{(n+l+1)!!} \lim_{J\to 0} \frac{\partial^{o+2l+2}}{\partial J^{o+2l+2}} \left[ L_{\frac{n-l}{2}}^{\frac{1}{2}+l}\left(\frac{\partial^2}{\partial J^2}\right)\right]^2 e^{\frac{J^2}{4}}\left[1+\mathrm{Erf}\left(\frac{J}{2}\right)\right], \tag{3.72}$$

with the error function $\mathrm{Erf}(x)$. The generalised Laguerre polynomials have the closed-form expression

$$L_n^\alpha(x) = \sum_{n'=0}^{n} (-1)^{n'} \binom{\alpha+n}{n-n'} \frac{x^{n'}}{n'!}, \tag{3.73}$$

with the binomial coefficient $\binom{m}{n}$. Furthermore, derivatives of the generating function can be obtained in general, yielding

$$\lim_{J\to 0} \frac{\partial^o}{\partial J^o} e^{\frac{J^2}{4}}\left[1+\mathrm{Erf}\left(\frac{J}{2}\right)\right] = \Gamma\left(\frac{o+1}{2}\right). \tag{3.74}$$

As as result, we can express the expectation value of powers of the momentum as

$$\langle \hat{k}^o \rangle = (M\omega)^{\frac{o}{2}} \frac{2^{\frac{2+n+l}{2}}\left(\frac{n-l}{2}\right)!}{(n+l+1)!!} \sum_{n',n''=0}^{\frac{n-l}{2}} (-1)^{n'+n''} \binom{\frac{n+l+1}{2}}{\frac{n-l-n'}{2}} \binom{\frac{n+l+1}{2}}{\frac{n-l-2n''}{2}} \frac{\Gamma\left[\frac{3+o+2(l+n'+n'')}{2}\right]}{n'!n''!}. \tag{3.75}$$

Note that $n-l$ is an even number such that the sum is well-defined. For the MDRs associated with $\xi_2$, this expression simplifies significantly. In fact, it is possible to provide a closed-form expression even in the case of nonvanishing, but constant $\mathcal{A}_i$ such that

$$\Delta E_n|_{\xi_1=\xi_3=0} = -\frac{\xi_2}{2}(Mc)\ell\left[M\mathcal{A}^2+\omega\left(n+\frac{3}{2}\right)\right] = -\frac{\xi_2}{2}(Mc)\ell\left[M\mathcal{A}^2+E_n\right]. \tag{3.76}$$

Here, the corrections introduced by nonvanishing $\mathcal{A}_i$ are constant, and can therefore be absorbed into a redefinition of the zero-point energy.

The harmonic oscillator holds significance beyond its pedagogical value. In recent years, considerable research has focused on investigating the potential of macroscopic harmonic oscillators as a means to examine minimal-length deformations [8, 120, 121]. Notably, in [120], bounds on the quadratic GUP-parameter $\beta$ were derived through such investigations. It is important to note that these analyses did not incorporate the necessary rescaling of the minimal length for compounds provided in Eq. (A.4). Taking into account this rescaling, the ensuing constraint becomes

$$\beta < \mathcal{O}(10^{48}), \tag{3.77}$$

bearing testament to the elusiveness of minimal-length deformations in the nonrelativistic regime. In order to shed light on the potential implications of quantum gravity phenomenology at low energies, we aim to establish a preliminary estimate of how the obtained results could be translated into constraints on the various MDR-parameters $\xi_n$. To accomplish this, we begin by deriving an approximate bound on the linear GUP-parameter $\alpha$, which, as discussed in Section 3.5, essentially corresponds to $\xi_3$. Subsequently, we proceed to approximate the resulting constraints on $\xi_1$ and $\xi_2$. We stress that these considerations cannot replace a full phenomenological derivation of the effect.

On the level of order-of-magnitude estimates, the linear and the quadratic GUP imply perturbative corrections $\Delta_{\text{GUP}}O$ to the predicted value of any observable $O$ which go like

$$(\Delta O)_{\text{GUP}} \sim O\alpha\ell\bar{k} \quad \text{and} \quad (\Delta O)_{\text{GUP}} \sim O\beta\left(\ell\bar{k}\right)^2, \tag{3.78}$$

respectively, with some momentum scale $\bar{k}$. If this observable has been measured to a relative precision $\delta O = \Delta O/O$, and no deviation from the case $\ell = 0$ has been detected, the model parameters can be constrained as

$$\alpha \sim \frac{\delta O}{\ell\bar{k}} \quad \text{and} \quad \beta \sim \frac{\delta O}{\left(\ell\bar{k}\right)^2}. \tag{3.79}$$

Above, we have provided an upper bound to the quadratic GUP of the form $\beta \leq \beta_0$. By virtue of Eq. (3.79), such a bound can be roughly translated to the linear GUP as

$$\alpha \leq \sqrt{\beta_0 \delta O}. \tag{3.80}$$

In [120], the observable in question is given by the frequency $\omega$ which is measured to a relative precision of $\delta\omega \sim 10^{-7}$, thus leading to a bound

$$\alpha \leq 10^{21}. \tag{3.81}$$

Bounds on the other MDR-parameters can be obtained considering that we can estimate $\langle p^\sigma \rangle \sim (Mv)^\sigma$, with the velocity $v \sim \bar{A}\omega$, and the maximal amplitude $\bar{A}$. From this consideration, we infer that bounds on $\xi_3$ may be roughly translatable to the other MDRs by the recipe

$$\alpha \sim \xi_3 \sim \frac{c}{v}\xi_2 \sim \left(\frac{c}{v}\right)^2 \xi_1. \tag{3.82}$$

As expected, we see an enhancement of the effect for other MDRs. For instance, in [120], the considered oscillator moves at a velocity $v \sim 10^{-11}c$. Thus, our preliminary considerations indicate that we may obtain bounds of the orders of magnitude

$$\xi_1 \leq \mathcal{O}(10^{-1}), \qquad \xi_2 \leq \mathcal{O}(10^{10}), \qquad \xi_3 = \mathcal{O}(10^{21}). \tag{3.83}$$

Thus, even though the input constraint in Eq. (3.77) appears to be far below the Planck scale, it could actually rule out those MDRs associated with the parameter $\xi_1$. We find a clear indication that nonrelativistic experiments are more than competitive in some areas of quantum gravity phenomenology.

### 3.6.2 Equivalence Principle

We now investigate the impact of MDR-induced corrections on the Weak Equivalence Principle (WEP). For simplicity, we assume that the corrections are isotropic, in other words, $\mathcal{A}_i = 0$, and that electromagnetic interactions are negligible ($A^e_i = \phi_e = 0$).

Near the surface of a very massive body, the gravitational potential can be approximated as $\phi = gz$, where $g$ is the gravitational acceleration. From Eq. (3.43), the corresponding Hamiltonian reads:

$$\hat{H}_{\ell,\mathrm{NR,N}} = \frac{\hat{p}^2}{2M_I} + Mgz - \frac{\ell}{2}\left(\xi_1 \hat{p} M c^2 + \xi_3 \frac{\hat{p}^3}{M}\right), \tag{3.84}$$

where the deformed inertial mass is defined as

$$M_I \equiv \frac{M}{1 - \xi_2 \ell M c} \simeq M\left(1 + \xi_2 \ell M c\right). \tag{3.85}$$

The corresponding Heisenberg equations of motion are:

$$M_I \dot{\hat{x}}^i = \hat{p}^i \left[1 - \frac{\ell M_I}{2}\left(\frac{\xi_1 M c^2}{\hat{p}} + 3\frac{\xi_3 \hat{p}}{M}\right)\right], \qquad \dot{\hat{p}}_i = -Mg\delta_{iz}. \tag{3.86}$$

Assuming the particle starts from rest at time $t = 0$, the expectation value of the absolute acceleration, $a = \langle|\ddot{\hat{x}}^i|\rangle$, becomes:

$$M_I a = \left(1 - 3\xi_3 \ell g M_I t\right) Mg \equiv M_g(t) g, \tag{3.87}$$

where the last equality defines a time-dependent effective gravitational mass $M_g$.

This result clearly demonstrates that the Weak Equivalence Principle, one of the most stringently tested principles in physics, is violated under Planck-scale corrections induced by MDRs.

The violation of the Weak Equivalence Principle (WEP) can be quantified via the **Eötvös** parameter, $\eta(A, B)$, for two freely falling bodies $A$ and $B$:

$$\eta(A,B) = 2\left\langle \frac{\dfrac{M_{\mathrm{g},A}}{M_{\mathrm{I},A}} - \dfrac{M_{\mathrm{g},B}}{M_{\mathrm{I},B}}}{\dfrac{M_{\mathrm{g},A}}{M_{\mathrm{I},A}} + \dfrac{M_{\mathrm{g},B}}{M_{\mathrm{I},B}}} \right\rangle \simeq c\ell(M_B - M_A)\left(\xi_2 + \xi_3 \beta_{\mathrm{rel}}\right), \tag{3.88}$$

where $\beta_{\rm rel} \simeq gt/c$ is the ratio of the test mass velocity to the speed of light.

The MICROSCOPE collaboration has placed the most stringent bound on the Eötvös parameter to date:

$$|\eta| < 10^{-14}. \tag{3.89}$$

Future experiments are expected to improve this limit by at least one additional order of magnitude.

Notably, MICROSCOPE involves macroscopic test masses. To account for the suppression of quantum-gravity effects with the increasing number of elementary constituents $\mathcal{N}$, we rescale the minimal length as $\ell \to \ell/\mathcal{N}$. Under this assumption, the Eötvös parameter becomes:

$$\eta(A,B) = \frac{c\ell}{\mathcal{N}}(M_{{\rm g},B} - M_{{\rm g},A})\left(\xi_1 \frac{c}{\mathcal{A}} + \xi_2 + \xi_3 \mathcal{A}\right), \tag{3.90}$$

where

$$\mathcal{A} \equiv \sqrt{h^{ij}\mathcal{A}_i\mathcal{A}_j} \gtrsim 10^{-3}c \tag{3.91}$$

is a lower bound for the center-of-mass velocity of the constituents.

Considering MICROSCOPE operates with mass differences of order $\sim 1\,\mathrm{kg}$ and a maximal relative velocity resolution of $\Delta\beta_{\rm rel} \sim 10^{-17}$, the resulting bounds are:

$$|\xi_2| \leq \mathcal{O}(10^4), \qquad |\xi_3| \leq \mathcal{O}(10^{21}). \tag{3.92}$$

Thus, MDRs associated with $\xi_2$ are constrained to energy scales up to three orders of magnitude below the Planck scale, while constraints on GUP-like MDRs (associated with $\xi_3$) remain relatively weak.

The suppression with increasing $\mathcal{N}$ can be circumvented by employing microscopic systems. For single atoms ($\mathcal{N} \sim 1$), the best constraints to date yield $|\eta| \leq \mathcal{O}(10^{-12})$ with velocities up to $v \sim 10^{-7}c$. This leads to the bounds:

$$|\xi_2| \leq \mathcal{O}(10^8), \qquad |\xi_3| \leq \mathcal{O}(10^{15}). \tag{3.93}$$

Interestingly, the constraint on $\xi_2$ is weaker than the macroscopic bound, while the bound on $\xi_3$ is significantly improved. This discrepancy arises from the higher velocities achieved in atomic interferometry compared to macroscopic setups.

### 3.6.3 Landau Levels

First, to facilitate a detailed analysis of the deformed dynamics described by Eq. (3.43), we make a number of simplifying assumptions. Specifically, we assume that the electric and gravitational potentials ($\phi$ and $\phi_{\rm g}$) vanish, and the Lorentz-violation is aligned along the global time-direction ($\mathcal{A}_i = 0$). With these assumptions in place, the corrections in the dynamics depend solely on the undeformed Hamiltonian. In other words, we obtain

$$\hat{H}_{\ell,\mathrm{NR,EM}} = \hat{H}_{0,\mathrm{NR,EM}} - \frac{\ell}{2M}\sum_{n=1}^{3}\xi_n (Mc)^{3-n}(2M\hat{H}_{0,\mathrm{NR,EM}})^{n/2}. \tag{3.94}$$

It is reasonable to expect that this property continues to hold at the nonperturbative level.[8] Consequently, stationary states remain unmodified. Since $\hat{H}_{\ell,\mathrm{NR,EM}} = \hat{H}_{\ell,\mathrm{NR,EM}}(\hat{H}_{0,\mathrm{NR,EM}})$, it is evident that the eigenstates of $\hat{H}_{0,\mathrm{NR,EM}}$ are identical to the eigenstates of $\hat{H}_{0,\mathrm{NR,EM}}$. Yet, their eigenenergies are modified as

$$\begin{aligned} E_{\ell,k_i} &= E_{0,k_i} - \frac{\ell}{2M}\sum_{n=1}^{3}\xi_n (Mc)^{3-n}(2ME_{0,k_i})^{n/2} \\ &= E_{0,k_i} - \frac{\ell}{2M}\sum_{n=1}^{3}\xi_n c^{3-n} M^{3-\frac{n}{2}}(2E_{0,k_i})^{n/2}, \end{aligned} \tag{3.95}$$

with the eigenvalue of the unperturbed Hamiltonian $E_{0,k_i}$, which depends on some possibly discrete variable $k_i$, the eigenvalue of the momentum operator. Note that this modification of the energy can, in general, not be absorbed into a redefinition of the time parameter because this redefinition would be dependent on the mass of the particle at hand. Once we consider particles of different masses, the correction reappears. Curiously, an energy dependence of physical "constants" may be possible in the rainbow-gravity approach [122].

As an illustrative example, we consider the configuration of a particle with charge $-|e|$ in a spacetime endowed with a static electric or magnetic field. Specifically, we can examine the scenario of a cosmic string coupled to an axial magnetic field [123, 124]. In cylindrical coordinates, the line element is given by

$$\mathrm{d}s^2 = -\mathrm{d}t^2 + \mathrm{d}\rho^2 + \alpha^2\rho^2\mathrm{d}\phi^2 + \mathrm{d}z^2\,, \tag{3.96}$$

where $\alpha \leq 1$ measures the angular deficit of this string, which defines a spacetime with conical structure. The vector potential that furnishes a magnetic field $\vec{B} = \vec{\nabla}\times\vec{A}$ with constant norm $h_{ij}B^iB^j = B^2$, defined just in the $z$-direction, has only one non-zero component $A_\phi(\rho) = B\rho/(2\alpha)$. The energy levels of this system are characterised by the discrete and continuous variables $k_i = (n, l, k_z)$, where $n \in \mathbb{N}$ represents the radial, $l \in \mathbb{Z}$ the angular and $k_z \in \mathbb{R}$ the $z$-component of the momentum. For a detailed derivation of the solution and the corresponding energy levels in the Minkowski case, we refer the reader to [125], and for the cosmic string correction to [124] from which we recover the energy levels

$$E_{0,(n,l,k_z)} = \frac{\hbar\omega_B}{2\alpha}\left(2n + \frac{|l|}{\alpha} - \frac{l}{\alpha} + 1\right) + \frac{\hbar^2k_z^2}{2M}\,, \tag{3.97}$$

[8] Here, the term "nonperturbative" refers to expansions in both $\ell$ and $1/c$.

where $\omega_B = |e|B/Mc$ is the cyclotron frequency of the configuration. Plugging this expression into Eq. (3.95) implies the shifted energy levels

$$E_{\ell,(n,l,k_z))} = E_{0,(n,l,k_z)} - \frac{\ell}{2M} \sum_{n'=1}^{3} \xi_{n'} c^{3-n'} M^{3-\frac{n'}{2}} (2E_{0,(n,l,k_z)})^{n'/2}. \tag{3.98}$$

The variable $k_i$ is of broader utility in the enumeration of stationary states, allowing for the expression of a general state at $t = 0$, denoted as $\psi(0)$, as follows

$$\psi(0) = \sum\!\!\!\!\!\!\!\int_{k_i} a_{k_i} \psi_{k_i}(0), \tag{3.99}$$

where the sum (integral) is over the discrete (continuous) enumerator $k_i$, and the coefficients $a_{k_i}$ are chosen such that $\sum\!\!\!\!\!\!\int_{k_i} |a_{k_i}|^2 = 1$. Then, the corresponding time evolved state (at $t = \Delta t$) becomes

$$\psi(\Delta t) = \sum\!\!\!\!\!\!\!\int_{k_i} e^{iE_{\ell,k_i}\Delta t} a_{\mathcal{P}} \psi_{k_i}(0). \tag{3.100}$$

As a result, these corrections introduce additional relative phases between stationary states during time evolution, which makes them suitable for exploration through interferometric table-top experiments. In this vein, the duration of the time evolution $\Delta t$ can be used as amplifier for the effect.

## 3.7 Discussion

Modified dispersion relations are prominent candidates for low-energy signatures of quantum gravity. Recent advances in measurement precision and quantum state control now make the nonrelativistic quantum regime a viable testing ground, not just high-energy experiments beyond the LHC scale. As emphasised in [6], experimental amplifiers include not only energy but also gains in precision, statistics, coherence time, and entangled particle numbers.

To systematically explore this regime, we have developed a $1/c$ expansion for MDR-inspired dynamics at first order in the Planck length . Our approach is model-agnostic, encompassing all analytic MDRs permitted at this order. We employed two complementary derivations to ensure

(i) a classical nonrelativistic limit followed by canonical quantisation,

(ii) a WKB-type reduction of a deformed Klein–Gordon equation describing the single-particle sector of a bosonic field theory.

The results from both methods agree for backgrounds with non-evolving induced geometries on spatial hypersurfaces. Although subtleties arise for general time-dependent backgrounds, these are not specific to MDRs and do not affect the core formalism.

An important result is the clarification of the relationship between modified dispersion relations (MDRs) and minimal-length models. As previously noted [80], generalized uncertainty principles (GUPs) with commutative geometry constitute a specific subset of MDRs, characterized by the weakest nonrelativistic signatures, which are further suppressed by factors of $1/c$. Constraints from high-energy astrophysical time-delay observations yield $\alpha \lesssim \mathcal{O}(1)$ for the linear GUP [89] and $\beta \lesssim \mathcal{O}(10^{16})$ for the quadratic GUP [37]. Consequently, the linear GUP is excluded up to the Planck scale, and the improved bound on the quadratic GUP strengthens previous limits by 17 orders of magnitude.

The formalism has been applied to several physical configurations:

- **Landau levels** in static spacetimes, where we found formulas for the corrections.
- **Flat-space quantum systems**, like the harmonic oscillator, show that some MDRs could be limited up to the Planck scale by table-top experiments.
- We found changes to the Schrödinger equation in a Newtonian potential. The resulting **weak equivalence principle violations** produce limits up to one order of magnitude below the Planck scale for some MDRs, while models tied to the bicrossproduct basis of deformed special relativity [85] are limited to scales of about $10^{15}$ GeV.

These results affirm that nonrelativistic experiments are competitive in quantum gravity phenomenology, extending the scope beyond approaches based exclusively on quantum superpositions [126, 127].

A conceptual distinction emerges between UV and IR signatures. In the far UV ($E \simeq kc$), high-energy behaviors in different models become nearly identical. For example, the $\kappa$-Poincaré bicrossproduct basis [85] and certain Lorentz invariance violating scenarios [86] show similar predictions, leading to model degeneracy. In contrast, IR ($E \simeq Mc^2$) signatures are distinct. Only $Ek^2$-type MDRs induce sizeable weak equivalence principle violations, highlighting the unique sensitivity of the low-energy regime.

MDRs exhibit a rich phenomenology in the IR that has yet to be explored. In contrast, the GUP, whose nonrelativistic effects have been extensively studied over the past 30 years, is most observable in the UV, not the IR. MDRs that produce significant effects in the nonrelativistic regime warrant further investigation.

Among the deformations arising from nonrelativistic dynamics, one case in particular is that in which the corrections involve non-integer powers of momentum. Chapter 4 explores this special regime, showing how certain MDRs naturally lead to an effective dynamics described by fractional quantum mechanics.

# CHAPTER 4

# Fractional Infrared Dynamics

In chapter 3, it was shown that corrections arising from modified dispersion relations motivated by quantum gravity induce systematic deformations of quantum dynamics in the nonrelativistic limit. Such deformations appear as additional contributions to the effective Hamiltonian, whose dependence on momentum can depart significantly from the usual quadratic kinematics. Notably, in certain scenarios, these corrections involve non-integer powers of the momentum, which, upon quantization, give rise to nonlocal differential operators [12].

This chapter explores the physical and conceptual consequences of these structures, with special emphasis on an infrared regime in which the deformed terms may dominate over the standard quadratic kinetic contribution to the effective dynamics. We show that, in this context, the deformed Schrödinger equation can be reinterpreted, at the level of the effective dynamics, within the formalism of fractional quantum mechanics, thereby establishing a direct connection between quantum gravity phenomenology and nonlocal quantum dynamics. This regime, which we refer to as the deep infrared regime, exhibits properties qualitatively analogous to those associated with effective dimensional reduction, commonly discussed in the ultraviolet sector of quantum gravity.

We discuss the origin of fractional operators from modified dispersion relations, the physical motivation for corrections involving fractional powers of the Planck scale, and possible experimental implications, as well as analogue models that capture the essential features of this dynamics.

## 4.1 Fractional Operators from MDRs

We begin by considering the general structure of modified dispersion relations motivated by quantum gravity, along with their nonrelativistic limit. As discussed in Chapter 3, such relations describe Planck-scale suppressed corrections to the standard relativistic dispersion relation, encoding effective interactions between matter degrees of freedom and an underlying quantum geometry. A general form of modified dispersion relation with corrections linear in the inverse Planck momentum can be written as [128]

$$M^2c^2 = \left(\frac{E}{c}\right)^2 - p^2 - p_{\mathrm{P}}^{-1} \sum_{n=0}^{2} \sum_{m=0}^{3-n} a_{n,m,3-n-m} (Mc)^n p^m \left(\frac{E}{c}\right)^{3-n-m}, \tag{4.1}$$

where $M$ is the particle mass, $E$ its energy, and $p$ its momentum. This expression encompasses a broad class of phenomenological models relevant for both high- and low-energy probes.

Such modifications are not merely phenomenological artifacts, but arise naturally in the semiclassical limit of several quantum gravity frameworks, including deformations of relativistic symmetries and curved momentum space scenarios [129, 130, 131, 132, 133]. From an experimental standpoint, contributions beyond the first order in the inverse Planck scale are typically subleading, as current tests do not reach sufficient sensitivity to probe higher-order corrections [6, 16, 134].

Taking the nonrelativistic limit of Eq. (4.1), the dominant contributions reduce to momentum-dependent corrections to the Galilean dispersion relation. A generic effective expression for the energy in this regime can be written as [128]

$$E = \frac{p^2}{2M} + \frac{p_{\mathrm{P}}^{-1}}{2M} \sum_{n=1}^{3} \xi_n (Mc)^{3-n} p^n, \tag{4.2}$$

where the dimensionless coefficients $\xi_n$ are linear combinations of the parameters appearing in Eq. (4.1). While the specific values of these coefficients depend on the underlying model, their qualitative role is to control deviations from the standard quadratic kinetic term.

Upon canonical quantization, the momentum-dependent corrections in Eq. (5.2) lead to modifications of the Schrödinger equation involving higher-order and, in certain cases, non-integer powers of the Laplacian operator $\Delta$ [128]. In particular, terms proportional to $p^\alpha$ in the dispersion relation give rise to operators of the form $(-\Delta)^{\alpha/2}$, introducing intrinsically nonlocal contributions to the effective quantum dynamics.

This observation provides the starting point for the analysis developed in the remainder of this chapter. Rather than focusing on specific bounds for the MDR parameters, we emphasize how such momentum-dependent corrections naturally motivate a description of the effective dynamics in terms of fractional quantum mechanics, especially in regimes where non-quadratic contributions dominate.

## 4.2 Fractional Powers of Planck-Scale Corrections from Fractal Black Holes

Many approaches to quantum gravity predict corrections to physical observables that scale with integer powers of the Planck length or energy. However, there exist physically motivated scenarios in which quantum-gravity effects give rise to corrections involving fractional powers of the Planck scale. Such behavior has been suggested, for instance, in studies of quantum fluctuations of black hole horizons, where fluctuations of the horizon radius may scale as $\ell_{\mathrm{P}}^{2/3}$ [135] or $\sqrt{\ell_{\mathrm{P}}}$ [136]. These results point toward an effective fractal structure of the horizon geometry, indicating that quantum gravity may modify the effective dimensionality of spacetime at very small scales.

Building on these considerations, Barrow introduced a generalized entropy–area relation in which black hole entropy is associated with a fractal horizon [137]. Within this framework, the entropy is given by

$$S_{\mathrm{frac}} \propto \left(\frac{A}{4\ell_{\mathrm{P}}^2}\right)^{d/2}, \tag{4.3}$$

where $A$ is the horizon area and $d \geq 2$ is an effective, generally non-integer, fractal dimension. The standard Bekenstein-Hawking result is recovered for $d = 2$, while deviations from this value encode possible quantum-gravity corrections to the microscopic structure of the horizon.

The connection between modified black hole thermodynamics and modified dispersion relations, or equivalently generalized uncertainty principles, has been extensively explored in the literature [138, 139, 140]. Within this context, it has been shown that generalized entropy–area relations can be consistently associated with dispersion relations involving fractional powers of the momentum. In particular, dispersion relations of the form

$$E \propto p^{d-1}, \tag{4.4}$$

lead to temperature–mass relations that reproduce the fractal entropy scaling above when applied to Hawking radiation arguments.

From the perspective of quantum gravity phenomenology, these results provide a concrete physical motivation for considering corrections suppressed by fractional powers of the Planck scale. Rather than being regarded as purely mathematical generalizations, such corrections may reflect an underlying fractal or multi-scale structure of quantum spacetime. This observation motivates the introduction of phenomenological modified dispersion relations containing both fractional momentum powers and fractional Planck-scale suppression.

To explore the implications of this idea in the nonrelativistic regime, we consider a generalized modified dispersion relation of the form

$$E^2 = c^2 p^2 + M^2 c^4 + \xi_{\alpha,\beta}\, \ell_{\mathrm{P}}^{-\beta} c^2 (Mc)^{2+\beta-\alpha} p^\alpha, \tag{4.5}$$

where $\alpha$ and $\beta$ are real parameters. The exponent $\alpha$ controls the momentum dependence of the correction, while $\beta$ regulates the fractional power of the Planck scale. Integer values of $\beta$ may be associated with standard Taylor expansions in $p\ell_{\mathrm{P}}$, whereas non-integer values naturally arise in more general expansions, such as Puiseux series [10], and may encode genuinely fractal features of quantum spacetime.

Taking the nonrelativistic limit of Eq. (4.5), one obtains an effective dispersion relation of the form

$$E = \frac{p^2}{2M} + \xi_{\alpha,\beta}\, \ell_{\mathrm{P}}^{-\beta} \frac{(Mc)^{2+\beta-\alpha}}{2M} p^\alpha \doteq \frac{p^2}{2M} + D_\alpha^{(\beta)}\, p^\alpha, \tag{4.6}$$

which generalizes the standard Galilean kinetic energy by including fractional momentum-dependent corrections. For $\beta = 1$ and integer values of $\alpha$, this expression reduces to the class of nonrelativistic corrections discussed in Section 4.1. More generally, Eq. (4.6) provides a unified phenomenological framework in which both integer and non-integer Planck-scale corrections can be systematically investigated.

This generalized dispersion relation forms the basis for the analysis developed in the following sections. In particular, upon quantization, the term proportional to $p^\alpha$ leads to fractional differential operators in the effective Schrödinger equation, establishing a direct connection between modified dispersion relations and fractional quantum mechanics.

## 4.3 Fractional Quantum Mechanics and Quantum Gravity Phenomenology

Fractional quantum mechanics offers a rigorous mathematical framework for quantum systems with non-quadratic dispersion relations. This approach originates from a generalization of Feynman's path integral quantization, where Brownian trajectories are replaced by Lévy flights that exhibit anomalous diffusion. In this context, the scaling of the particle trajectories is given by $x(t) \sim t^{1/\alpha}$, with $0 < \alpha \leq 2$, where $\alpha$ denotes the Lévy index. The conventional Brownian scenario is recovered when $\alpha = 2$.

Laskin demonstrated that quantum dynamics formulated on Lévy paths yields a generalized Schrödinger equation, which can also be derived via canonical quantization of a Hamiltonian of the form $H = D_\alpha p^\alpha + V$ [141]. The corresponding fractional Schrödinger equation is given by

$$i\hbar \frac{\partial}{\partial t} \Psi(\mathbf{x}, t) = \left[ D_\alpha (-\hbar^2 \Delta)^{\alpha/2} + V(\mathbf{x}, t) \right] \Psi(\mathbf{x}, t). \tag{4.7}$$

This equation reduces to the standard Schrödinger equation when $\alpha = 2$.

As outlined in previous sections, the nonrelativistic limit of modified dispersion relations results in effective Hamiltonians with momentum dependent corrections of the form $p^\alpha$. Quantization of these corrections produces a modified Schrödinger equation of the form

$$i\hbar\frac{\partial}{\partial t}\Psi(\mathbf{x},t) = \left[-\frac{\hbar^2}{2M}\Delta + V(\mathbf{x},t) + \xi_{\alpha,\beta}p_{\mathrm{P}}^{-\beta}\frac{(Mc)^{2-\alpha+\beta}}{2M}\left(-\hbar^2\Delta\right)^{\alpha/2}\right]\Psi(\mathbf{x},t), \tag{4.8}$$

This equation explicitly includes a fractional kinetic term. The correspondence indicates that the deformed nonrelativistic dynamics arising from modified dispersion relations can be interpreted within the framework of fractional quantum mechanics at the level of effective dynamics.

Although the fractional exponent $\alpha$ is limited to the interval $0 < \alpha \leq 2$, this range suffices for phenomenological applications. Corrections involving higher powers of momentum are generally suppressed below current Planck-scale sensitivity and are therefore not considered here [128].

The fractional Laplacian appearing in Eq. (4.8) can be rigorously defined in terms of the Riesz derivative [10], whose action on the wave function is given by

$$\Delta^{\alpha/2}\Psi(\vec{x},t) = -\frac{1}{(2\pi)^3}\int d^3k\, e^{i\vec{k}\cdot\vec{x}}k^\alpha\,\Phi(\vec{k},t), \tag{4.9}$$

where $\Psi(\vec{x},t)$ and $\Phi(\vec{k},t)$ are related through the Fourier transformation. The operator is Hermitian and preserves parity, thus maintaining the fundamental symmetries of quantum theory [142]. Its nonlocal nature leads to quantum dynamics that exhibit delocalization effects, which are central to the phenomenological interpretation presented in the remainder of this chapter.

### 4.3.1 The Deep Infrared Regime

Phenomenological studies of Lorentz invariance violation often employ modified dispersion relations as effective descriptions, without committing to a specific underlying theory of quantum gravity. In this context, dispersion relations are frequently treated as exact expressions within a given energy regime, allowing one to search for deviations from standard relativistic or nonrelativistic dynamics [143].

From a complementary theoretical perspective, modified dispersion relations have also been used to investigate dimensional flow phenomena in quantum gravity. In these studies, exact dispersion relations are used to analyze diffusion processes or thermodynamic properties, revealing scale-dependent effective dimensions that typically manifest themselves in the ultraviolet or transplanckian regime [144, 145, 146, 147].

In this analysis, we start from a relativistic modified dispersion relation and derive its nonrelativistic limit, leading to an effective Galilean invariance violating dispersion relation. From a pragmatic phenomenological standpoint, the generalized nonrelativistic dispersion relation

$$E = \frac{p^2}{2M} + D_\alpha^{(\beta)} p^\alpha, \tag{4.10}$$

may be regarded as an effective description of particle dynamics at low energies, where the correction term is suppressed by fractional powers of the Planck scale. Similar considerations may be extended to composite systems, in which the effective Planck scale is modified by the number of constituents [148].

A central observation is that, for fractional exponents satisfying $\alpha < 2$, the correction term proportional to $p^\alpha$ dominates over the standard quadratic kinetic term in the limit of sufficiently small momenta. We define the deep infrared regime as the domain in which this fractional contribution governs the effective dynamics. Quantitatively, this regime is characterized by the inequality

$$p \ll \left(2MD_\alpha^{(\beta)}\right)^{\frac{1}{2-\alpha}}. \tag{4.11}$$

In this limit, the dispersion relation simplifies to the pure fractional form

$$E \simeq D_\alpha^{(\beta)}\, p^\alpha, \tag{4.12}$$

and the corresponding quantum dynamics is naturally described within the framework of fractional quantum mechanics. The quadratic kinetic term becomes subdominant, and the dynamics exhibits intrinsically nonlocal features.

To illustrate the phenomenological implications of this regime, one may consider a low-temperature quantum system composed of $N$ particles of mass $M$, such as a Bose-Einstein condensate. Under standard assumptions from fractional statistical mechanics [142], the internal energy scales as

$$E \sim N\frac{k_\mathrm{B}T}{2\alpha}. \tag{4.13}$$

Combining this relation with Eqs. (4.11) and (4.12) leads to a characteristic temperature scale

$$T \ll T_\mathrm{dir} = \frac{\alpha}{Mk_\mathrm{B}}\left[\xi_{\alpha,\beta}(Mc)^{2+\beta-\alpha}p_\mathrm{P}^{-\beta}\right]^{\frac{3-\alpha}{2-\alpha}}, \tag{4.14}$$

which defines an upper bound for the validity of the deep infrared regime. This temperature scale should be interpreted as an order-of-magnitude estimate, dependent on the phenomenological assumptions underlying the modified dispersion relation.

Figure 4.1 displays the dependence of $T_\mathrm{dir}$ on the parameters $\alpha$ and $\beta$ for representative choices of physical constants. The surface illustrates how fractional corrections can lead to characteristic temperature scales well above or below experimentally accessible values, depending on the location in parameter space.

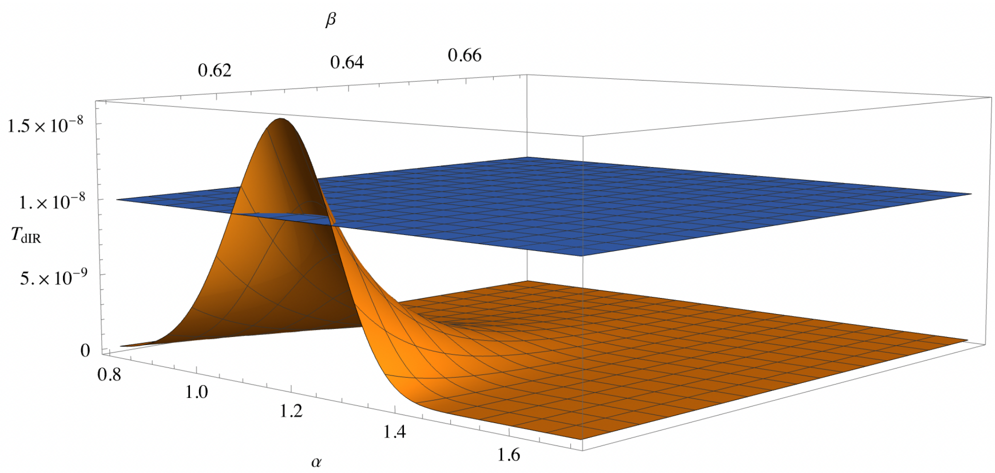


Figure 4.1: The dependence of $T_{\mathrm{dir}}$ on the parameters $\alpha$ and $\beta$ is depicted by the orange surface, while the safe ceiling is indicated by the blue plane.

Within this illustrative framework, regions of the $(\alpha, \beta)$ parameter space for which $T_{\mathrm{dir}}$ exceeds a given reference temperature may be regarded as phenomenologically disfavored, under the assumptions adopted. Figure 4.2 shows indicative regions corresponding to different reference temperature ceilings. These regions should be interpreted with caution, as they depend on the specific modeling choices and do not represent model-independent exclusions.

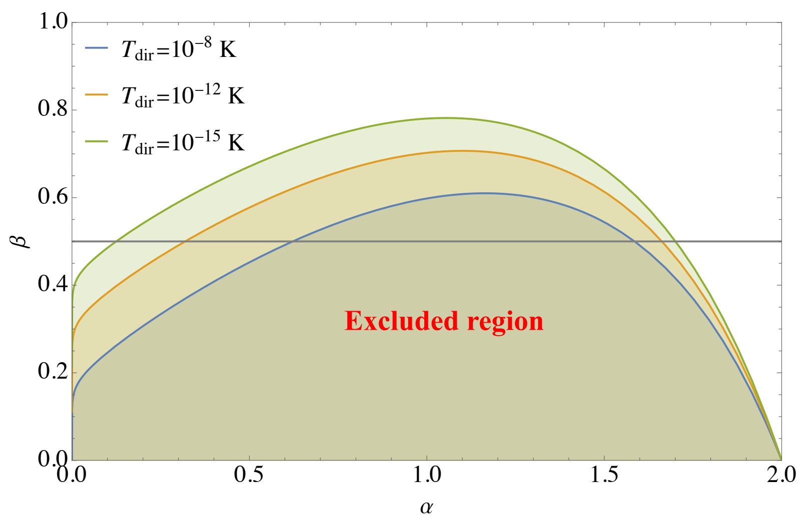


Figure 4.2: The exclusion regions formed by the $\alpha$ and $\beta$ parameters for the temperatures $T_{\mathrm{dir}}$.

Overall, this analysis demonstrates that the deep infrared regime provides a concrete phenomenological setting in which fractional quantum dynamics induced by dispersion relations could, in principle, become relevant in low-energy quantum systems. While the estimates presented here are illustrative, they highlight the potential interplay between infrared quantum dynamics, nonlocality, and Planck-scale physics.

### 4.3.2 Fractional Harmonic Dimension

Regarding pure fractional quantum mechanics, several results have been derived, including the spectrum of the harmonic oscillator and the hydrogen atom [11]. For the harmonic oscillator with a potential $V(x) = q^2x^2$, the Bohr-Sommerfeld quantization rule, $2\pi\hbar\left(n+\frac{1}{2}\right) = \oint p\,dx$, can be employed to calculate the spectrum of the fractional harmonic oscillator in one spatial dimension. In this case, the energy eigenvalues are given by

$$E_{n,1}^{(\alpha)} = \left(\frac{\pi\hbar D_\alpha^{(\beta)^{1/\alpha}} q}{B\left(\frac{1}{2},\frac{1}{\alpha}+1\right)}\right)^{\frac{2\alpha}{2+\alpha}} \left(n+\frac{1}{2}\right)^{\frac{2\alpha}{2+\alpha}}, \tag{4.15}$$

where the subscript 1 indicates one dimension, and the $B$-function is defined as

$$\frac{1}{\gamma}B\left(\frac{1}{\gamma},\frac{1}{\alpha}+1\right) = \int_0^1 dy\,(1-y^\gamma)^{1/\alpha}\,.$$

Observe that Eq.(4.15) reduces to the standard energy spectrum when $\alpha = 2$, highlighting the dimensional dependence of the oscillator:

$$E_n^{(2)} = 2\hbar q\sqrt{D_2^{(\beta)}}\left(n+\frac{d}{2}\right), \qquad d = 1, \tag{4.16}$$

such that if $D_2^{(\beta)} = 1/(2M)$ and $q = \omega\sqrt{M/2}$, we obtain the textbook energy levels $E_n^{(2)} = \hbar\omega(n + d/2)$, where $d$ is the oscillator dimension, which in this case is $d = 1$.

In the standard case, knowing the energy spectrum $E_n^{(2)}$ and the harmonic frequency $\omega$ allows us to determine the oscillator's dimension using the formula $d = 2E_0/(\hbar\omega)$. However, this property is not valid in the fractional case. The concept of dimension becomes tricky in fractional quantum mechanics, where a fractal dimension often emerges naturally (see, e.g., the fractal dimension of the black hole and cosmological horizons [137, 149, 150, 151, 152], and the fractal dimension of Lévy paths [142]). Thus, a similar phenomenon might occur in this approach.

The natural candidate for an undeformed observable that depends on the system's dimension is the energy levels of the oscillator. To derive a meaningful formula for the dimension, we compare the deformed energy levels with the undeformed ones in $d$ dimensions, depending only on the Lévy index $\alpha$. Using the dimensionless formulation of fractional quantum mechanics and the energy levels of the harmonic oscillator from section 9.3 of [142], we define the dimensionless energy as

$$\begin{aligned}
\epsilon_{n,1}^{(\alpha)} &= \frac{E_{n,1}^{(\alpha)}}{\left((D_\alpha^{(\beta)})^2\hbar^2 q^{2\alpha}\right)^{1/(2+\alpha)}} \\
&= \left[\frac{\pi}{B\left(\frac{1}{2},\frac{1}{\alpha}+1\right)}\left(n+\frac{1}{2}\right)\right]^{2\alpha/(2+\alpha)}.
\end{aligned} \tag{4.17}$$

This expression should be compared with the case $\alpha = 2$ in $d_\alpha$ dimensions, given by

$$\epsilon_{n,d_\alpha}^{(\alpha)} = \frac{2\hbar q\sqrt{D_2^{(\beta)}}}{\left((D_2^{(\beta)})^2\hbar^4 q^4\right)^{1/4}}\left(n+\frac{d}{2}\right) = 2\left(n+\frac{d_\alpha}{2}\right). \tag{4.18}$$

Equating (4.17) and (4.18) as $\epsilon_{n,1}^{(\alpha)} = \epsilon_{n,d_\alpha}^{(\alpha)}$ and setting $n = 0$ for simplicity, we find

$$d_\alpha = \left[\frac{\pi}{B\left(\frac{1}{2},\frac{1}{\alpha}+1\right)}\left(n+\frac{1}{2}\right)\right]^{2\alpha/(2+\alpha)}. \tag{4.19}$$

The dependence of this dimension on $\alpha$ is depicted in Fig.4.3. At this extreme regime, this dimension depends solely on the MDR power and not on the system's physical properties. This feature also occurs in the spectral and thermal dimensions within the UV limit [143, 147, 153]. This quantity indeed resembles a fractal dimension, as it is slightly larger than 1 for $0 < \alpha < 2$, approaching a 2-dimensional geometry, similar to the Koch curve [154, 142]. The maximum value is $d_{0.413} \approx 1.167$, and the linear case gives $d_1 \approx 1.115$.

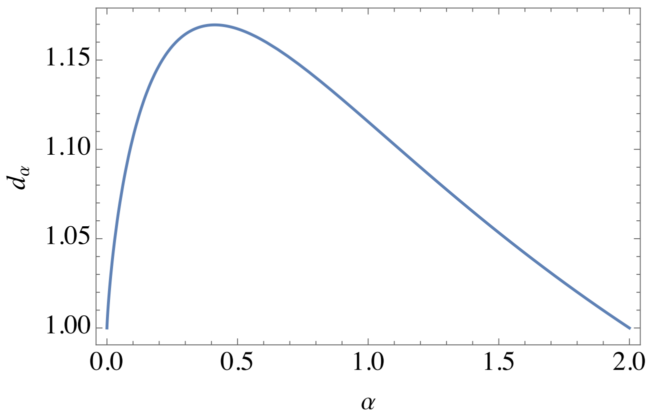


Figure 4.3: Harmonic fractional dimension $d_\alpha$ as a function of the Lévy index $\alpha$.

Given that similar fluctuations occur in the UV regime, this may represent an interplay between the trans-Planckian UV and the deep IR behaviors, where similar properties emerge.

## 4.4 Experimental analogue

Despite the challenges in testing the existence of fractional quantum mechanics at the Planck scale, we can gain insights by translating experiments conducted with fractional quantum systems to the quantum gravity context. In [155], an experiment was conducted using an optical apparatus in the temporal domain to realize a fractional Schrödinger equation. The Schrödinger equation considered in [155] is

$$i\frac{\partial}{\partial z}\Psi = \left[-\frac{|\beta_2|}{2}\frac{\partial^2}{\partial\tau^2} + i\frac{\beta_3}{6}\frac{\partial^3}{\partial\tau^3} + \frac{D}{2}\left(-\frac{\partial^2}{\partial\tau^2}\right)^{\alpha/2}\right]\Psi, \tag{4.20}$$

where $\beta_2$ and $\beta_3$ are experimental parameters, $D$ is the fractional dispersion coefficient, $z$ is the propagation distance and $\tau = T - z/V_{\text{gr}}$ is the reduced time, where $T$ is the physical time and $V_{\text{gr}}$ is the group velocity of the carrier wave [156]. This equation describes the slowly varying amplitude $\Psi$ of the electric field triggered by the travel of an optical pulse through a complex dispersive material.

In such optics experiments, the group velocity of the carrier wave $V_{\text{gr}}$ is the natural velocity scale, allowing us to map the propagation and temporal coordinates $(\tau, z)$ to new coordinates $(t, x)$ that will be used in our analysis as $z = tV_{\text{gr}}$ and $\tau = x/V_{\text{gr}}$ in (4.20). This group velocity is found from the relation between the wavenumber $k$ and frequency $\omega$ of the carrier as $k = (D/2)|\omega|^\alpha - (\beta_2/2)\omega^2 - (\beta_3/6)\omega^3$, which implies in

$$\frac{1}{V_{\text{gr}}(\alpha)} = \frac{dk}{d\omega} = \frac{\alpha D}{2}|\omega(k)|^{\alpha-1} - \beta_2|\omega(k)| - \frac{\beta_3}{2}|\omega(k)|^2\,, \tag{4.21}$$

where $|\omega(k)|$ is the frequency as a function of the wavenumber $k$ found from the dispersion relation. Therefore, considering fixed wavelength $\lambda = 1/k$ and other experimental parameters $D$ and $\beta_{2,3}$, for each $\alpha$, we have a different $\omega$ and, consequently, a different $V_{\text{gr}}$.

If we proceed with this map and multiply (4.20) by $\hbar$, it goes to

$$i\hbar\frac{\partial}{\partial t}\Psi = \left[-\frac{\hbar|\beta_2|V_{\text{gr}}^3}{2}\frac{\partial^2}{\partial x^2} + i\frac{\hbar\beta_3 V_{\text{gr}}^4}{6}\frac{\partial^3}{\partial x^3} + \frac{\hbar D|V_{\text{gr}}|^{\alpha+1}}{2}\left(-\frac{\partial^2}{\partial x^2}\right)^{\alpha/2}\right]\Psi\,.$$

This expression is equivalent to

$$i\hbar\frac{\partial}{\partial t}\Psi = \Big[-\frac{\hbar^2}{2M}\frac{\partial^2}{\partial x^2} - i\frac{\xi_3\hbar^3}{2Mp_{\text{P}}}\frac{\partial^3}{\partial x^3} + \xi_{\alpha,\beta}p_{\text{P}}^{-\beta}\frac{(Mc)^{3-\alpha+\beta}\hbar^\alpha}{2M}\left(-\frac{\partial^2}{\partial x^2}\right)^{\alpha/2}\Big]\Psi,$$

where the parameters are identified as

$$M = \frac{\hbar}{V_{\mathrm{gr}}^3}\frac{1}{|\beta_2|}, \qquad \xi_3 = -\frac{MV_{\mathrm{gr}}^4 p_{\mathrm{P}}}{3\hbar^3}\beta_3,$$
$$\xi_{\alpha,\beta} = p_{\mathrm{P}}^{\beta} M V_{\mathrm{gr}}^{\alpha+1}\hbar^{1-\alpha}(Mc)^{\alpha-\beta-2}D. \tag{4.22}$$

Except for the term proportional to $\xi_3$, this equation is equivalent to the one described in this chapter, given by Eq.(4.8). Hence, the experiment performed in [155] can be considered an analog of testing the Lorentz-violating Schrödinger equation with an optical system, representing an analogue model of in-vacuo dispersion.

In this chapter, we shall focus in the case in which $\beta_3 = 0$. The experimental parameters $\alpha\,, \beta_2\,, D$ and the wavelength of the carrier wave $\lambda$ are

$$|\beta_2| = 21 \times 10^{-3}\,\mathrm{ps}^2/\mathrm{m}, \qquad D = 21 \times 10^{-3}\,\mathrm{ps}^{\alpha}/\mathrm{m},$$
$$\lambda = 810\,\mathrm{nm}, \qquad \alpha = 0.25, \quad \alpha = 1.25. \tag{4.23}$$

In both cases, the experimental results matched the behavior predicted by simulations. The initial pulse, represented by a Gaussian function in time, showed delocalization after traversing the nonlinear medium. For $\alpha = 1.25$, the wave packet split and displayed an interference pattern, while for $\alpha = 0.25$, a soliton rain profile emerged, with each soliton centered around different time values. This system, analogous to a wave packet traveling in quantum spacetime, suggests that a wave packet would exhibit spatial delocalization in a quantum spacetime. Such nonlocal behavior is not surprising, as the notion of locality in quantum gravity has been questioned [48].

The frequency of the carrier wave can be found from the dispersion relation, but due to the magnitude of the experimental parameters, it is basically the same for both $\alpha$'s, being $\omega \approx 1.1 \times 10^{10}\,\mathrm{s}^{-1}$. Using this information in (4.21), we have $V_{\mathrm{gr}} = 4.4\,\mathrm{km}/s$. Using the experimental parameters in (4.23) and the mapping (4.22), this optical system effectively describes a particle with mass $M = 5.9 \times 10^{-32}$ kg, which is roughly of the order of magnitude of the electron mass $M_e = 9 \times 10^{-31}$ kg.

The experimentally analyzed cases correspond to the dimensionless parameters $\xi_{0.25,1} = 3.5 \times 10^6$ and $\xi_{1.25,1} = 2.6 \times 10^9$. In order to have $\xi_{\alpha,\beta} \approx 1$ (which would be natural for quantum gravity effects), we need to have $\beta \sim 0.75$ (for $\alpha = 0.25$) and $\beta \sim 0.6$ (for $\alpha = 1.25$). Therefore, our conclusion is that such experiments are actually testing the fractal nature of spacetime, by testing in-vacuo dispersion due to quantum gravity for fractional powers in the momentum and fractional powers in the Planck scale.

Simulations show wave packet splitting in both scenarios, and we anticipate similar experimental results. Furthermore, in the analysis carried out in [155], such splitting increases with propagation, indicating an effect that accumulates over time in our analogy.

## 4.5 Discussion

We revisited the modified Schrödinger dynamics induced by MDRs and extended it to include corrections with noninteger powers of the momentum. We showed that, in this regime, the effective dynamics naturally fall within the formalism of fractional quantum mechanics, a rich area of research with numerous experimental possible tests.

Conceptually, these results indicate that the IR limit of quantum gravity may exhibit qualitative features beyond small polynomial perturbations of the standard Schrödinger Hamiltonian. The MDRs do not necessarily produce only higher-order analytic corrections. Instead, they can induce genuinely new structures in the effective theory, such as fractional or intrinsically nonlocal kinetic operators.

From this perspective, the fractional dynamics derived in this chapter should not be regarded as an *ad hoc* modification of quantum mechanics. Rather, they emerge from the same kinematic formalism introduced in the previous chapters. This observation suggests the presence of a distinct deep infrared regime. In this regime, nonanalytic terms dominate over the usual Galilean kinetic contribution. There, the dynamics may exhibit scale-invariant or fractal-like features, conceptually analogous but physically very different from the transplanckian behavior expected in the UV.

By identifying a Planck-scale modified Schrödinger equation with fractional quantum mechanics, we recognized that experiments testing this approach serve as analog models of quantum gravity, where nonlocal behavior of the wave function emerges.

Up to this point, we have considered systematic corrections to MDRs. However, in many quantum gravity approaches, Planck-scale effects can manifest stochastically. Chapter 5, therefore, abandons the systematic scenario and investigates how stochastic fluctuations in MDRs can induce gravitational decoherence.

# CHAPTER 5

## Stochastic Planck-Scale Effects in Gravcats

This chapter examines a complementary aspect of the framework by analyzing stochastic realizations of Planck-scale effects and their influence on coherence and entanglement in mesoscopic quantum systems. While the previous chapters focused on systematic Planck-scale modifications of quantum dynamics, here we address how quantum-gravitational stochasticity can alter the dynamics of bipartite systems in which gravity itself mediates quantum correlations [6, 157].

Specifically, we study how Lorentz Invariance Violation (LIV) can cause decoherence in gravitational cat states [126, 127]. In these states, massive particles are placed in spatial superpositions and interact only through their shared gravitational potential. The analysis in this chapter is based on the results presented in [158].

## 5.1 Master Equation from Stochastic Dispersion Relation

As discussed throughout this thesis, one of the most promising avenues of research in quantum gravity lies in the phenomenological perspective, whereby the quantum nature of spacetime may imprint itself on the kinematic properties of particles. These deviations from the classical behavior are coupled to the energy and momentum of the test particles and are suppressed by the quantum gravity energy scale. This phenomenon can be represented by an effective modification of the Hamiltonian. Various quantum gravity models predict different mechanisms for such deviations. To capture these corrections and analyze their observable signatures, a phenomenological approach often considers a modified dispersion relation for particles with energy $E$, momentum $p$, and mass $M$ of the form:

$$M^2c^2 = \left(\frac{E}{c}\right)^2 - p^2 - \ell\xi_n(Mc)^{n-3}p^{3-n}, \tag{5.1}$$

where $\ell^{-1}$ is the quantum gravity scale, which here has dimensions of momentum and we expect it to be of the order of the Planck momentum $E_{\mathrm{P}}/c \approx 6.5\,\mathrm{kg\,m/s}$, where $E_{\mathrm{P}} \approx 1.22 \times 10^{19}\,\mathrm{GeV}$ is the Planck energy, $c$ is the speed of light, and $\xi_n$ are parameters expected to be of order unity. As discussed previously, this expression incorporates general corrections that depend on the energy and momentum of the test particles.

Relativistic astrophysics provides the most common scenario for searching for effects resulting from these corrections, as they are amplified by particle energies. However, recent studies have suggested that such corrections might also leave imprints at nonrelativistic scales, which are currently being constrained with Planck-scale sensitivity. In this case, as discussed in [128], the most relevant contributions come from corrections proportional to powers of the momentum and mass:

$$E = \frac{p^2}{2M} + \frac{\ell}{2M}\xi_n (Mc)^{3-n} p^n. \tag{5.2}$$

Quantum systems have provided the most important window for investigating these infrared effects. By performing a spacetime foliation and either quantizing Eq. (5.2) or calculating the nonrelativistic limit of the Klein-Gordon equation compatible with (5.2), the Schrödinger equation takes the form [128]

$$\hat{H} = \hat{K} + e\phi_e + M\phi_g - \xi_n \ell (Mc)^{3-n} (2M)^{\frac{n-2}{2}} \hat{K}^{n/2}, \tag{5.3}$$

$$\hat{K} = -\frac{h^{ij}}{2M} \left(\nabla_i - ieA_i^e\right)\left(\nabla_j - ieA_j^e\right) \tag{5.4}$$

where $\hat{K}$ is the kinetic energy with a minimal coupling with the electromagnetic potential (in this case, we do have contributions from a gravitomagnetic potential), $\phi_e$ is the electromagnetic scalar potential on a particle of charge $e$, $\phi_g$ is the scalar gravitational potential on a particle of mass $M$ and $h^{ij}$ are the space components of the metric in a $3+1$-decomposition.

We refer to $\hat{H}_0 = \hat{K} + e\phi_e + M\phi_g \doteq \hat{K} + \hat{V}$ as the undeformed Hamiltonian, and $\hat{H}_{\ell,n} = -\xi_n \ell (Mc)^{3-n} (2M)^{\frac{n-2}{2}} \hat{K}^{n/2}$ represents the Hamiltonian correction due to MDR. This Hamiltonian governs the time evolution of the state vector $|\phi\rangle$, and its corresponding pure state density matrix $\varrho = |\psi\rangle\langle\psi|$ follows the Liouville-von Neumann equation

$$i\hbar\partial_t|\psi\rangle = (\hat{H}_0 + \hat{H}_{\ell,n})|\psi\rangle \Rightarrow \partial_t\varrho = -\frac{i}{\hbar}[\hat{H}_0 + \hat{H}_{\ell,n}, \varrho]. \tag{5.5}$$

In order to analyze this equation, we follow the steps described in [159]. We define a new Hamiltonian and its stochastic perturbation as

$$\hat{H}_0' = \hat{H}_0 + g(\hat{K})\,, \tag{5.6}$$

$$\hat{H}_{\ell,n}' = \hat{H}_{\ell,n} - g(\hat{K})\,, \tag{5.7}$$

where $g(\hat{K}) = \langle \hat{H}_{\ell,n} \rangle$ and $\langle * \rangle$ means averaging over the stochastic process. This guarantees that $\langle \hat{H}'_{\ell,n} \rangle = 0$.

The stochastic nature of $\xi_n$ will induce a master equation describing an open quantum system, as we now demonstrate. Following the approach in [157], we treat the deformed Hamiltonian contribution $\hat{H}_{\ell,n}$ as describing the particle's interaction with the gravitational degrees of freedom. We work in the interaction picture by defining the state $|\psi^I\rangle$ as

$$|\psi\rangle = e^{-i\hat{H}'_0 t/\hbar}|\psi^I\rangle. \tag{5.8}$$

This allows us to write the Schrödinger equation as

$$i\hbar\partial_t|\psi^I\rangle = e^{i\hat{H}'_0 t/\hbar}\hat{H}'_{\ell,n}e^{-i\hat{H}'_0 t/\hbar}|\psi^I\rangle \doteq \hat{H}'^I_{\ell,n}|\psi^I\rangle. \tag{5.9}$$

Consequently, the Liouville-von Neumann equation for the density matrix $\varrho^I = |\psi^I\rangle\langle\psi^I|$ in the interaction picture becomes

$$\partial_t \varrho^I = -\frac{i}{\hbar}[\hat{H}'^I_{\ell,n}, \varrho^I]. \tag{5.10}$$

The formal solution to this equation is

$$\varrho^I(t) = \varrho^I(0) - \frac{i}{\hbar}\int_0^t [\hat{H}'^I_{\ell,n}(t'), \rho^I(t')]dt'. \tag{5.11}$$

Substituting (5.11) back into (5.10) yields

$$\partial_t\varrho^I(t) = -\frac{i}{\hbar}[\hat{H}'^I_0(t), \varrho^I(0)] - \frac{1}{\hbar^2}\int_0^t \left[\hat{H}'^I_0(t), [\hat{H}'^I_0(t'), \varrho^I(t')]\right]dt', \tag{5.12}$$

where we employ the Born-Markov approximation to insert $\hat{H}'^I_0(t)$ inside the integral as a function of $t$ only. We treat $\xi_n = \sqrt{t_{QG}}\chi_n(t)$ as Gaussian noise with fixed average and sharp autocorrelation:

$$\langle \xi_n(t) \rangle = 1, \quad \langle \chi_n(t), \chi_n(t') \rangle = \delta(t - t'), \tag{5.13}$$

where $t_{QG}$ is the quantum gravity timescale, presumably of Planck-time order.

Since the evolution equation fluctuates, we consider the average density matrix $\langle \varrho \rangle \doteq \rho$ to study the quantum system. The average differential equation can be found using the cumulant expansion method, expanding $\rho^I$'s equations of motion in terms of the cumulant of the operator $[\hat{H}'^I_\ell, *]$ [160]:

$$\partial_t\rho^I = -\int_0^t \langle \left[\hat{H}'^I_{\ell,n}(t), [\hat{H}'^I_\ell(t'), \rho^I(t)]\right] \rangle dt'. \tag{5.14}$$

Assuming $\hat{H}'^{I}_{\ell,n}(t)$ follows Gaussian white noise statistics yields the evolution equation:

$$\partial_t \rho^I = -\frac{\sigma_n^2}{\hbar^2} t_{QG} \left[ (\hat{K}^I)^{n/2}, [(\hat{K}^I)^{n/2}, \rho^I] \right], \tag{5.15}$$

where $\sigma_n = \ell (Mc)^{3-n} (2M)^{\frac{n-2}{2}}$. For the density matrix $\rho = e^{-i\hat{H}_0' t/\hbar} \rho^I e^{i\hat{H}_0' t/\hbar}$, we obtain our main result, a Lindblad equation:

$$\partial_t \rho(t) = -\frac{i}{\hbar} \left[ \hat{K} + \hat{V} - \sigma_n \hat{K}^{n/2}, \rho(t) \right] - \frac{\sigma_n^2}{\hbar^2} t_{QG} \left[ \hat{K}^{n/2}(t), \left[ \hat{K}^{n/2}(t), \rho(t) \right] \right]. \tag{5.16}$$

This equation describes an open quantum system experiencing decoherence due to quantum spacetime fluctuations. The interaction strength with the environment is characterized by $\sigma_n$, which depends on the system's mass. For $n = 1$, our Lindbladian $\sqrt{\hat{K}} \propto \hat{p}$ resembles that in [161], though the latter uses momentum components $\hat{p}_i$ as Lindbladians. For $n = 2$, the Lindblad term becomes similar to [162], with $\hat{p}^2 \propto \hat{K}$ as the Lindbladian. The $n = 3$ case introduces a novel $\hat{K}^{3/2}$ term.

To estimate the decoherence timescale, we consider a free nonrelativistic particle with $\hat{H}_0 = \hat{K} - \sigma_n K^{n/2}$. In the momentum representation, the density matrix elements $\rho_{p,q} = \langle p|\rho|q\rangle$ (where $|p\rangle$ is a momentum eigenstate) evolve as:

$$\rho_{pq}(t) = \rho_{pq}(0) \exp\left[ -\frac{i}{\hbar} \left( \Delta\tilde{E} \right) t \right] \exp\left[ -\sigma_n \left( \Delta E^{n/2} \right)^2 t \right]. \tag{5.17}$$

where $\tilde{E} = E - \sigma_n E^{n/2}$, $\Delta\tilde{E} = \tilde{E}(p) - \tilde{E}(q)$ and $\left(\Delta E^{n/2}\right)^2 = \left( E^{n/2}(p) - E^{n/2}(q) \right)^2$. Off-diagonal elements are suppressed by the $\sigma_n$ damping factor, with decoherence time $\tau_D = 1/(\sigma_n \left(\Delta E^{n/2}\right)^2)$. Substituting $\ell = c/E_P$, the decoherence time becomes:

$$\tau_{D,n} = \frac{2^{2-n} \hbar^2}{(Mc^2)^{4-n} \left(\Delta E^{n/2}\right)^2} \frac{E_P^2}{t_{QG}}. \tag{5.18}$$

For comparison with relativistic quantum gravity decoherence models, we set $M = E/c^2$ and $\Delta E^{n/2} \sim E^{n/2}$. Taking $t_{QG} = t_P = \hbar/E_P$ yields an $n$-independent decoherence time:

$$\tau_D \propto \hbar \frac{E_P^3}{E^4}, \tag{5.19}$$

sharing the energy dependence of the Ellis-Mohanty-Nanopoulos model [163]. Our goal is to examine LIV effects on entanglement in gravitationally interacting massive quantum states.

## 5.2 Gravitational Cat States

Consider a system of two particles, each confined in a double-well potential with local minima at positions $x_{\min} = \pm L/2$ that interact gravitationally as in Fig.5.1. Under the conditions discussed in [164], where the second excited energy level lies far above the first excited and ground states, we can approximate each particle as a two-level system. The Hamiltonian for a two-level particle is given by the $z$-Pauli matrix $\hat{K} = \frac{\epsilon}{2}\sigma_z$, with eigenstates $|0\rangle$ and $|1\rangle$ corresponding to eigenenergies $\pm\epsilon/2$, where $\epsilon$ represents the energy gap between states. These states define the computational basis.

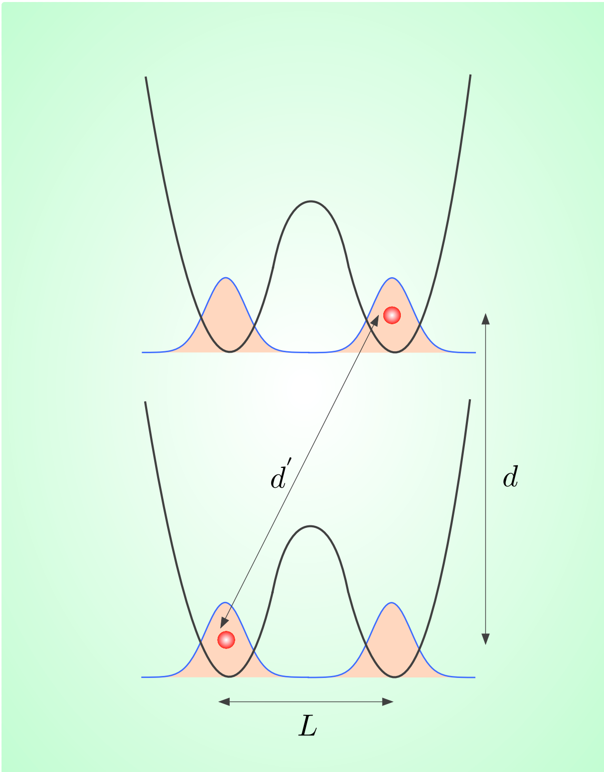


Figure 5.1: Representation of the gravcat states. The two particles are located in an even double-well potential with minima separated by distance $L$. The interparticle distance is $d$ or $d'$ when the particles occupy the same or different potential minima, respectively.

Since the particles can be well-localized in the left or right well of the double-well potential, they can also be described by superpositions of the eigenstates of the left and right positions, denoted $|\pm\rangle$. These particles are in a superposition of positions and energies. Due to the uncertainty in the location of each particle, there is a superposition in the gravitational potential that describes their interaction. We refer to these as gravitational cat (gravcat) states.

The system Hamiltonian is given by [164]:

$$\hat{H}_0 = (E - \Gamma)\mathbb{1} \otimes \mathbb{1} + \frac{\epsilon}{2}(\mathbb{1} \otimes \sigma_z + \sigma_z \otimes \mathbb{1}) - \Omega\sigma_x \otimes \sigma_x, \tag{5.20}$$

where $E > \epsilon$ is a reference energy shifted by $\pm\epsilon$, $\Gamma = \frac{1}{2}\alpha\left(\frac{1}{d} + \frac{1}{d'}\right)$, $\Omega = \frac{1}{2}\alpha\left(\frac{1}{d} - \frac{1}{d'}\right)$, and $\alpha = Gm^2$. While the constant terms proportional to $E$ and $\Gamma$ do not contribute to Lindblad evolution, we retain them in the Hamiltonian because in the following section we will consider $\hat{K}^{n/2}$ as the Lindbladian, which requires a positive definite kinetic energy operator.

The Liouville-von Neumann evolution $\partial_t \rho = -i[\hat{H}_0, \rho(t)]$ for the initial state $|\psi_0\rangle = \sin(\theta)|00\rangle + \cos(\theta)|11\rangle$

$$\rho(0) = \begin{pmatrix} \cos^2(\theta) & 0 & 0 & \sin(\theta)\cos(\theta) \\ 0 & 0 & 0 & 0 \\ 0 & 0 & 0 & 0 \\ \sin(\theta)\cos(\theta) & 0 & 0 & \sin^2(\theta) \end{pmatrix} \tag{5.21}$$

yields the following non-zero matrix elements:

$$\begin{aligned} \Delta &= \sqrt{\Omega^2 + \epsilon^2}, \quad \omega = \frac{2\Delta}{\hbar}, \\ A &= \Omega\cos(2\theta) + \epsilon\sin(2\theta) \\ B &= \Omega\epsilon\cos(2\theta) + \epsilon^2\sin(2\theta) \\ C &= -\Omega\epsilon\cos(2\theta) + \Omega^2\sin(2\theta) \end{aligned}$$

$$\rho_{11}(t) = \frac{1}{2} + \frac{-\Omega\epsilon\sin(2\theta) + \epsilon^2\cos(2\theta) + \Omega A\cos(\omega t)}{2(\Omega^2 + \epsilon^2)} \tag{5.22}$$

$$\rho_{44}(t) = \frac{1}{2} + \frac{\Omega\epsilon\sin(2\theta) - \epsilon^2\cos(2\theta) - \Omega A\cos(\omega t)}{2(\Omega^2 + \epsilon^2)} \tag{5.23}$$

$$\rho_{14}(t) = \frac{1}{2(\Omega^2 + \epsilon^2)}\left[-i\frac{\Delta}{\hbar}A\sin(\omega t) + B\cos(\omega t) + C\right] \tag{5.24}$$

For the initial condition with $\theta = 0$ (an unentangled state), the system evolves into an entangled state, as quantified by the concurrence [165]:

$$\mathcal{C}(t) = 2\max\left\{|\rho_{23}| - \sqrt{\rho_{11}\rho_{44}}, |\rho_{14}| - \sqrt{\rho_{22}\rho_{33}}, 0\right\}. \tag{5.25}$$

The characteristic timescale for entanglement generation is:

$$\tau_E = \frac{\hbar}{\sqrt{\Omega^2 + \epsilon^2}}. \tag{5.26}$$

This timescale $\tau_E$ determines the oscillation period of the entanglement, while $\Omega$ governs the entanglement strength.

For an initially unentangled state $\theta = 0$, we obtain:

$$\mathcal{C}_{\theta=0}(t) = 2\frac{\Omega}{\hbar^2}\tau_E^2|\sin(t/\tau_E)|\sqrt{\epsilon^2 + \Omega^2\cos^2(t/\tau_E)}. \tag{5.27}$$

Notably, when $\theta = 0$ and $\Omega = 0$, we find $\mathcal{C} = 0$. This observation underlies the concept that particles in position superposition states can develop entanglement mediated by their gravitational interaction.

The next step involves investigating the effects of Lorentz invariance violation on this system.

## 5.3 LIV Effect on Entanglement Between Gravcat States

Consider that the double-well potential of each particle is generated by the interaction of our system with an electromagnetic field. This could be realized, for instance, via the minimal coupling to a magnetic vector potential in the $y$ direction of the form $\vec{A} = (0, bx^2, 0)$ in Cartesian coordinates. In fact, according to the prescription (5.4), in the position representation, the Hamiltonian (kinetic term with minimal coupling) of this system is of the form

$$\hat{K} = \frac{1}{2M}\left[p_z^2 + \hat{P}_x^2 + e^2b^2\left(\frac{p_y}{eb} - x^2\right)^2\right], \tag{5.28}$$

where $p_y$ and $p_z$ are the momenta of the particle and $\hat{P}_x$ is the momentum operator in the $x$-direction. Apart from the constant displacement given by $p_z$, the interaction term $e^2b^2(p_y/eb - x^2)^2$ is a double well potential, whose shape can be controlled by $p_y$, $e$ and $b$ and the interwell coupling occurs in the $x$-direction. An example of such system consists in those found from Bose-Einstein condensation, for instance in [166], some conditions are given on the potential such that, in each well, the two lowest energy states are closely spaced and well separated from higher energy levels of the potential. Although experimentally difficult due to electrostatic repulsion, in principle, this system can be formed under certain conditions [167].

Therefore, assuming that the two-level configuration is generated by a minimal coupling with $\vec{A}$, we can identify the kinetic energy operator as $\hat{K} = E\mathbb{1}\otimes\mathbb{1} + \frac{\epsilon}{2}(\mathbb{1}\otimes\sigma_z + \sigma_z\otimes\mathbb{1})$. From Eq.(5.16), powers of this operator will play the role of Lindbladians in this analysis.

Since $\hat{K}$ is diagonal, we can directly consider its components raised to the power $n/2$, which remain real-valued due to the condition $E > \epsilon$. This ensures the Hermiticity of the kinetic energy operator, which serves as the Lindblad operator in this approach.

Substituting this information into the Lindblad evolution some components of the density matrix evolve in an undeformed way:

$$\begin{aligned}\rho'_{11}(t) &= -\rho'_{44}(t) = -i\Omega\left(\rho_{14}(t) - \rho_{41}(t)\right)/\hbar,\\ \rho'_{22}(t) &= -\rho'_{33}(t) = -i\Omega\left(\rho_{23}(t) - \rho_{32}(t)\right)/\hbar,\\ \rho'_{23}(t) &= -i\Omega\left(\rho_{22}(t) - \rho_{33}(t)\right)/\hbar,\end{aligned}$$

while the LIV effects are restricted to the component

$$\rho'_{14}(t) = -\frac{A_n^2 t_{QG}}{\hbar^2}\rho_{14}(t) - i\frac{A_n}{\hbar}\rho_{14}(t) - \frac{i\left(\Omega\rho_{11}(t) - \Omega\rho_{44}(t) + 2\epsilon\rho_{14}(t)\right)}{\hbar}, \tag{5.29}$$

where $A_n = \sigma_n\left[(E-\epsilon)^{n/2} - (E+\epsilon)^{n/2}\right]^2$ quantifies the attenuation of the off-diagonal component $\rho_{14}$ and effectively determines the decoherence timescale of the model. The parameter $n$ exclusively influences the constant $A_n$, meaning that studying the qualitative behavior of this Lindblad evolution only requires specifying initial conditions and values for $A_n$.

The decoherence timescale in our approach is given by $\tau_{D,n} = A_n^{-2}\hbar^2/t_{QG}$, or equivalently (recalling that $\ell = p_P^{-1} = c/E_P$):

$$\tau_{D,n} = \frac{2^{2-n}}{\left[(E-\epsilon)^{n/2} - (E+\epsilon)^{n/2}\right]^2}\frac{\hbar^2}{(Mc^2)^{4-n}}\frac{E_P^2}{t_{QG}}. \tag{5.30}$$

In Fig. 5.2(b), we analyzed the systematic LIV case, i.e., in which the quantum gravity scale does not fluctuate, which is achieved by requiring $t_{QG} = 0$ in (5.29). The larger is the LIV parameter, the more attenuated is the maximum of the concurrence. This means that even in the absence of fluctuations of the quantum gravity scale in the dispersion relation, the LIV parameter suppresses entanglement formation. From (5.29), we see that the solution is given by Eqs. (5.22)–(5.24), where we map $\epsilon \mapsto \epsilon + A_n/2$.

For the stochastic case, i.e., when $t_{QG} \neq 0$, Fig. 5.2(c) demonstrates that the interaction initially dominates the system's evolution, generating entanglement between particles. However, LIV effects gradually dampen the density matrix's off-diagonal elements. The oscillation extrema remain largely unchanged as they are governed by the entanglement timescale (5.26), which depends solely on $\Omega$ and $\epsilon$. The characteristic timescales depend on the dispersion relation details encoded in parameter $n$ through (5.30).

Figure 5.2(d) shows the population dynamics for $\theta = 0$ (initially separable state). When $\Omega > \epsilon$, the stronger interaction drives pronounced oscillations between $\rho_{11}$ and $\rho_{44}$ before decoherence effects ultimately equilibrate them to 0.5.

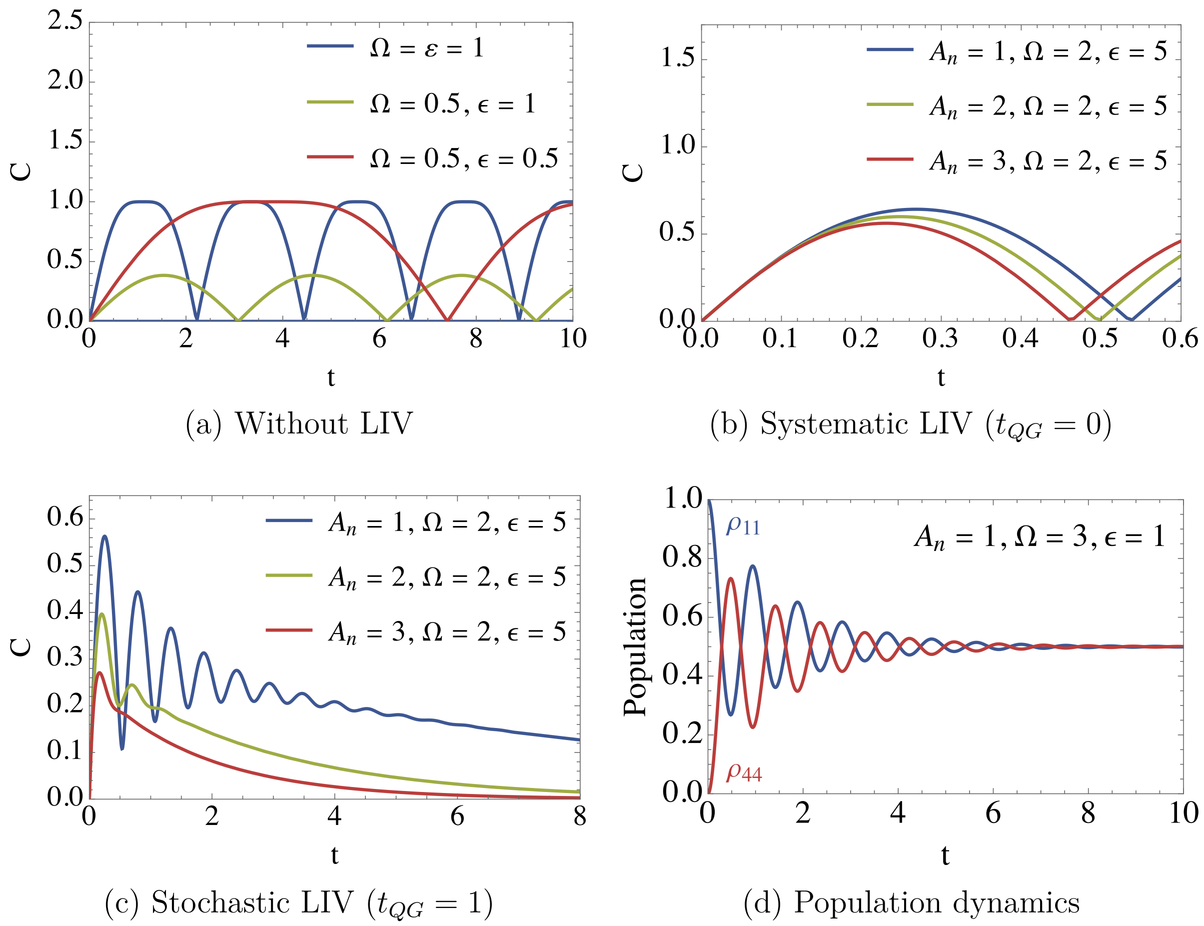


Figure 5.2: Figs.(a)-(c) describe the concurrence for an initially unentangled state ($\theta = 0$) for the cases without LIV ($A_n = 0$), with systematic LIV ($t_{QG} = 0$), and with stochastic LIV ($t_{QG} = 1$), respectively. Fig.(d) describes the population with stochastic LIV ($t_{QG} = 1$). We set $\hbar = c = 1$.

### 5.3.1 Mesoscopic Particles

Following [126], we consider particles with separation $d = 200\,\mu\text{m}$, position shift $L = 100\,\mu\text{m}$, mass $M = 10^{-14}\,\text{kg}$, and frequency $\omega = \epsilon/\hbar = 1\,\text{Hz}$. The resulting entanglement timescale $\tau_E \sim 1\,\text{s}$ matches the requirements for measurable gravitationally induced entanglement phases in the proposed experimental setup. While these numerical values coincide, they represent distinct physical quantities. A shorter $\tau_E$ would simply compress the oscillations shown in Fig. 5.2(c), with entanglement remaining observable on average if decoherence is sufficiently suppressed.

For these parameters, the LIV decoherence timescale becomes $\tau_{D,1} \approx 2 \times 10^{19}\,\text{s} \sim 600$ billion years for $n = 1$, increasing further for larger $n$. This represents a lower bound, as arguments suggesting the quantum gravity energy scale should grow with particle number would push this timescale even higher. Consequently, LIV effects would not produce measurable decoherence in this configuration.

To assess the generality of this conclusion, we note that [126] predicts measurable gravitational entanglement between masses $m_1$ and $m_2$ over timescale $\tau$ when:

$$\frac{Gm_1m_2}{\hbar(d-L)}\tau + \frac{Gm_1m_2}{\hbar(d+L)}\tau \sim 1. \tag{5.31}$$

For the reasonable $\tau \sim 1$s timescale, this requires $Gm_1m_2/D \sim \hbar\,$s, where $D$ is the system length scale. Meanwhile, the LIV decoherence timescale becomes $\frac{2^{2-n}\hbar}{(Mc^2)^{4-n}E^n}E_P^3$ when approximating $(\Delta E^{n/2})^2 \sim E^n$ and setting $t_{QG} = t_P = \hbar/E_P$. For sufficiently high energy scales $E$, this fundamental LIV decoherence could compete with coherence maintenance requirements:

$$\frac{2^{2-n}\hbar}{(Mc^2)^{4-n}E^n}E_P^3 \sim 1\,\text{s}. \tag{5.32}$$

This corresponds to energy scales:

Table 5.1: Energy scales and corresponding frequencies for $n = 1, 2, 3$.

| $n$ | Energy $E_n$ (J) | Energy $E_n$ (eV) | Frequency $\omega_n$ (Hz) |
|---|---|---|---|
| 1 | $2.5 \times 10^{-15}$ | 15.6 keV | $\sim 10^{18}$ |
| 2 | $1.0 \times 10^{-6}$ | 6.2 TeV | $\sim 10^{27}$ |
| 3 | $8.0 \times 10^{-4}$ | 5 PeV | $\sim 10^{30}$ |

This implies the need for a relativistic treatment beyond our Galilean framework for practical reasons. For the considered mesoscopic system, collisional and thermal decoherence sources dominate over LIV effects [168].

### 5.3.2 Generalization to Different Lindbladians

The parameter $n$, which determines the correction power, appears exclusively in the decoherence factor $A_n$ (Eq. (5.29)). This allows generalization to cases involving different momentum operator powers $\hat{K}^{n/2}$ and alternative $\sigma_n$ values. For example, a generic Lindblad equation:

$$\partial_t\rho(t) = -\frac{i}{\hbar}\left[\hat{H}_0, \rho(t)\right] - \sigma_n\left[\hat{K}^{n/2}(t), \left[\hat{K}^{n/2}(t), \rho(t)\right]\right], \tag{5.33}$$

with $n = 4$ and $\sigma_n = \sigma_{PI} = 16M^2\ell_P^4 t_P/\hbar^6$, recovers the Petruzziello-Illuminati model based on the Generalized Uncertainty Principle [157]. The decoherence time $\tau_D^{PI} = 1/(\sigma_{PI}(\Delta E^2)^2)$ becomes $\tau_D^{PI} \sim 10^{141}$ s for our mesoscopic particles. Reference [159] analyzed similar decoherence effects in mechanical oscillators.

## 5.4 Discussion

Using tools presented in [157], we constructed a Lindblad equation based on a modified dispersion relation with a fluctuating Planck-scale parameter. In this context, the quantum spacetime, characterized by deviations from the standard relativistic expression, functions as an unavoidable environment that necessarily interacts with every quantum system. Equipped with this evolution equation, we analyzed its impact on a system composed of two cat states interacting gravitationally in a superposition of position eigenstates (gravcat states). For closed quantum systems, these particles evolve into an entangled pair mediated by Newtonian gravitational interaction. We calculated the concurrence as an entanglement quantifier for this system and observed its oscillatory behavior over time.

When incorporating terms originating from quantum spacetime effects, we examined the system's evolution and found that entanglement gradually vanishes due to the influence of stochastic Planck-scale parameters. Our analysis revealed that because quantum gravity effects are extremely small, the timescale for such fluctuations to dissipate quantum correlations is remarkably long. Consequently, such systems would more likely experience decoherence from other environmental factors before quantum spacetime effects become significant in the infrared regime. (The ultraviolet regime appears to bring this timescale to more accessible levels, though this would require more sophisticated analytical tools.)

The gravcat states we considered represent a simplified version of systems discussed in the literature concerning interactions between spatial superposition states. Therefore, it would be valuable for future investigations to examine more detailed proposals, such as those in [126, 127, 169, 168], before drawing definitive conclusions. This is particularly important because quantum gravity effects, even in the infrared regime, can sometimes produce unexpected amplifications of apparently mild effects [170].

Beyond stochastic fluctuations, quantum gravity may also result in the noncommutativity of spacetime. Chapter 6 examines how deformation in the energy composition law, a feature of noncommutative spacetimes, can generate and modulate quantum correlations between physical systems, even without direct interaction.

CHAPTER 6

# Noncommutative Quantum Correlations

The central question this chapter explores is whether deformations in the symmetries of quantum spacetime can affect quantum systems even in the absence of direct gravitational interactions. In the previous chapters, we examined how MDRs alter single-particle motion and how stochastic fluctuations induce decoherence.

In quantum mechanics, correlations between distinct particles arise from direct interactions or from a shared environment. Free particles that evolve independently do not become entangled. This principle forms the basis of both scattering theory and the operational concept of locality in nonrelativistic quantum systems.

In the context of noncommutative or deformed spacetimes, the composition of energy and momentum no longer follows the standard linear addition law. Instead, it is governed by generalized algebraic structures such as Hopf algebras, leading to modified conservation laws. This deformation implies that even for free particles, the total momentum of a multiparticle system is not simply the sum of the individual contributions.

Such modifications can be encoded through a coproduct structure for the energy-momentum operators. For example, within the $\kappa$-Poincaré framework, the deformed addition of two single-particle momenta introduces non-linear terms proportional to the deformation parameter, which is expected to be suppressed by the Planck scale. Importantly, these deformations admit a nonrelativistic limit in which residual traces of quantum spacetime effects may still be present.

A direct consequence of these deformed symmetries is that the time evolution of quantum systems is altered. Instead of being fully governed by unitary Hamiltonian dynamics, the system is effectively described by a Lindblad-type equation, reflecting the fact that quantum spacetime behaves as an open environment. In this picture, decoherence arises as a fundamental phenomenon, not due to conventional environmental interactions but as a manifestation of the underlying quantum structure of spacetime.

This framework provides the foundation for the analysis developed in this chapter. By focusing on two-particle systems, we aim to investigate how deformed symmetry transformations induce effective interactions that compete with decoherence, leading to the emergence and persistence of quantum correlations. Throughout this chapter, we use natural units $\hbar = c = 1$, unless otherwise stated.

## 6.1 Deformation of Spacetime Symmetries

One of the most studied examples of noncommutative spacetimes is the so called $\kappa$-Minkowski spacetime given by the following commutation relation between coordinates

$$\left[x^0, x^i\right] = i\ell x^i\,, \qquad \left[x^i, x^j\right] = 0, \tag{6.1}$$

where Latin indices span space coordinates, and $\ell$ is a length scale, supposedly of the order of the Planck length.[1] A generic feature of noncommutative spacetimes is that the description of free particles as plane waves is generalized to noncommutative ordered exponentials [130] : $e^{ik_\mu x^\mu}$ :, since the parameters appearing in these exponentials are coordinates of a non-Abelian Lie group.

This means that if quantum states are given in the momentum representation, they are labeled by momentum coordinates on the group $|k(g)\rangle$ such that the action of the translation generators, which are the spatial momentum operators, is $P_\mu|k(g)\rangle = k_\mu(g)|k(g)\rangle$. As a consequence, these momentum eigenvalues obey a deformed composition law $k_\mu(g) \oplus k_\mu(h) = k_\mu(gh)$. From this, we can define the inverse group element $k(g^{-1})$ in which $k(g) \oplus k(g^{-1}) = 0$. The action of the momentum operator on the dual space elements allows one to define the antipode operator $S(P)$ such that $P_\mu\langle k(g)| = k_\mu(g^{-1})\langle k(g)| = \langle k(g)|S(P_\mu)$. Besides that, the representation of the momentum operator on a two-particle state is given by the coproduct map

$$\Delta P_\mu \left(|g\rangle \otimes |h\rangle\right) = k_\mu(gh) \left(|g\rangle \otimes |h\rangle\right)\,. \tag{6.2}$$

This general approach finds a natural application in the $\kappa$-Minkowski spacetime (see, for instance [171, 161] and references therein), in which these structures are given by

$$S(P_0) = -P_0 + \ell \mathbf{P}^2 \Pi_0^{-1}\,, \tag{6.3}$$

$$S(P_i) = -P_i \Pi_0^{-1}\,, \tag{6.4}$$

$$\Delta P_0 = P_0 \otimes \Pi_0 + \Pi_0^{-1} \otimes P_0 + \ell \sum_i P_i \Pi_0^{-1} \otimes P_i\,, \tag{6.5}$$

$$\Delta P_i = P_i \otimes \mathbb{1} + \mathbb{1} \otimes P_i\,, \tag{6.6}$$

[1] It is also commonly used the notation $\kappa = \ell^{-1}$ to refer the energy scale $\kappa$, in natural units, as the one that governs quantum gravity corrections.

where

$$\Pi_0 = \ell P_0 + \sqrt{1 - \ell^2 P^\mu P_\mu}\,, \tag{6.7}$$

$$\Pi_0^{-1} = \frac{\sqrt{1 - \ell^2 P^\mu P_\mu} - \ell P_0}{1 - \ell^2 \mathbf{P}^2}\,, \tag{6.8}$$

$$P^\mu P_\mu = -P_0^2 + \mathbf{P}^2 = -P_0^2 + \sum_i P_i P_i\,. \tag{6.9}$$

This way of expressing the generators of translations and its action on two-particle states is called the *classical basis* of the $\kappa$-Poincaré algebra [172]. It is named this way because the symmetry generators and, consequently, the mass Casimir operator of the algebra is undeformed for single particle systems, and the modifications are concentrated on the multi-particle sector. An interesting aspect of this approach is that it admits a nonrelativistic limit that retains traces of the quantum gravity scale, i.e., after recovering the speed of light $c$ withing the symmetry generators and quantum gravity parameter $\ell$, one can consider the nonrelativistic (Galilean) limit by taking $c \to \infty$. In this classical basis, the nonrelativistic limit of the antipode and coproduct takes the form:

$$S(P_0) = -P_0 - i\ell \mathbf{P}^2, \tag{6.10}$$

$$S(P_i) = -P_i + \ell P_i P_0\,, \tag{6.11}$$

$$\Delta P_0 = P_0 \otimes \mathbb{1} + \mathbb{1} \otimes P_0 - i\ell \sum_i P_i \otimes P_i, \tag{6.12}$$

$$\Delta P_i = P_i \otimes \mathbb{1} + \mathbb{1} \otimes P_i\,. \tag{6.13}$$

The form of the coproduct operators leads to a modified, non-Abelian conservation law for energy and momentum. When applied to a composite system $|g\rangle \otimes |h\rangle$, the momentum eigenvalues of the composite system are then given by:

$$g_0 \oplus h_0 = g_0 + h_0 + \ell \vec{g} \cdot \vec{h}, \tag{6.14}$$

$$g_i \oplus h_i = g_i + h_i, \tag{6.15}$$

where $(g_0, g_i)$ represents the energy and momentum (in Cartesian coordinates) of the single-particle state $|g\rangle$ (and similarly for $h$).

### 6.1.1 Effective Lindblad Evolution

The presence of deformed symmetries induces a deformation of the commutator, given by the adjoint action presented in [171, 161]. This action selects a representative of the vector space $\mathcal{R}_G$, spanned by the generators of the symmetry algebra $G \in \mathcal{R}_G$, and acts on the quantum system $\mathcal{A}_{\mathcal{H}}$ defined on a Hilbert space $\mathcal{H}$ as:

$$\mathrm{ad}_{\clubsuit}\spadesuit : \mathcal{R}_G \times \mathcal{A}_{\mathcal{H}} \to \mathcal{A}_{\mathcal{H}}, \quad \mathrm{ad}_G O = (\mathrm{id} \otimes S)\Delta G \diamond O, \tag{6.16}$$

where id is the identity operator, $\Delta G$ is the coproduct operator, $S$ is the antipode map, and $\diamond$ is the operator defined as:

$$(a \otimes b) \diamond O \doteq aOb. \tag{6.17}$$

When the coproduct operator is of the form $\Delta G = \sum_i a_i \otimes b_i$, then $(\mathrm{id} \otimes S)\Delta G = \sum_i a_i \otimes S(b_i)$, which implies that $\mathrm{ad}_G O = \sum_i a_i O S(b_i)$. If $O = \rho$ is the density matrix of a quantum system and $\Delta G = P_0 \otimes \mathbb{1} + \mathbb{1} \otimes P_0$, then $\mathrm{ad}_{P_0}\rho = [P_0, \rho]$. This means that the evolution equation of a system with Galilean invariance can be written as $i\partial_t \rho = \mathrm{ad}_{P_0}\rho$. For a quantum spacetime with deformed symmetries, the generalization of this evolution equation in a way that preserves the hermiticity of $\rho$ is:

$$i\partial_t \rho = \frac{1}{2}\left\{\mathrm{ad}_{P_0}\rho - [\mathrm{ad}_{P_0}\rho]^\dagger\right\}. \tag{6.18}$$

A straightforward calculation based on the above definition can be described as follows. Using the coproduct and antipode in the nonrelativistic limit, the adjoint action reads

$$\mathrm{ad}_{P_0}\rho = (\mathrm{id} \otimes S)\Delta P_0 \diamond \rho = P_0 \rho - \rho S(P_0). \tag{6.19}$$

Substituting the antipode $S(P_0) = -P_0 - i\ell \mathbf{P}^2$, we obtain

$$\mathrm{ad}_{P_0}\rho = [P_0, \rho] - i\ell \mathbf{P}^2 \rho. \tag{6.20}$$

The generator of the dynamics is constructed by enforcing Hermiticity through

$$i\partial_t \rho = \frac{1}{2}\left\{\mathrm{ad}_{P_0}\rho - [\mathrm{ad}_{P_0}\rho]^\dagger\right\}. \tag{6.21}$$

Using $(\mathbf{P}^2\rho)^\dagger = \rho \mathbf{P}^2$ and $\mathbf{P}^2 = \sum_i P_i^2$, this yields

$$\partial_t \rho = -i[P_0, \rho] - \frac{\ell}{2}\left(\mathbf{P}^2\rho + \rho\mathbf{P}^2 - 2\sum_i P_i \rho P_i\right), \tag{6.22}$$

which has the standard double-commutator structure of a Lindblad equation.

This implies that the noncommutative spacetime acts effectively as an environment of an open quantum system. Considering a free nonrelativistic particle, we can describe the elements of the density matrix in the momentum representation as $\rho_{pq} = \langle \mathbf{p}|\rho|\mathbf{q}\rangle$, $\mathbf{p}$ represents the components of the particle's momentum. From the dispersion relation

$E(p) = p^2/2m$, the evolution of these elements is

$$\partial_t \rho_{pq} = \left[ -\frac{i}{\hbar}(E(p) - E(q)) - \frac{\ell}{2}(\mathbf{p} - \mathbf{q})^2 \right] \rho_{pq}. \tag{6.23}$$

whose solution is

$$\rho_{pq}(t) = \rho_{pq}(0) \exp\left[ -it\,(E(p) - E(q)) - \frac{\ell t}{2}(\mathbf{p} - \mathbf{q})^2 \right]. \tag{6.24}$$

We observe that the off-diagonal elements ($\mathbf{p} \neq \mathbf{q}$) of the density matrix exponentially decay. The time scale of such decay is called decoherence time, and in this model is given by

$$\tau_D = \frac{2}{\ell(\mathbf{p} - \mathbf{q})^2}. \tag{6.25}$$

Since the length scale of quantum gravity should be very small, the decoherence time should be very large and the decoherence is suppressed by quantum gravity deformations. The presence of a Lindblad equation implies that a quantum spacetime acts as a source of fundamental decoherence in quantum systems [161]. In the next section, we shall deal with corrections coming from the Hamiltonian side of the evolution equation, when we are able to separate the quantum system in two sectors, defined by two particles, where the conservation law implies a modified Hamiltonian of the system.

## 6.2 Two-Particle Model with Deformed Composition Law

The modification of the energy conservation law, given by Eq. (6.14), leads to the definition of the Hamiltonian for a system of two free particles as:

$$H = H_0 \otimes \mathbb{1} + \mathbb{1} \otimes H_0 + \ell \sum_i P_i \otimes P_i, \tag{6.26}$$

where $H_0$ is the Hamiltonian of a free particle. Notably, the new term in (6.26) resembles a momentum-dependent potential that may induce correlations between the particles.

In the following, we will analyze the case of two interacting particles, each occupying a defined energy state.

### 6.2.1 Two-Energy States

To estimate these effects, we consider a simple case of two particles, each modeled as a two-level system. Individually, each particle can occupy energy states with energies $E_{(g)} = \dfrac{\epsilon - \omega}{2}$ or $E_{(e)} = \dfrac{\epsilon + \omega}{2}$, where $\epsilon > \omega$ ensures positive energies. If the energy composition were undeformed, the Hamiltonian of this system would be:

$$H_{\text{und}} = \epsilon \mathbb{1} \otimes \mathbb{1} + \frac{\omega}{2}(\sigma_z \otimes \mathbb{1} + \mathbb{1} \otimes \sigma_z), \tag{6.27}$$

where $\sigma_z$ is the $z$-Pauli matrix. The two-particle state would then be described by two indices $|ij\rangle$, where $(ij) = \{g, e\}$ labels whether the first or second particle is in the ground or excited state.

Now, suppose the particles are in a superposition of momenta. Typically, this would not affect the system's description, but since the inner product of momenta influences the energy of the composite system, the direction of each momentum becomes important. For simplicity, we consider a one-dimensional case, which suffices for our purposes. Here, each particle can move in either the positive ($|+\rangle$) or negative direction ($|-\rangle$), meaning the composite system is described by a state $|ij\alpha\beta\rangle$, where $(\alpha, \beta) = \{+, -\}$ labels the direction of the first or second particle.

In our model, each particle can have either positive or negative momentum. This means that the eigenvectors of direction for each particle can be written as a linear combination of energy eigenstates:

$$|\pm\rangle = \frac{1}{\sqrt{2}}(|g\rangle \pm |e\rangle). \tag{6.28}$$

This approximation is reasonable, as it can be verified by combining energy eigenfunctions of a 1D harmonic oscillator in the momentum representation, showing that this combination is concentrated in the positive or negative branch of momentum.

From the undeformed dispersion relation (since we are at the classical basis), we construct an operator that gives the modulus of the momentum of a two-level state, sharing the same energy eigenstates but with different energies for each level:

$$|P| = \text{diag}\left(\sqrt{m(\epsilon + \omega)}, \sqrt{m(\epsilon - \omega)}\right). \tag{6.29}$$

To account for the momentum direction, we note that the $x$-Pauli matrix has eigenstates given by Eq. (6.28). Thus, the Hamiltonian describing the evolution of this system is:

$$\mathcal{H} = \epsilon(\mathbb{1})^4 + \frac{\omega}{2}\left(\sigma_z \otimes \mathbb{1} \otimes \mathbb{1} \otimes \mathbb{1} + \mathbb{1} \otimes \sigma_z \otimes \mathbb{1} \otimes \mathbb{1}\right) + \ell |P| \otimes |P| \otimes \sigma_x \otimes \sigma_x, \tag{6.30}$$

where $(\mathbb{1})^4 = \mathbb{1} \otimes \mathbb{1} \otimes \mathbb{1} \otimes \mathbb{1}$, and $\mathbb{1}$ is the $2 \times 2$ identity matrix. This Hamiltonian is a $16 \times 16$ matrix, such that a direct computation shows that it is constituted by four $4 \times 4$ block matrices as follows:

$$\mathcal{H} = \begin{pmatrix} H_{11} & 0 & 0 & 0 \\ 0 & H_{-11} & 0 & 0 \\ 0 & 0 & H_{1-1} & 0 \\ 0 & 0 & 0 & H_{-1-1} \end{pmatrix}, \tag{6.31}$$

where

$$H_{ab}=\begin{pmatrix} \epsilon+\frac{a+b}{2}\omega & 0 & 0 & \ell m\sqrt{(\epsilon+a\omega)(\epsilon+b\omega)} \\ 0 & \epsilon+\frac{a+b}{2}\omega & \ell m\sqrt{(\epsilon+a\omega)(\epsilon+b\omega)} & 0 \\ 0 & \ell m\sqrt{(\epsilon+a\omega)(\epsilon+b\omega)} & \epsilon+\frac{a+b}{2}\omega & 0 \\ \ell m\sqrt{(\epsilon+a\omega)(\epsilon+b\omega)} & 0 & 0 & \epsilon+\frac{a+b}{2}\omega \end{pmatrix} \tag{6.32}$$

with $(a,b)=\{-1,1\}$. Since the evolution of this system involves Lindblad operators, we need to describe the momentum of the composite system. Given that the Lindblad operators are multiplied by $\ell$ in (6.22) and are expected to contribute only slightly, the momentum composition remains undeformed. The operator representing the sum of the momenta of the two particles is:

$$\mathcal{P}=|P|\otimes\mathbb{1}\otimes\sigma_x\otimes\mathbb{1}+\mathbb{1}\otimes|P|\otimes\mathbb{1}\otimes\sigma_x, \tag{6.33}$$

where we account for the possibility that the particles may be moving in different directions. This operator can also be expressed in block form, similar to the Hamiltonian in (6.34) as

$$\mathcal{P}=\begin{pmatrix} P_{11} & 0 & 0 & 0 \\ 0 & P_{-11} & 0 & 0 \\ 0 & 0 & P_{1-1} & 0 \\ 0 & 0 & 0 & P_{-1-1} \end{pmatrix}, \tag{6.34}$$

where

$$P_{ab}=\sqrt{m}\begin{pmatrix} 0 & \sqrt{\epsilon+a\omega} & \sqrt{\epsilon+b\omega} & 0 \\ \sqrt{\epsilon+a\omega} & 0 & 0 & \sqrt{\epsilon+b\omega} \\ \sqrt{\epsilon+b\omega} & 0 & 0 & \sqrt{\epsilon+a\omega} \\ 0 & \sqrt{\epsilon+b\omega} & \sqrt{\epsilon+a\omega} & 0 \end{pmatrix}. \tag{6.35}$$

Although $P_{ab}$ has not an $X$-shape, the matrix $(P_{ab})^2$ has this form, just like the Hamiltonian (6.32). As this operator appears explicitly in the Lindblad equation (6.22), this suggests that a natural ansatz for the density matrix consists also in a block-diagonal matrix $\rho=\operatorname{diag}(\rho_{11},\rho_{-11},\rho_{1-1},\rho_{-1-1})$, where each $\rho_{ab}$ is a $4\times 4$ $X$-shaped matrix. In fact, assuming this ansatz, the last term of the Lindblad equation (6.22) $-2\mathcal{P}\rho\mathcal{P}$ also assumes a block diagonal form of $X$-shaped matrices labeled by parameters $(a,b)$ running $\{-1,1\}$.

As a consequence of these observations, we can reduce the problem of handling the system of differential equations described by a $16\times 16$ matrix to four sets of systems of differential equations given by $4\times 4$ matrices, labeled by the parameters $(a,b)$. Specifically, for each block of matrices, obeys a Lindblad equation of the form:

$$\partial_t\rho_{ab}+i\left[H_{ab},\rho_{ab}\right]+\frac{\ell}{2}\left(P_{ab}^2\rho_{ab}+\rho_{ab}P_{ab}^2-2P_{ab}\rho_{ab}P_{ab}\right)=0. \tag{6.36}$$

Since the particles can move in any direction, there is a 25% probability for the system to be in one of the four possible configurations of parameters $(a, b) = \{-1, 1\}$. Therefore, the density matrix used to compute correlations must be averaged as:

$$\bar{\rho} = 0.25\left(\rho_{-1-1} + \rho_{-11} + \rho_{1-1} + \rho_{11}\right). \tag{6.37}$$

with elements

$$\bar{\rho}_{ij} \doteq [\bar{\rho}]_{ij} = 0.25\left([\rho_{-1-1}]_{ij} + [\rho_{-11}]_{ij} + [\rho_{1-1}]_{ij} + [\rho_{11}]_{ij}\right) \tag{6.38}$$

To analyze this state, we consider solutions to the Lindblad equation, following an ansatz similar to the one adopted in [173], assuming the initial condition:

$$|\Psi\rangle = \sin\theta|eg\rangle + \cos\theta|ge\rangle, \tag{6.39}$$

which represents an unentangled state when $\theta = 0$ and a maximally entangled state (Bell state) when $\theta = \pi/4$. Thus, the parameter $\theta$ allows us to control the initial level of entanglement. The corresponding averaged matrix for this initial conditions is

$$\bar{\rho}(t=0) = \begin{pmatrix} 0 & 0 & 0 & 0 \\ 0 & \cos^2(\theta) & \sin(\theta)\cos(\theta) & 0 \\ 0 & \sin(\theta)\cos(\theta) & \sin^2(\theta) & 0 \\ 0 & 0 & 0 & 0 \end{pmatrix}. \tag{6.40}$$

In appendix B.1, we solve this Lindblad equation analytically, and derive its asymptotic behavior for late times.

## 6.3 Quantum Correlations

Quantum spacetime is typically responsible for introducing dissipation in the form of decoherence in quantum systems (see, for instance, [157]). However, a unique signature of the deformation of the relativity principle is the presence of modified composition laws for energy and momentum. For single-particle states, decoherence emerges as a consequence of the modified evolution equation (6.22), as discussed in [161]. However, for multiple particles, the introduction of interaction-like terms that depend on the momenta of each particle may introduce correlations that initially compete with decoherence effects. In this section, we will consider four quantifiers of correlations: concurrence, as a measure of entanglement; the $l_1$-norm of coherence, quantum mutual information, and local quantum Fisher information.

### 6.3.1 Concurrence

Entanglement is the most profound quantum correlation between systems and was first highlighted in the work by Einstein, Podolsky, and Rosen [174], which aimed to point out an incompleteness in the quantum description of the world. The modern definition of entanglement dates back to the works by Werner [175], where this concept was extended to mixed states. Today, entanglement plays a fundamental role in quantum cryptography [176], quantum computing [177], and quantum teleportation [178].

A useful quantifier of entanglement for a two-qubit state, described by an $X$-shaped matrix, is the concurrence. For a $4 \times 4$ matrix, it reads [165, 179]:

$$\mathcal{C} = 2 \max \left\{ |\bar{\rho}_{23}| - \sqrt{\bar{\rho}_{11}\bar{\rho}_{44}}, |\bar{\rho}_{14}| - \sqrt{\bar{\rho}_{22}\bar{\rho}_{33}}, 0 \right\}, \tag{6.41}$$

where the density matrix used is the averaged one described in (6.37). The system of differential equations (6.36) for the initial condition (6.39) was solved analytically for arbitrary $\theta$ in section B.1. The asymptotic behavior of the system is quoted below:

$$\lim_{t\to\infty} \rho_{11} = \lim_{t\to\infty} \rho_{22} = \lim_{t\to\infty} \rho_{33} = \lim_{t\to\infty} \rho_{44} = \frac{1}{4}, \tag{6.42}$$

$$\lim_{t\to\infty} \rho_{14} = \lim_{t\to\infty} \rho_{23} = \frac{\sin(\theta)\cos(\theta)}{2} = \frac{\sin(2\theta)}{4}. \tag{6.43}$$

We verify that the diagonal elements of the density matrix eventually larger than the off-diagonal ones when $\theta \neq \pi/4$. This means that in a finite time, the concurrence becomes null. For the case where $\theta = \pi/4$, this happens asymptotically.

In Fig. 6.1, we observe the concurrence for different initial conditions. The qualitative behavior of the quantities discussed in this chapter does not change significantly for different values of the parameter $\ell$. Only the scale in which they occur is modified. Therefore, without loss of generality, we consider $\ell$ with the same order of magnitude of the other parameters of the model. We see that a system of two particles can be prepared in an unentangled state ($\theta = 0$) and become entangled over time due to the modified energy conservation in deformed relativity (black, solid curve). By increasing the angle to $\theta = 0.05$, we see that although the state is initially partially entangled, decoherence effects reduce the concurrence to zero. However, the modified composition law effects are still strong enough to reentangle the system before it becomes completely unentangled (blue, dash-dotted curve). For $\theta = \pi/12$, the system starts more entangled before experiencing a drop in this correlation (purple, dashed curve). This behavior repeats for the initial Bell state ($\theta = \pi/4$) (red, dotted curve). We considered unrealistically large values of the parameters for the sake of clarity of the figures, but this does not affect the main results. In fact, we are considering a value of the $\ell$-parameter of the same order of the other parameters in this plot, but in reality, it should be much smaller, since it is related to the Planck length scale of quantum gravity.

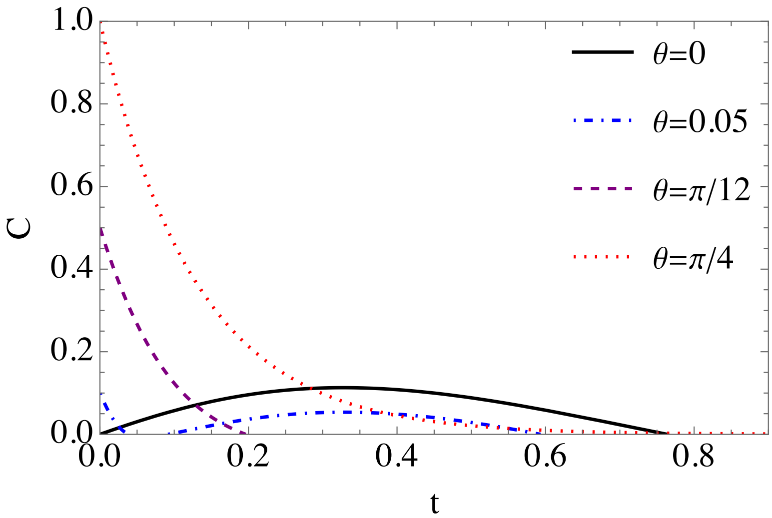


Figure 6.1: Concurrence for different initial conditions determined by $\theta$. The parameters used are $\ell = 1$, $m = 1$, $\epsilon = 1$, and $\omega = 0.5$.

Notice that such mechanism is conceptually different than the one from the gravitationally-induced entanglement procedure [126, 127] that we discussed in the previous chapter. In that case, the Newtonian potential and a superposition of position states (which creates an effective superposition of gravitational interactions) is responsible for creating entanglement between the two massive particles. In our case, we interpret that after an interaction, considering that the particles are in a momentum superposition, the initially separate state of the two quantum particles, becomes entangled due to the noncommutative properties of spacetime. In the former case, it has been argued that the Newtonian interaction creates a communication channel that violates the Local Operation and Classical Communication (LOCC) theorem, which, as a consequence, therefore implies that the gravitational interaction is of quantum nature in essence. In our case, we consider that the particles are free, i.e., there is no interaction potential that serves as a channel for communication between them. The term $\vec{p}_1 \cdot \vec{p}_2$ that corrects the undeformed Hamiltonian is not, in fact, an interaction term due to some force. Although it, in a broad sense, "interacts" the particles through a scalar product, its presence here is purely kinematical in nature.

The extra, non-local term that deforms the energy conservation is introduced by the same mechanism that creates decoherence between the particles, i.e., the underlying quantum algebra that is responsible for the preservation of the relativity principle at the Planck scale. In fact, as we verified in Fig.6.1, the time scale of the decoherence is the same as the entanglement generation. This entanglement generation is due to the apparent non-locality of this extra term in the conservation law. Non-local terms can, in fact, create entanglement and circumvents the LOCC theorem [180].

The non-local nature of modified conservation laws in corrections of classical systems due to quantum gravity has been a matter of debate in the past years [181], which has led to the development of the Principle of Relative Locality [48], that states that the locality of interactions is an observer-dependent statement, that can be effectively described via modified composition laws. While the Relative Locality framework considers energy-momentum conservation using classical mechanics tools, we are exploring the possible non-local behavior from a quantum mechanical perspective (due to entanglement). Although entanglement emerges in this approach, we also have the presence of decoherence effects, that naturally suppresses such behavior to a limited time window.

If we consider the product state determined by $\theta = 0$, then, from [182], the time scale that governs the entanglement of this system is given by $T_{\text{ent}} = (\ell \Delta P^2)^{-1}$, where $\Delta P$ is the standard quantum uncertainty of the momentum. If we average the uncertainty of the observable as $\Delta P = 0.25 \sum_{ab} \Delta P_{ab}$ and express the result by restoring the speed of light and Planck's constant, we find:

$$T_{\text{ent}} = \frac{\hbar E_{\text{QG}}}{2mc^2 \epsilon}, \tag{6.44}$$

where $E_{\text{QG}} = \ell^{-1}$ is the quantum gravity energy scale that measures deviations from standard symmetries. Notice that this expression has an energy dependence similar to the decoherence time found in [161], $\tau_D \sim 2E_{\text{QG}}/p^2 \sim E_{\text{QG}}/(mE)$. For the parameters used in Fig. 6.1, $T_{\text{ent}}$ is of the order of 0.5 in natural units, which is consistent with Fig. 6.1. To understand this, let us suppose that we prepare such an unentangled superposition of two free particles. The uncertainty in the momentum of each particle translates into the time that it takes to observe the entanglement generation between them.

If the energy scale of the particles is $\epsilon$, then $T_{\text{ent}}\epsilon \sim \hbar E_{\text{QG}}/(mc^2)$. For instance, consider a pair of ions [183] with a mass of the order $m = 3.7 \times 10^{10}\,\text{eV}$, where the energy scale of electronic transitions is of the order $\epsilon \sim 1\,\text{eV}$, the Planck energy $E_{\text{QG}} = E_{\text{Planck}} = 1.2 \times 10^{28}\,\text{eV}$ and $\hbar = 6.6 \times 10^{-16}\text{eV} \cdot \text{s}$. We can estimate the entanglement time scale $T_{\text{ent}} = 214\,\text{s} \approx 3.6\,\text{min}$. If an entangled pair of ions has approximately 100 elementary particles and supposing that the quantum gravity energy scale grows linearly with the number of particles [81, 148], the entanglement time becomes of the order of hours. This means that it would be necessary to preserve the quantum properties of this superposition of two particle system along this time scale in order to probe entanglement generation due to the uncertainty in their momenta. Besides that, if the quantum gravity scale $E_{\text{QG}}$ grows with the number of elementary particles, then the entanglement time scale grows too. Notice that this time scale is larger than the one typically considered in the gravitationally induced entanglement proposals [126, 127] of $\sim 1$ s (also for different experimental setups, of course). But if one is capable of designing such an experiment, it would be possible at least to set interesting constraints on the quantum gravity scale not so far from the Planck scale.

An interesting opportunity could be achieved when we consider long lived qubits, like trapped ions. For instance, in [184] it is reported coherence time exceeding one hour for a single qubit. Coherence time of system of qubits can serve as laboratory tests for deformations of the conservation of energy and deformed Hamiltonians. Of course, in models in which $\Delta P$ can be enlarged would reduce the entangling time, which could be interesting for experimental tests.

Curiously, if we make $\epsilon = mc^2$ in (6.44), and we compare it with the entanglement time scale of the gravitationally induced setting $T_{\mathrm{GIE}} = \hbar L/(Gm^2)$ (where $L$ is the scale of the relative distance between the particles of the system), a straightforward calculation shows that $L = \ell$. This means that at the Planckian regime, the gravitational interaction between the particles involved in the scenario discussed in this chapter cannot be ignored.

### 6.3.2 The $l_1$-Norm of Coherence

Coherence is an important ingredient in various areas of physics, such as quantum optics, quantum information, solid-state physics, and biology [185]. The first axiomatic approach to quantifying coherence was proposed in [186], and since then, several approaches have been developed. For a review, we refer the reader to [187]. In this chapter, we use the $l_1$-norm of coherence, introduced by [188], which is a quantifier based on matrix norms and can be straightforwardly applied to the type of density matrix we are analyzing.

For an $X$-shaped density matrix, it reads:

$$C_{l_1} = \sum_{i \neq j} |\bar{\rho}_{ij}| = 2(|\bar{\rho}_{14}| + |\bar{\rho}_{23}|), \tag{6.45}$$

which simply measures the magnitude of the off-diagonal elements of $\bar{\rho}$.

In Fig. 6.2, we see that for $\theta < \pi/4$, the Hamiltonian creates correlations and initially dominates over decoherence effects, sharing the behavior of the concurrence discussed in the previous subsection. Over time, the Lindbladian terms eventually balance the deformed composition law contribution. Asymptotically, we observe a perfect balance between the creation of correlations due to the Hamiltonian and decoherence effects due to the Lindblad equation, which preserves the coherence of the system when $\theta \neq 0$. This is due to the asymptotic behavior of the density matrix elements shown in appendix B.1. Notably, for an initial Bell state ($\theta = \pi/4$), since the system begins maximally coherent, these two contributions balance each other from the outset. In fact, the open quantum spacetime also creates correlations in this system, as we will discuss in Section 6.4, meaning that while it dissipates entanglement, it helps maintain other correlations between the particles for initially partially entangled states.

We observe that such behavior is due to the survival of the off-diagonal elements of the density matrix as can be seen in Eq.(6.43). For an initially unentangled state, the off-diagonal elements vanish in time as can be seen in Fig. 6.3a. In this case, we see that the off-diagonal elements $|\bar{\rho}_{14}|$ (orange curve) and $|\bar{\rho}_{23}|$ (purple curve) asymptotically

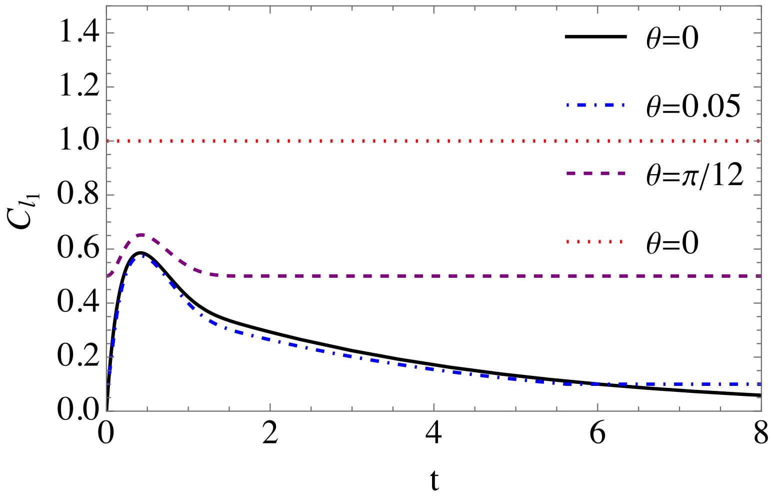


Figure 6.2: The $l_1$-norm of coherence for different initial conditions determined by $\theta$. The parameters used are $\ell = 1$, $m = 1$, $\epsilon = 1$, and $\omega = 0.5$.

survive and assume the same value. Also notice in Fig. 6.3a that, at initial times, the element $|\bar{\rho}_{23}|$ (purple curve) is indeed larger than $\bar{\rho}_{11}\bar{\rho}_{44}$ (blue curve), which is the reason why there is an initial entanglement due to the modified composition law. Also notice in Fig. 6.3b that for an initially partially entangled state, the off-diagonal elements grow again and approach each other according to (6.43).

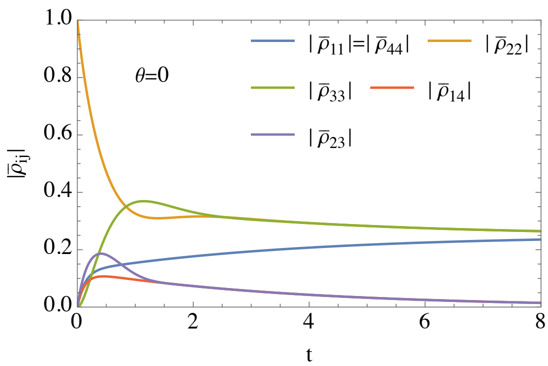


(a) Behavior of the average density matrix for $\theta = 0$.

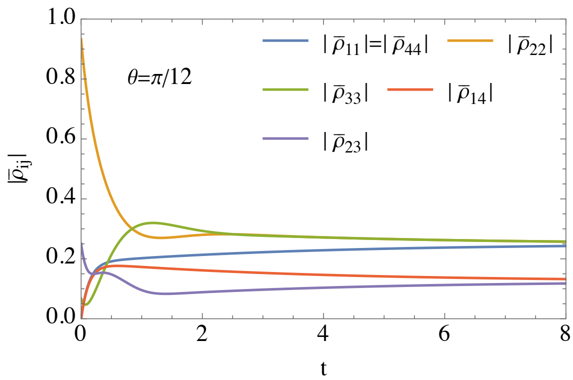


(b) Behavior of the average density matrix for $\theta = \pi/12$.

Figure 6.3: Behavior of the average density matrix elements $\bar{\rho}_{ij}$ for the initial condition $\theta = 0$ and $\theta = \pi/12$. We assume parameters $\ell = 1$, $m = 1$, $\epsilon = 1$, $\omega = 0.5$.

This behavior is not entirely new in condensed matter systems. For instance, a similar phenomenon can be observed in [173], which considers a spin-1/2 Ising-$XYZ$ chain model. There, one also observes the disappearance and resurgence of entanglement and coherence, with the stabilization of quantum correlations over time.

### 6.3.3 Quantum Mutual Information

An important quantifier of quantum correlations beyond entanglement is the Quantum Discord. By calculating it, we can determine whether the balance between the Hamiltonian and the Lindbladian dissipates all quantum correlations or only entanglement. The definition of quantum discord uses the concept of *mutual information* between two random variables [189, 190], which is the correlations that we will consider in this subsection. For a system consisting of two subsystems, say $A$ and $B$ (e.g., the two particles considered in this chapter), the density matrix is written as $\rho^{AB}$, which in our case is $\bar{\rho}$. The quantum mutual information is given by:

$$I(\rho^{AB}) = S(\rho^A) + S(\rho^B) - S(\rho^{AB}), \tag{6.46}$$

where $S(\rho) = -\mathrm{Tr}[\rho \log_2 \rho]$ is the von Neumann entropy, which measures the uncertainty of a quantum state $\rho$.

The quantity $\rho^A$ is the reduced density operator of subsystem $A$, defined as:

$$\rho^A = \mathrm{Tr}_B[\rho^{AB}], \tag{6.47}$$

where $\mathrm{Tr}_B$ is the partial trace over subsystem $B$, given by:

$$\mathrm{Tr}_B[\rho^{AB}] = \sum_{k=1}^{d} (\mathbb{1}_A \otimes \langle k_B|)\rho^{AB}(\mathbb{1}_A \otimes |k\rangle_B), \tag{6.48}$$

where $d$ is the dimension of subsystem $B$, $\mathbb{1}_A$ is the identity operator of subsystem $A$ (in our case, $\mathrm{diag}(1,1)$), and $\{|k\rangle_B\}$ is an orthonormal basis of subsystem $B$ [191, 192]. In our case, $d = 2$, and we consider the computational basis $\{|k\rangle_B\} = \{|0\rangle, |1\rangle\}$. For a $4 \times 4$ matrix with elements $[\rho^{AB}]_{ij} = \rho_{ij}$, we have:

$$\rho^A = \mathrm{Tr}_B(\rho^{AB}) = \begin{pmatrix} \rho_{11} + \rho_{33} & \rho_{12} + \rho_{34} \\ \rho_{21} + \rho_{43} & \rho_{22} + \rho_{44} \end{pmatrix}, \tag{6.49}$$

$$\rho^B = \mathrm{Tr}_A(\rho^{AB}) = \begin{pmatrix} \rho_{11} + \rho_{22} & \rho_{13} + \rho_{24} \\ \rho_{31} + \rho_{42} & \rho_{33} + \rho_{44} \end{pmatrix}. \tag{6.50}$$

This procedure provides a way to derive the state of $A$ by tracing out the degrees of freedom of $B$, and vice versa. It ensures the correct measurement statistics for measurements made on subsystems $A$ and $B$ [193].

For a classical system, there is an equivalent way to define mutual information. The Shannon entropy is the classical counterpart of the von Neumann entropy. Consider a classical system described by two random variables $X$ and $Y$, where $p_x$ is the probability that $X$ takes the value $x$, $p_y$ is the probability that $Y$ takes the value $y$, and $p_{x,y}$ is the probability that a measurement of $(X,Y)$ yields $(x,y)$. The Shannon entropy for $X$ is given by $H(X) = -\sum_x p_x \log_2 p_x$.

From Bayes' rule, the probability that $X$ takes the value $x$, given that $Y$ takes the value $y$, is $p_{x|y} = p_{xy}/p_y$. This allows us to write:

$$H(X,Y) = -\left(\sum_y p_y \log_2 p_y\right)\left(\sum_x p_{x|y}\right) - \sum_y p_y \left(\sum_x p_{x|y} \log_2 p_{x|y}\right) = H(Y) + H(X|Y), \tag{6.51}$$

where $H(X|Y) = \sum_y H(X|y)$ is the conditional entropy, representing the amount of information needed to describe the outcome of $X$ given the outcome of $Y$. Thus, there are two equivalent ways, $I$ and $J$, to describe mutual information for a classical system:

$$I(X,Y) = H(X) + H(Y) - H(X,Y), \tag{6.52}$$

$$J(X,Y) = H(X) - H(X|Y). \tag{6.53}$$

A quantum analog of the conditional entropy for a bipartite system $\rho^{AB}$ was introduced by Ollivier and Zurek [190]:

$$S(A|\{\Pi_i^B\}) = \sum_i p_i S(\rho_i^A), \tag{6.54}$$

where $\{\Pi_i^B\}$ are orthogonal measurement operators on subsystem $B$, and $p_i = \mathrm{Tr}[\Pi_i^B \rho^{AB}]$ is the probability of obtaining outcome $i$. Additionally, $\rho_i^A = \mathrm{Tr}_B[\Pi_i^B \rho^{AB}]/p_i$ is the post-measurement state of subsystem $A$. Thus, the quantum version of $J$ defined in (6.53) is:

$$J(\rho^{AB})_{\{\Pi_i^B\}} = S(\rho^A) - S(A|\{\Pi_i^B\}), \tag{6.55}$$

which depends on the measurement operator $\Pi_i^B$ and represents the amount of information gained about $A$ by measuring $B$. The quantum discord is the difference between the expressions (6.46) and (6.55), minimized over all von Neumann measurements [2]. It is not a simple task to minimize this difference and several works have been dedicated to finding analytical expressions for this quantifier [194, 195, 196, 197]. To analyze study correlations of the discord type, we will consider the Local Quantum Fisher Information in the next subsection. Below, we will describe the quantum mutual information between the two particles as a quantifier of correlations. In Appendix B.2, we express this quantity for any $X$-state.

[2] A general quantum measurement is described by a collection $\{E_i\}$ of measurement operators that satisfy the completeness equation: $\sum_i E_i^\dagger E_i = \mathbb{1}$. For a projective measurement, the operators $E_i$ are orthogonal projectors: $E_i E_j = \delta_{ij} E_i$. A von Neumann measurement is a special type of projective measurement where the measurement operators $E_i$ are orthogonal projectors with rank one (i.e., their image is a column matrix).

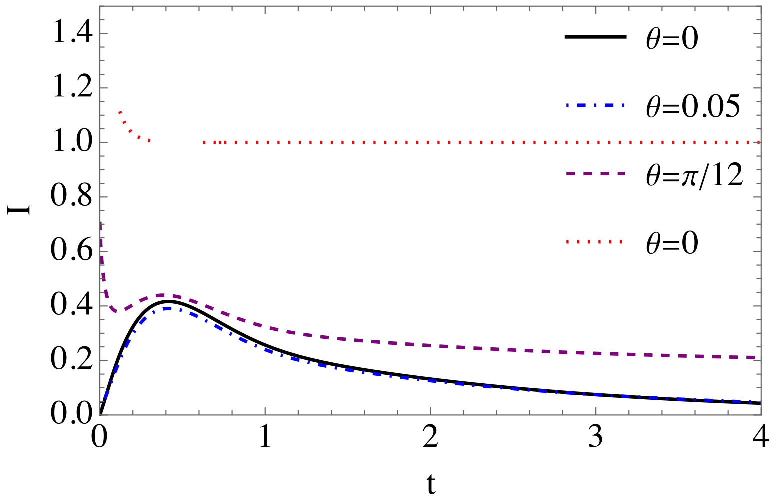


Figure 6.4: Quantum Mutual Information for different initial conditions determined by $\theta$. We assume parameters $\ell = 1$, $m = 1$, $\epsilon = 1$, $\omega = 0.5$.

We depict the mutual information for different initial conditions in Fig. 6.4. It also stabilizes over very long times, indicating that while entanglement degrades over time, other quantum correlations between the two particles persist.

We also depict the behavior of the three correlations discussed in this chapter so far for an initially unentangled state in Fig. 6.5. It is evident that there is a hierarchy between coherence, quantum mutual information and entanglement.

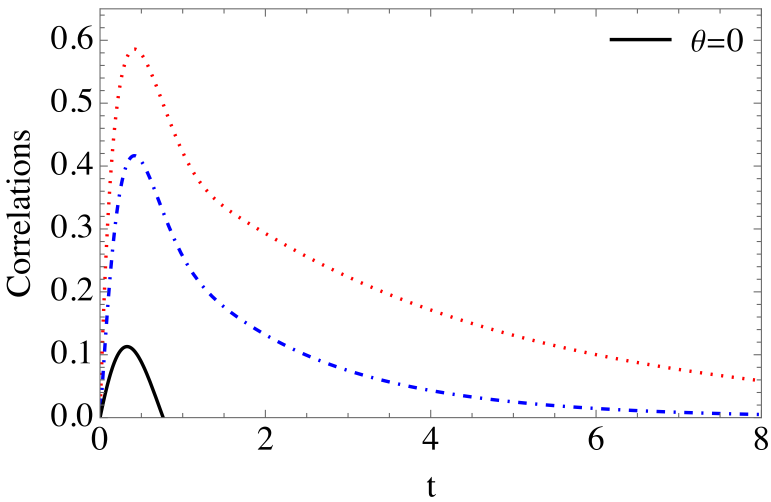


Figure 6.5: Comparison of the different quantifiers for coherence, quantum mutual information and entanglement studied in the chapter for $\theta = 0$. The red/dotted curve represents the $l_1$-norm of coherence. The blue/dash-dotted curve represents quantum mutual information. The black/solid curve represents concurrence.

### 6.3.4 Local Quantum Fisher Information

The Quantum Fisher Information (QFI) is a fundamental concept in quantum estimation theory, which measures how much information a quantum state carries about a parameter to be estimated. It is related to the maximum precision with which we can estimate a parameter through the quantum Cramér-Rao bound [198, 199, 200, 201, 202, 203].

In many applications of quantum mechanics and quantum information, we aim to estimate a parameter $\phi$ that affects a quantum state $\rho(\phi)$. This parameter can represent, for example: a magnetic field applied to a quantum system, an evolution time of a quantum state or a phase shift in an optical system. The idea is to measure a quantum system to obtain as much information as possible about $\phi$.

The Quantum Fisher Information is a generalization of classical Fisher Information to quantum states. The formal definition is:

$$F_Q(\phi) = \mathrm{Tr}\left(\rho(\phi)L_\phi^2\right) , \tag{6.56}$$

where $L_\phi$ is the quantum score operator, also called the Helstrom operator, defined implicitly by the Lyapunov equation:

$$\frac{d\rho(\phi)}{d\phi} = \frac{1}{2}(\rho(\phi)L_\phi + L_\phi\rho(\phi)). \tag{6.57}$$

The operator $L_\phi$ represents the best choice of observable for estimating the parameter $\phi$.

The QFI is widely used in various areas of physics and quantum information, such as: quantum metrology, for improving the precision of sensitive measurements, such as interferometry and quantum sensors; quantum communication, for optimizing the transmission and detection of signals encoded in quantum states; quantum computing, for optimizing algorithms based on phase estimation and entangled states, quantum thermodynamics, for understanding the efficiency of quantum heat engines.

In particular, when the parametric states $\rho_\phi$ can be obtained from an initial probe state $\rho$ subjected to a unitary transformation $U_\phi = e^{iH\phi}$ dependent on $\phi$ and generated by a Hermitian operator $H$, that is, $\rho_\phi = U_\phi^\dagger \rho U_\phi$. In this case, the Quantum Fisher Information $F(\rho_\phi)$, which we denote by $F(\rho, H)$, is given by:

$$F(\rho, H) = \sum_{i\neq j} \frac{(p_i - p_j)^2}{p_i + p_j} |\langle\psi_i|H|\psi_j\rangle|^2 . \tag{6.58}$$

Here, we use the spectral decomposition of $\rho$, that is,

$$\rho = \sum_i p_i|\psi_i\rangle\langle\psi_i|, \tag{6.59}$$

with $p_i \geq 0$ and $\sum_i p_i = 1$ . The main terms here are:

- $p_i$: eigenvalues of the density matrix $\rho$, obtained from its spectral decomposition $\rho = \sum_i p_i |\psi_i\rangle\langle\psi_i|$.
- $|\psi_i\rangle$: eigenvectors corresponding to $\rho$.
- $H$: Hermitian operator associated with the unitary evolution of the system.
- $\frac{(p_i-p_j)^2}{p_i+p_j}$: weight that quantifies the difference between the eigenvalues of the quantum state $\rho$.
- $|\langle\psi_i|H|\psi_j\rangle|^2$: matrix element of $H$ between the eigenvectors $|\psi_i\rangle$ and $|\psi_j\rangle$.

The important point here is that the QFI is independent of $\phi$. The phase estimation sensitivity, for any type of measurement, is limited by the Crámer-Rao bound $(\Delta\phi)^2 \geq 1/F(\rho, H)$ [204, 205, 206]. Therefore, this quantity provides a lower bound on the precision of the estimation. The knowledge of this limitation is of fundamental importance for quantum metrology, when using quantum mechanics to describe physical systems. For instance, considering the case in which one has an unknown parameter $\alpha$ that controls the strength of a given Hamiltonian that acts on a system during a known time $t$, the unitary evolution of the system is determined by the operator $t\alpha H = \phi H$ for a known observable $H$. Since this argument can be applied for different operations, like rotations through the angular momentum, for example, this estimator is of fundamental importance for several areas of physics that employ different techniques, like interferometry [204].

Now, consider a bipartite quantum state $\rho_{AB}$ of dimension $2 \times d$ in the Hilbert space $H = H_A \otimes H_B$. We assume that the dynamics of the first part is governed by the local phase shift transformation $e^{-i\phi H_A}$, where $H_A \equiv H_a \otimes I_B$ is the local Hamiltonian. In this case, the QFI reduces to the Local Quantum Fisher Information (LQFI), given by:

$$F(\rho, H_A) = \mathrm{Tr}(\rho H_A^2) - \sum_{i\neq j} \frac{2p_i p_j}{p_i + p_j} |\langle\psi_i|H_A|\psi_j\rangle|^2 \,. \tag{6.60}$$

The Local Quantum Fisher Information (LQFI) was introduced to deal with quantum correlations of the discord type. This quantifier allows a deeper understanding of how quantum correlations influence metrological precision. It has desirable properties that any good quantifier of quantum correlations should satisfy:

- It is non-negative and vanishes for bipartite states without discord (classically correlated states).
- It is invariant under local unitary operations.
- For pure states, it coincides with the geometric discord.

The goal of choosing the local Hamiltonian was to capture the quantum correlations between the subsystems. If the system is purely classical, then the LQFI will be zero, as a local observer does not detect quantum effects.

The quantification of quantum correlations in terms of the Local Quantum Fisher Information $Q(\rho)$ is defined as the minimization of the QFI over all local Hamiltonians $H_A$ acting on part $A$:

$$Q(\rho) = \min_{H_A} F(\rho, H_A)\,. \tag{6.61}$$

The general form of a local Hamiltonian is

$$H_A = \vec{\sigma} \cdot \vec{r},$$

with $|\vec{r}| = 1$ and $\vec{\sigma} = (\sigma_x \equiv \sigma_1, \sigma_y \equiv \sigma_2, \sigma_z \equiv \sigma_3)$ being the usual Pauli matrices.

It can be verified that

$$Tr(\rho H_A^2) = 1,$$

and the second term in equation (2) can be rewritten as:

$$\sum_{i \neq j} \frac{2p_i p_j}{p_i + p_j} |\langle \psi_i | H_A | \psi_j \rangle|^2 = \vec{r}^\dagger M \vec{r},$$

where the elements of the symmetric matrix $M$ of dimension $3 \times 3$ are given by:

$$M_{lk} = \sum_{i \neq j} \frac{2p_i p_j}{p_i + p_j} \langle \psi_i | \sigma_l \otimes I_B | \psi_j \rangle \langle \psi_j | \sigma_k \otimes I_B | \psi_i \rangle. \tag{6.62}$$

To minimize $F(\rho, H_A)$, it is necessary to maximize the quantity $\vec{r}^\dagger M \vec{r}$ over all unit vectors $\vec{r}$. The maximum value of this expression corresponds to the largest eigenvalue of the matrix $M$.

Therefore, the minimum value of the Local Quantum Fisher Information $Q(\rho)$ is given by:

$$Q(\rho) = 1 - \lambda_{\max}(M),$$

where $\lambda_{\max}$ represents the largest eigenvalue of the symmetric matrix $M$ defined in equation (6.62).

Fig. 6.6 illustrate the behavior of $LQFI$ as a function of time $t$, comparing the $LQFI$ for the initial state ($\theta = 0$) with that of the initial state ($\theta = \pi/4$). This figure reveals that the quantum correlations embedded in the $LQFI$ for the initially non-entangled state are more robust than those for the initially entangled state. This occurs because entangled states are more sensitive to decoherence than separable states, causing the

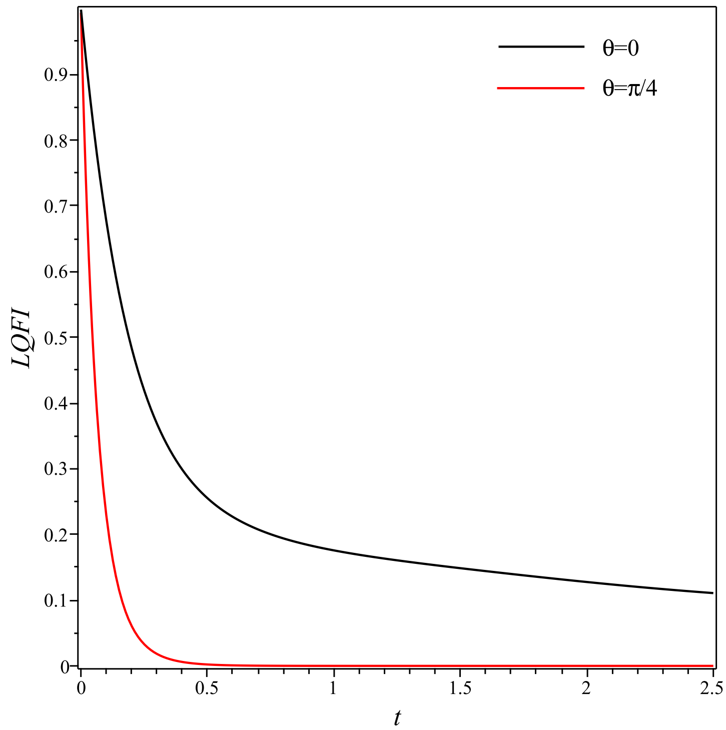


Figure 6.6: The local quantum Fisher information ($LQFI$) as a function of time $t$ for different initial quantum states. The black curve represents the $LQFI$ for the non-entangled initial state ($\theta = 0$), while the red curve corresponds to the entangled initial state ($\theta = \pi/4$). The parameters used are $\ell = 1$, $m = 1$, $\epsilon = 1$, and $\omega = 0.5$.

$LQFI$ to degrade more rapidly.

We summarize the qualitative behavior of the correlations in Table 6.1.

Table 6.1: Qualitative summary of the behavior of the correlations.

| **Correlation** | **Effect of contact with quantum spacetime environment** |
|---|---|
| Concurrence (entanglement) | Destroyed in a finite time for $\theta \neq \pi/4$. Asymptotically vanishes otherwise. |
| $l_1$-norm of coherence | Asymptotically preserved for $\theta \neq 0$. Asymptotically vanishes otherwise. |
| Quantum Mutual Information | Asymptotically preserved for $\theta \neq 0$. Asymptotically vanishes otherwise. |
| Local Quantum Fisher Information | Destroyed in finite time for $\theta = \pi/4$. Asymptotically vanishes or survives otherwise. |

## 6.4 Competing Planck-Scale Effects

To better understand the effect of the deformed Hamiltonian in creating correlations and the Lindbladians in destroying them, we introduce two deformation parameters, $\ell_H$

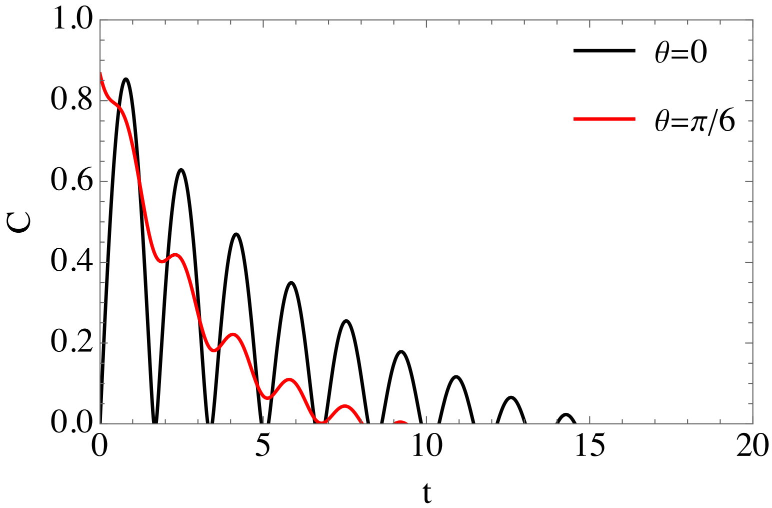


Figure 6.7: Concurrence for different initial conditions determined by $\theta$. The parameters used are $\ell_H = 1$, $\ell_L = 0.05$, $m = 1$, $\epsilon = 1$, and $\omega = 0.5$.

and $\ell_L$, to control these contributions. The Hamiltonian is given by:

$$\begin{aligned}\mathcal{H} = \epsilon(\mathbb{1})^4 + \frac{\omega}{2}\left(\sigma_z \otimes \mathbb{1} \otimes \mathbb{1} \otimes \mathbb{1} + \mathbb{1} \otimes \sigma_z \otimes \mathbb{1} \otimes \mathbb{1}\right) \\ + \ell_H |P| \otimes |P| \otimes \sigma_x \otimes \sigma_x,\end{aligned} \tag{6.63}$$

and the Lindblad equation is given by:

$$\partial_t \rho_{ab} + i\left[\mathcal{H}_{ab}, \rho_{ab}\right] + \frac{\ell_L}{2}\left(\mathcal{P}_{ab}^2 \rho_{ab} + \rho_{ab}\mathcal{P}_{ab}^2 - 2\mathcal{P}_{ab}\rho_{ab}\mathcal{P}_{ab}\right) = 0. \tag{6.64}$$

### 6.4.1 Lindbladian Weaker than Hamiltonian ($\ell_L \ll \ell_H$)

The effect of the different contributions to the Lindblad equation can be seen in Fig. 6.7, where we assume different values for the deformation parameters. The dissipation effect is described by $\ell_L = 0.05$, while the deformed Hamiltonian is described by $\ell_H = 1$. For an initially unentangled state ($\theta = 0$, black curve), we observe a dynamic phenomenon of alternating sudden death and sudden birth of quantum entanglement between the particles, whose amplitude is progressively attenuated by the dissipation introduced by the Lindblad term. In contrast, for a partially entangled initial state ($\theta = \pi/6$, blue curve), the concurrence drops quicker until it vanishes.

Similarly, the $l_1$-norm of coherence and quantum mutual information exhibit oscillatory behavior, as shown in Figs. 6.8 and 6.9. For an initially unentangled state ($\theta = 0$, black curve) and for the partially entangled state ($\theta = \pi/6$, red curve), the coherence oscillates but tends to stabilize over time, as observed in the case where $\ell_H = \ell_L$. To further study the role of these contributions, let us consider the opposite case.

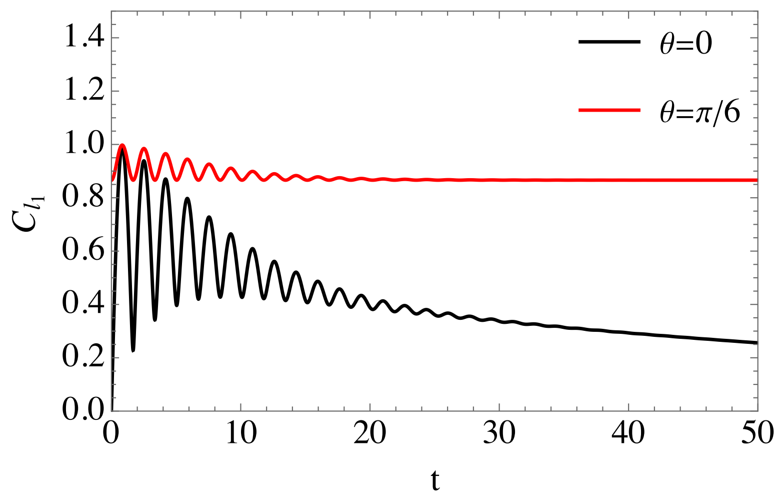


Figure 6.8: The $l_1$-norm of coherence for different initial conditions determined by $\theta$. The parameters used are $\ell_H = 1$, $\ell_L = 0.05$, $m = 1$, $\epsilon = 1$, and $\omega = 0.5$.

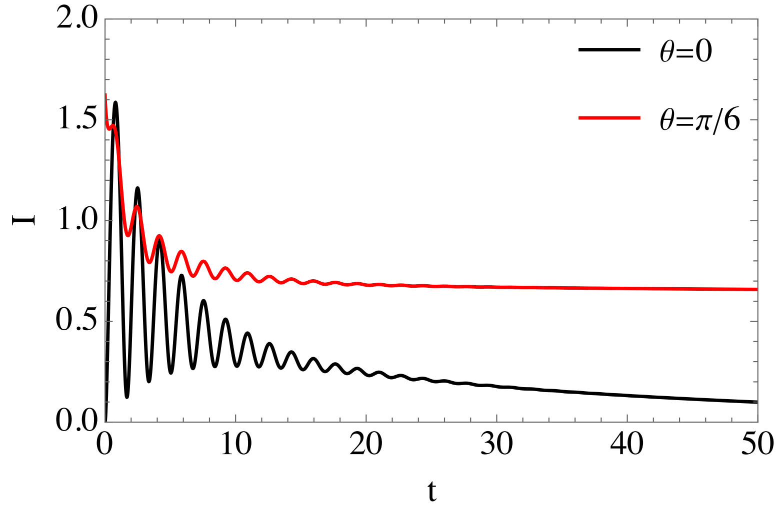


Figure 6.9: Quantum mutual information for different initial conditions determined by $\theta$. The parameters used are $\ell_H = 1$, $\ell_L = 0.05$, $m = 1$, $\epsilon = 1$, and $\omega = 0.5$.

### 6.4.2 Hamiltonian Weaker than Lindbladian ($\ell_H \ll \ell_L$)

In this case, when the system starts in an unentangled state, the deformed composition law contribution is not strong enough to produce non-zero concurrence. For an initially entangled state, the concurrence evolves similarly to the behavior shown in Fig. 6.1 for the same set of parameters.

Regarding the $l_1$-norm of coherence and quantum mutual information, the system behaves similarly to Figs. 6.2 and 6.4. This provides evidence that the quantum spacetime, which acts as an environment of the two-qubit system, actively preserving the coherence of the system. Although it dissipates entanglement, it helps create and preserve classical and quantum correlations beyond entanglement. The reason for this behavior is in the fact that the Lindbladian $P_{ab}$ is not diagonal due to the superposition of momenta in this model, as can be seen in (6.35). This property is responsible for giving a non-null contribution from the open system represented by the quantum spacetime and creating superpositions in this model.

## 6.5 Discussion

We analyzed how modifications to the Hamiltonian of a system of particles, arising from deformations of the relativistic symmetries, influence quantum correlations. Specifically, we constructed a model describing two particles in a superposition of energies and momenta, corresponding to a system of four qubits. This system exhibits intriguing properties, such as the emergence of entanglement due to the modified Hamiltonian and the role of the quantum spacetime as an environment that dissipates entanglement while simultaneously creating and preserving other classical and quantum correlations between the particles. This behavior was observed when we individually examined the contributions of the quantum gravity parameters from the deformed energy composition law (Hamiltonian) and from the Lindblad equation.

The unique ability of the deformed Hamiltonian to generate entanglement between the particles in the system is a distinctive effect of a deformation of relativistic symmetries. If coherence is maintained during the time scale of the entanglement time described in this chapter, then systems of qubits could be considered to test deformations of the composition of energy due to quantum gravity. The study of $N$-partite systems could also be beneficial to understand the effect of quantum gravity on more general systems [207].

# CHAPTER 7

## Conclusions

This thesis examines the manifestation of Lorentz symmetry violations and deformations at the Planck scale within nonrelativistic quantum systems. It specifies the conditions under which effects, generally considered to be strongly suppressed, may become dynamically significant in the infrared regime. Due to the limited experimental/observational accessibility of the Planck scale, the analysis employs a phenomenological approach, considering low-energy quantum systems as potential amplifiers of Planck scale physics when the appropriate kinematical and dynamical regimes are identified.

The central objective of this study is to translate modifications of relativistic kinematics, inspired by quantum gravity, into experimentally meaningful signatures within nonrelativistic quantum mechanics. The valuable contributions of this thesis are summarized below.

**Nonrelativistic limit of modified dispersion relations:** A general and systematic procedure was developed to obtain effective nonrelativistic Hamiltonians from broad classes of modified dispersion relations. This approach shows that Planck-scale deformations manifest as higher-order, generally nonlocal operators in the Schrödinger dynamics.

**Emergence of fractional and nonlocal dynamics:** Dispersion relations with non-integer powers of momentum result in effective dynamics that qualitatively differ from the standard quadratic kinetic structure. In the deep infrared regime, such contributions can dominate the system's evolution, leading to fractional and intrinsically nonlocal quantum behavior. This relationship forms a conceptual link between Planck-scale kinematical deformations and fractional quantum mechanics, indicating that anomalous geometric or fractal-like properties of spacetime could produce observable effects in low-energy dynamics.

**Gravitationally induced decoherence from stochastic fluctuations:** Planck-scale fluctuations can be modeled as stochastic modifications of the dispersion relation, leading to an effective open-system description in which quantum spacetime serves as an environment that induces decoherence.

**Correlation and entanglement from deformed symmetry structures:** In scenarios with deformed momentum-composition laws or noncommutative spacetimes, the structure of spacetime can generate effective interactions between otherwise free subsystems. These interactions dynamically create correlations and entanglement, even in the absence of direct coupling. This indicates that quantum spacetime may play an active dynamical role, rather than serving as a passive background.

Table 7.1: Lorentz symmetry effects in NR quantum systems induced by MDRs.

| Scenario | Lorentz symmetry | NR Infrared manifestation | Chapters |
|---|---|---|---|
| Systematic effects with integer power in momentum | MDRs (LIV or DSR) | Deformed Schrödinger dynamics; non-quadratic kinetic terms | Ch. 3 |
| Systematic effects with fractional power in momentum | MDRs with fractional powers (LIV) | Presence of fractional operators; nonlocal quantum dynamics | Ch. 4 |
| Stochastic effects | Fluctuating MDRs (LIV) | Lindblad dynamics; gravitational decoherence of quantum states | Ch. 5 |
| Symmetry-induced correlations | Deformed energy composition laws (DSR) | Emergent interactions, entanglement without direct coupling and decoherence | Ch. 6 |

Table 7.1 provides an overview of the physical mechanisms examined in this study and demonstrates that different forms of Lorentz symmetry breaking or deformation produce qualitatively distinct signatures in the nonrelativistic regime.

The findings of this thesis suggest that nonrelativistic quantum systems serve not only as approximations to relativistic theories but also as complementary tools for investigating fundamental spacetime structure. Precision tabletop experiments, quantum optical platforms, and mesoscopic systems, therefore, represent promising laboratories for advancing quantum gravity phenomenology.

# Bibliography

[1] Matvei Bronstein. Quantum theory of weak gravitational fields. *Gen. Rel. Grav.*, 44:267–283, 2012.

[2] Sabine Hossenfelder. Minimal length scale scenarios for quantum gravity. *Living Reviews in Relativity*, 16:2, 2013.

[3] Claus Kiefer. *Quantum Gravity*. Oxford University Press, Oxford, 2007.

[4] J. Polchinski. *String theory. Vol. 1: An introduction to the bosonic string*. Cambridge Monographs on Mathematical Physics. Cambridge University Press, 12 2007.

[5] Carlo Rovelli. Loop Quantum Gravity. *Living Rev. Rel.*, 1:1, oct 1997.

[6] Giovanni Amelino-Camelia. Quantum-Spacetime Phenomenology. *Living Rev. Rel.*, 16:5, 2013.

[7] Stefano Liberati. Tests of Lorentz invariance: a 2013 update. *Class. Quant. Grav.*, 30:133001, apr 2013.

[8] Igor Pikovski, Michael R. Vanner, Markus Aspelmeyer, Myungshik Kim, and Caslav Brukner. Probing Planck-scale physics with quantum optics. *Nature Phys.*, 8:393–397, 2012.

[9] Jacob D. Bekenstein. Is a tabletop search for Planck scale signals feasible? *Phys. Rev. D*, 86(12):124040, nov 2012.

[10] Nick Laskin. Fractional quantum mechanics. *Physical Review E*, 62(3):3135, 2000.

[11] Nick Laskin. Fractional Schrodinger equation. *Phys. Rev. E*, 66:056108, 2002.

[12] Gislaine Varão, Iarley P. Lobo, and Valdir B. Bezerra. Fractional quantum mechanics meets quantum gravity phenomenology. *EPL*, 148(3):30001, 2024.

[13] J. Ambjorn, J. Jurkiewicz, and R. Loll. Spectral dimension of the universe. *Phys. Rev. Lett.*, 95:171301, 2005.

[14] Gianluca Calcagni. Fractal universe and quantum gravity. *Phys. Rev. Lett.*, 104:251301, 2010.

[15] Iarley P Lobo, Gislaine Varão, Giulia Gubitosi, Moises Rojas, and Valdir B Bezerra. Coherence and entanglement in a non-commutative spacetime. *Classical and Quantum Gravity*, 42(22):225010, nov 2025.

[16] Andrea Addazi et al. Quantum gravity phenomenology at the dawn of the multi-messenger era. *Prog. Part. Nucl. Phys.*, 125:103948, 2022.

[17] Giovanni Amelino-Camelia. Quantum-Gravity Phenomenology: Status and Prospects. *Mod. Phys. Lett. A*, 17:899–922, apr 2002.

[18] Giovanni Amelino-Camelia. Relativity in space-times with short distance structure governed by an observer independent (Planckian) length scale. *Int. J. Mod. Phys. D*, 11:35–60, 2002.

[19] John F. Donoghue. General relativity as an effective field theory: The leading quantum corrections. *Phys. Rev. D*, 50:3874–3888, may 1994.

[20] C. Alden Mead. Possible Connection Between Gravitation and Fundamental Length. *Phys. Rev.*, 135(3B):B849–B862, aug 1964.

[21] T Padmanabhan. Limitations on the operational definition of spacetime events and quantum gravity. *Class. Quantum Gravity*, 4(4):L107–L113, jul 1987.

[22] Michele Maggiore. A Generalized Uncertainty Principle in Quantum Gravity. *Phys. Lett. B*, 304:65–69, jan 1993.

[23] Luis J. Garay. Quantum gravity and minimum length. *Int. J. Mod. Phys. A*, 10:145–166, mar 1994.

[24] Fabio Scardigli. Generalized uncertainty principle in quantum gravity from micro-black hole gedanken experiment. *Phys. Lett. B*, 452:39, 1999.

[25] Jerzy Kowalski-Glikman and Andrea Bevilacqua. Doubly special relativity and relative locality. *PoS*, CORFU2021:322, 2022.

[26] Giovanni Amelino-Camelia, Laurent Freidel, Jerzy Kowalski-Glikman, and Lee Smolin. Relative locality: A deepening of the relativity principle. *Gen. Rel. Grav.*, 43:2547–2553, 2011.

[27] J. L. Synge, editor. *Relativity: The General theory.* North-Holland Publishing Company, Amsterdam, Netherlands, 1960.

[28] J. J. Relancio and S. Liberati. Towards a geometrical interpretation of rainbow geometries for quantum gravity phenomenology. *Class. Quant. Grav.*, 38(13):135028, oct 2020.

[29] J. J. Relancio and S. Liberati. Phenomenological consequences of a geometry in the cotangent bundle. *Phys. Rev. D*, 101(6):64062, feb 2020.

[30] Christian Pfeifer and José Javier Relancio. Deformed relativistic kinematics on curved spacetime: a geometric approach. *Eur. Phys. J. C*, 82(2):150, 2022.

[31] Saulo Albuquerque, Valdir B. Bezerra, Iarley P. Lobo, Gabriel Macedo, Pedro H. Morais, Ernesto Rodrigues, Luis C. N. Santos, and Gislaine Varão. Quantum Configuration and Phase Spaces: Finsler and Hamilton Geometries. *Physics*, 5:90–115, 2023.

[32] Giovanni Amelino-Camelia. Doubly Special Relativity. *Nature*, 418:34–35, jul 2002.

[33] Jerzy Kowalski-Glikman. De Sitter space as an arena for Doubly Special Relativity. *Phys. Lett. B*, 547:291–296, jul 2002.

[34] Joao Magueijo and Lee Smolin. Lorentz invariance with an invariant energy scale. *Phys. Rev. Lett.*, 88:190403, dec 2002.

[35] David Mattingly. Modern tests of Lorentz invariance. *Living Rev. Rel.*, 8:5, 2005.

[36] Michele Maggiore. A generalized uncertainty principle in quantum gravity. *Phys. Lett. B*, 304:65, 1993.

[37] Achim Kempf, Gianpiero Mangano, and Robert B. Mann. Hilbert space representation of the minimal length uncertainty relation. *Phys. Rev. D*, 52:1108, 1995.

[38] S. Mignemi. Extended uncertainty principle and the geometry of (anti)-de Sitter space. *Mod. Phys. Lett. A*, 25:1697–1703, sep 2009.

[39] G. Amelino-Camelia, John Ellis, N. E. Mavromatos, D. V. Nanopoulos, and Subir Sarkar. Potential Sensitivity of Gamma-Ray Burster Observations to Wave Dispersion in Vacuo. *Nature*, 393:763–765, dec 1997.

[40] Vlasios Vasileiou, Jonathan Granot, Tsvi Piran, and Giovanni Amelino-Camelia. A Planck-scale limit on spacetime fuzziness and stochastic Lorentz invariance violation. *Nature Phys.*, 11(4):344–346, 2015.

[41] Uri Jacob and Tsvi Piran. Lorentz-violation-induced arrival delays of cosmological particles. *Journal of Cosmology and Astroparticle Physics*, 2008(01):031, jan 2008.

[42] Sidney R. Coleman and Sheldon L. Glashow. High-energy tests of lorentz invariance. *Physical Review D*, 59:116008, 1999.

[43] Ted Jacobson, Stefano Liberati, and David Mattingly. Threshold effects and planck scale lorentz violation: Combined constraints from high-energy astrophysics. *Physical Review D*, 67(12):124011, 2003.

[44] Giovanni Amelino-Camelia, Laurent Freidel, Jerzy Kowalski-Glikman, and Lee Smolin. Relative locality and the soccer ball problem. *Phys. Rev. D*, 84(8):087702, apr 2011.

[45] Yuri Bonder, Elias Okon, and Daniel Sudarsky. Can spacetime curvature induce quantum transitions? *Phys. Rev. D*, 92:124050, 2015.

[46] Giovanni Amelino-Camelia. Doubly-Special Relativity: First Results and Key Open Problems. *Int. J. Mod. Phys. D*, 11:1643, oct 2002.

[47] Don Colladay and Alan Kostelecky. Lorentz-Violating Extension of the Standard Model. *Phys. Rev. D*, 58:116002, sep 1998.

[48] Giovanni Amelino-Camelia, Laurent Freidel, Jerzy Kowalski-Glikman, and Lee Smolin. The principle of relative locality. *Phys. Rev. D*, 84:084010, 2011.

[49] Andrea Addazi, Pierluigi Belli, Rita Bernabei, Antonino Marcianò, and Homa Shababi. Phenomenology of the Pauli exclusion principle violations due to the non-perturbative generalized uncertainty principle. *Eur. Phys. J. C*, 80(8):795, aug 2020.

[50] Giovanni Amelino-Camelia, John Ellis, Nick E. Mavromatos, Dimitri V. Nanopoulos, and Subir Sarkar. Tests of quantum gravity from observations of gamma-ray bursts. *Nature*, 393:763–765, 1998.

[51] Vlasios Vasileiou, Jonathan Granot, Tsvi Piran, and Giovanni Amelino-Camelia. Constraints on lorentz invariance violation from fermi-large area telescope observations of gamma-ray bursts. *Physical Review D*, 87(12):122001, 2013.

[52] Sidney R. Coleman and Sheldon L. Glashow. Neutrino tests of special relativity. *Physics Letters B*, 405:249–252, 1997.

[53] V. Alan Kostelecky and Matthew Mewes. Lorentz and cpt violation in neutrinos. *Physical Review D*, 69:016005, 2004.

[54] Jorge S. Diaz and V. Alan Kostelecky. Neutrino oscillations and lorentz violation. *Physics Letters B*, 700:25–31, 2011.

[55] Alexander D. Cronin, Jorg Schmiedmayer, and David E. Pritchard. Optics and interferometry with atoms and molecules. *Reviews of Modern Physics*, 81:1051–1129, 2009.

[56] Vittorio Giovannetti, Seth Lloyd, and Lorenzo Maccone. Advances in quantum metrology. *Nature Photonics*, 5:222–229, 2011.

[57] Luca Pezzè, Augusto Smerzi, Markus K. Oberthaler, Roman Schmied, and Philipp Treutlein. Quantum metrology with nonclassical states of atomic ensembles. *Reviews of Modern Physics*, 90:035005, 2018.

[58] Clifford M. Will. The Confrontation between General Relativity and Experiment. *Living Rev. Rel.*, 17:4, 2014.

[59] Claus Lämmerzahl. A Hamilton operator for quantum optics in gravitational fields. *Phys. Lett. A*, 203(1):12–17, jul 1995.

[60] Piero Nicolini. Nonlocal and generalized uncertainty principle black holes, feb 2012.

[61] Philip K. Schwartz and Domenico Giulini. Post-Newtonian corrections to Schrödinger equations in gravitational fields. *Class. Quant. Grav.*, 36(9):095016, 2019. [Erratum: Class.Quant.Grav. 36, 249502 (2019)].

[62] R. Arnowitt, S. Deser, and C. W. Misner. Dynamical Structure and Definition of Energy in General Relativity. *Phys. Rev.*, 116(5):1322–1330, dec 1959.

[63] Richard L Arnowitt, Stanley Deser, and Charles W Misner. Canonical variables for general relativity. *Phys. Rev.*, 117:1595–1602, 1960.

[64] T. Padmanabhan. *Gravitation.* Cambridge University Press, jan 2010.

[65] Sean M. Carroll, Jeffrey A. Harvey, V. Alan Kostelecky, Charles D. Lane, and Takemi Okamoto. Noncommutative Field Theory and Lorentz Violation. *Phys. Rev. Lett.*, 87:141601, may 2001.

[66] R. Casadio and F. Scardigli. Generalized Uncertainty Principle, Classical Mechanics, and General Relativity. *Phys. Lett. B*, 807:135558, apr 2020.

[67] Pasquale Bosso, Giuseppe Gaetano Luciano, Luciano Petruzziello, and Fabian Wagner. 30 years in: Quo vadis generalized uncertainty principle? *Class. Quant. Grav.*, 40(19):195014, 2023.

[68] A. Mostafazadeh and F. Zamani. Quantum mechanics of Klein-Gordon fields. I. Hilbert space, localized states, and chiral symmetry. *Annals Phys.*, 321:2183–2209, 2006.

[69] Matej Pavsic. How the Geometric Calculus Resolves the Ordering Ambiguity of Quantum Theory in Curved Space. *Class. Quant. Grav.*, 20:2697–2714, nov 2001.

[70] Bryce Seligman DeWitt. Point Transformations in Quantum Mechanics. *Phys. Rev.*, 85(4):653–661, feb 1952.

[71] Fabian Wagner. Generalized uncertainty principle or curved momentum space? *Phys. Rev. D*, 104(12):126010, dec 2021.

[72] Fabian Wagner. Towards quantum mechanics on the curved cotangent bundle. *Classical and Quantum Gravity*, 41(4):045006, 2024.

[73] Claus Kiefer and Tejinder P. Singh. Quantum gravitational corrections to the functional Schrodinger equation. *Phys. Rev. D*, 44:1067–1076, 1991.

[74] Luciano Petruzziello and Fabian Wagner. Gravitationally induced uncertainty relations in curved backgrounds. *Phys. Rev. D*, 103(10):104061, 2021.

[75] Domenico Giulini and André Großardt. The Schrödinger–Newton equation as a non-relativistic limit of self-gravitating Klein–Gordon and Dirac fields. *Class. Quantum Gravity*, 29(21):215010, nov 2012.

[76] Jerzy Kowalski-Glikman and Sebastian Nowak. Doubly Special Relativity and de Sitter space. *Class. Quant. Grav.*, 20:4799–4816, apr 2003.

[77] S. I. Kruglov. Modified wave equation for spinless particles and its solutions in an external magnetic field. *Mod. Phys. Lett. A*, 28(6):1350014, 2013.

[78] Bibhas Ranjan Majhi and Elias C. Vagenas. Modified Dispersion Relation, Photon's Velocity, and Unruh Effect. *Phys. Lett. B*, 725:477–480, jul 2013.

[79] S. A. Franchino-Viñas and J. J. Relancio. Geometrizing the Klein–Gordon and Dirac equations in doubly special relativity. *Class. Quant. Grav.*, 40(5):054001, 2023.

[80] S. Hossenfelder. Multi-Particle States in Deformed Special Relativity. *Phys. Rev. D*, 75:105005, feb 2007.

[81] Sabine Hossenfelder. The Soccer-Ball Problem. *SIGMA*, 10:74, mar 2014.

[82] Giovanni Amelino-Camelia. Planck-scale soccer-ball problem: a case of mistaken identity. *Entropy*, 19(8):400, jul 2014.

[83] Ahmed Farag Ali, Saurya Das, and Elias C. Vagenas. The Generalized Uncertainty Principle and Quantum Gravity Phenomenology. *Twelfth Marcel Grossmann Meet.*, pages 2407–2409, jan 2010.

[84] J. M. Carmona and J. L. Cortes. Infrared and ultraviolet cutoffs of quantum field theory. *Phys. Rev. D*, 65:025006, 2001.

[85] J. Kowalski-Glikman and S. Nowak. Doubly Special Relativity theories as different bases of $\kappa$–Poincaré algebra. *Phys. Lett. B*, 539:126–132, mar 2002.

[86] Alan Kostelecky and Neil Russell. Data Tables for Lorentz and CPT Violation. *Rev. Mod. Phys.*, 83(1):11–31, jan 2011.

[87] Florian Girelli, Stefano Liberati, and Lorenzo Sindoni. Planck-scale modified dispersion relations and Finsler geometry. *Phys. Rev. D*, 75:064015, 2007.

[88] Giovanni Amelino-Camelia, Leonardo Barcaroli, Giulia Gubitosi, Stefano Liberati, and Niccoló Loret. Realization of doubly special relativistic symmetries in Finsler geometries. *Phys. Rev. D*, 90(12):125030, 2014.

[89] Ahmed Farag Ali, Saurya Das, and Elias C. Vagenas. Discreteness of Space from the Generalized Uncertainty Principle. *Phys. Lett. B*, 678(5):497–499, jun 2009.

[90] Ahmed Farag Ali, Saurya Das, and Elias C. Vagenas. A proposal for testing Quantum Gravity in the lab. *Phys. Rev. D*, 84(4):044013, jul 2011.

[91] G. Amelino-Camelia, V. D'Esposito, G. Fabiano, D. Frattulillo, P. A. Höhn, and F. Mercati. Quantum euler angles and agency-dependent space-time. *Progress of Theoretical and Experimental Physics*, 2024(3):033A01, 2024.

[92] Pasquale Bosso, Luciano Petruzziello, and Fabian Wagner. Minimal length: A cut-off in disguise? *Phys. Rev. D*, 107(12):126009, 2023.

[93] André H. Gomes. Constraining GUP Models Using Limits on SME Coefficients. *Class. Quantum Gravity*, 39(22):225017, may 2022.

[94] André H. Gomes. Constraining GUP Models Using Limits on SME Coefficients. In *9th Meet. CPT Lorentz Symmetry*, jun 2022.

[95] Giovanni Amelino-Camelia, Giuseppe Fabiano, and Domenico Frattulillo. Total momentum and other noether charges for particles interacting in a quantum spacetime. *Symmetry*, 17(2), 2025.

[96] Shiraz Minwalla, Mark Van Raamsdonk, and Nathan Seiberg. Noncommutative Perturbative Dynamics. *JHEP*, 02:20, dec 1999.

[97] Richard J. Szabo. Quantum field theory on noncommutative spaces. *Phys. Rept.*, 378:207–299, 2003.

[98] V. A. Acciari et al. Bounds on Lorentz invariance violation from MAGIC observation of GRB 190114C. *Phys. Rev. Lett.*, 125(2):021301, 2020.

[99] A. Abramowski et al. Search for Lorentz Invariance breaking with a likelihood fit of the PKS 2155-304 Flare Data Taken on MJD 53944. *Astropart. Phys.*, 34:738–747, 2011.

[100] M. L. Ahnen et al. Constraining Lorentz invariance violation using the Crab Pulsar emission observed up to TeV energies by MAGIC. *Astrophys. J. Suppl.*, 232(1):9, 2017.

[101] Saurya Das and Elias C. Vagenas. Universality of Quantum Gravity Corrections. *Phys. Rev. Lett.*, 101:221301, oct 2008.

[102] Lay Nam Chang, Djordje Minic, Naotoshi Okamura, and Tatsu Takeuchi. Exact solution of the harmonic oscillator in arbitrary dimensions with minimal length uncertainty relations. *Phys. Rev. D*, 65(12):125027, jun 2002.

[103] Ivan Dadic, Larisa Jonke, and Stjepan Meljanac. Harmonic oscillator with minimal length uncertainty relations and ladder operators. *Phys. Rev. D*, 67:087701, 2003.

[104] Pasquale Bosso and Giuseppe Gaetano Luciano. Generalized Uncertainty Principle: from the harmonic oscillator to a QFT toy model. *Eur. Phys. J. C*, 81(11):982, sep 2021.

[105] Sándor Benczik, Lay Nam Chang, Djordje Minic, and Tatsu Takeuchi. Hydrogen-atom spectrum under a minimal-length hypothesis. *Phys. Rev. A*, 72(1):012104, jul 2005.

[106] J. Slawny. Bound states of hydrogen atom in a theory with minimal length uncertainty relations. *J. Math. Phys.*, 48(5):053515, 2007.

[107] Lay Nam Chang, Zachary Lewis, Djordje Minic, and Tatsu Takeuchi. On the Minimal Length Uncertainty Relation and the Foundations of String Theory. *Adv. High Energy Phys.*, 2011:493514, may 2011.

[108] T. L. Antonacci Oakes, R. O. Francisco, J. C. Fabris, and J. A. Nogueira. Ground State of the Hydrogen Atom via Dirac Equation in a Minimal Length Scenario. *Eur. Phys. J. C*, 73:2495, aug 2013.

[109] F. Brau. Minimal Length Uncertainty Relation and Hydrogen Atom. *J. Phys. A*, 32:7691–7696, may 1999.

[110] Saurya Das and R. B. Mann. Planck scale effects on some low energy quantum phenomena. *Phys. Lett. B*, 704:596–599, sep 2011.

[111] Saurya Das and Elias C. Vagenas. Phenomenological Implications of the Generalized Uncertainty Principle. *Can. J. Phys.*, 87:233–240, jan 2009.

[112] Dongfeng Gao and Mingsheng Zhan. Constraining the generalized uncertainty principle with cold atoms. *Phys. Rev. A*, 94(1):13607, jul 2016.

[113] M. Khodadi, K. Nozari, A. Bhat, and S. Mohsenian. Probing Planck Scale Spacetime By Cavity Opto-Atomic $^{87}$Rb Interferometry. *PTEP*, 2019(5):053E03, apr 2018.

[114] Djamil Bouaziz. Kratzer's molecular potential in quantum mechanics with a generalized uncertainty principle. *Ann. Phys.*, 355:269–281, dec 2013.

[115] Fidele J. Twagirayezu. Generalized uncertainty principle corrections on atomic excitation. *Ann. Phys. (N. Y).*, 422:168294, nov 2020.

[116] Parth Girdhar and Andrew C. Doherty. Testing Generalised Uncertainty Principles through Quantum Noise. *New J. Phys.*, 22(9):93073, may 2020.

[117] Pasquale Bosso, Luciano Petruzziello, Fabian Wagner, and Fabrizio Illuminati. Spin operator, Bell nonlocality and Tsirelson bound in quantum-gravity induced minimal-length quantum mechanics. *Commun. Phys.*, 6(1):114, may 2023.

[118] Albert Messiah. *Quantum Mechanics*. Number Bd. 2 in Dover books on physics. Dover Publications, 1999.

[119] J. J. Sakurai and Jim Napolitano. *Modern Quantum Mechanics*. Cambridge University Press, Cambridge, UK, sep 2020.

[120] Mateusz Bawaj, Ciro Biancofiore, Michele Bonaldi, Federica Bonfigli, Antonio Borrielli, Giovanni Di Giuseppe, Lorenzo Marconi, Francesco Marino, Riccardo Natali, Antonio Pontin, Giovanni A. Prodi, Enrico Serra, David Vitali, and Francesco Marin. Probing deformed commutators with macroscopic harmonic oscillators. *Nat. Commun.*, 6:7503, nov 2014.

[121] P. A. Bushev, J. Bourhill, M. Goryachev, N. Kukharchyk, E. Ivanov, S. Galliou, M. E. Tobar, and S. Danilishin. Testing of Generalized Uncertainty Principle With Macroscopic Mechanical Oscillators and Pendulums. *Phys. Rev. D*, 100(6):66020, mar 2019.

[122] Joao Magueijo and Lee Smolin. Gravity's rainbow. *Class. Quant. Grav.*, 21:1725–1736, 2004.

[123] Alexander Vilenkin. Gravitational field of vacuum domain walls and strings. *Phys. Rev. D*, 23(4):852–857, feb 1981.

[124] Cláudio Furtado, Bruno G.C. da Cunha, Fernando Moraes, E.R.Bezerra de Mello, and V.B. Bezzerra. Landau levels in the presence of disclinations. *Phys. Lett. A*, 195(1):90–94, nov 1994.

[125] Orion Ciftja. Detailed solution of the problem of landau states in a symmetric gauge. *European Journal of Physics*, 41(3):035404, 2020.

[126] Sougato Bose, Anupam Mazumdar, Gavin W. Morley, Hendrik Ulbricht, Marko Toroš, Mauro Paternostro, Andrew Geraci, Peter Barker, M. S. Kim, and Gerard Milburn. Spin Entanglement Witness for Quantum Gravity. *Phys. Rev. Lett.*, 119(24):240401, 2017.

[127] Chiara Marletto and Vlatko Vedral. Gravitationally-Induced Entanglement Between Two Massive Particles is Sufficient Evidence of Quantum Effects in Gravity. *Phys. Rev. Lett.*, 119(24):240402, 2017.

[128] Fabian Wagner, Gislaine Varão, Iarley P. Lobo, and Valdir B. Bezerra. Quantum-spacetime effects on nonrelativistic Schrödinger evolution. *Phys. Rev. D*, 108(6):066008, 2023.

[129] Jerzy Lukierski, Anatol Nowicki, and Henri Ruegg. New quantum Poincare algebra and k deformed field theory. *Phys. Lett. B*, 293:344–352, 1992.

[130] S. Majid and H. Ruegg. Bicrossproduct structure of kappa Poincare group and noncommutative geometry. *Phys. Lett. B*, 334:348–354, 1994.

[131] Giovanni Amelino-Camelia, Malú Maira da Silva, Michele Ronco, Lorenzo Cesarini, and Orchidea Maria Lecian. Spacetime-noncommutativity regime of Loop Quantum Gravity. *Phys. Rev. D*, 95(2):024028, 2017.

[132] G. Amelino-Camelia, John R. Ellis, N. E. Mavromatos, and Dimitri V. Nanopoulos. Distance measurement and wave dispersion in a Liouville string approach to quantum gravity. *Int. J. Mod. Phys. A*, 12:607–624, 1997.

[133] Laurent Freidel and Etera R. Livine. 3D Quantum Gravity and Effective Noncommutative Quantum Field Theory. *Phys. Rev. Lett.*, 96:221301, 2006.

[134] R. Alves Batista, G. Amelino-Camelia, D. Boncioli, and et al. White paper and roadmap for quantum gravity phenomenology in the multi-messenger era. *Classical and Quantum Gravity*, 42(3):032001, 2025.

[135] Rafael D. Sorkin. How wrinkled is the surface of a black hole? In *1st Australasian Conference (ACGRG1) on General Relativity and Gravitation (Gravitational Waves, Mathematical Relativity, Quantum Gravity)*, 2 1996.

[136] Donald Marolf. On the quantum width of a black hole horizon. *Springer Proc. Phys.*, 98:99–112, 2005.

[137] John D. Barrow. The Area of a Rough Black Hole. *Phys. Lett. B*, 808:135643, 2020.

[138] Ronald J. Adler, Pisin Chen, and David I. Santiago. The Generalized uncertainty principle and black hole remnants. *Gen. Rel. Grav.*, 33:2101–2108, 2001.

[139] Giovanni Amelino-Camelia, Michele Arzano, Yi Ling, and Gianluca Mandanici. Black-hole thermodynamics with modified dispersion relations and generalized uncertainty principles. *Class. Quant. Grav.*, 23:2585–2606, 2006.

[140] Yi Ling, Bo Hu, and Xiang Li. Modified dispersion relations and black hole physics. *Phys. Rev. D*, 73:087702, 2006.

[141] Nikolai Laskin. Fractional quantum mechanics and Levy paths integrals. *Phys. Lett. A*, 268:298–305, 2000.

[142] N. Laskin. *Fractional Quantum Mechanics*. G - Reference,Information and Interdisciplinary Subjects Series. World Scientific, 2018.

[143] Giovanni Amelino-Camelia, Michele Arzano, Giulia Gubitosi, and Joao Magueijo. Dimensional reduction in the sky. *Phys. Rev. D*, 87(12):123532, 2013.

[144] Dario Benedetti. Fractal properties of quantum spacetime. *Phys. Rev. Lett.*, 102:111303, 2009.

[145] Petr Horava. Spectral Dimension of the Universe in Quantum Gravity at a Lifshitz Point. *Phys. Rev. Lett.*, 102:161301, 2009.

[146] Gianluca Calcagni, Astrid Eichhorn, and Frank Saueressig. Probing the quantum nature of spacetime by diffusion. *Phys. Rev. D*, 87(12):124028, 2013.

[147] Giovanni Amelino-Camelia, Francesco Brighenti, Giulia Gubitosi, and Grasiele Santos. Thermal dimension of quantum spacetime. *Phys. Lett. B*, 767:48–52, 2017.

[148] Giovanni Amelino-Camelia. Challenge to Macroscopic Probes of Quantum Spacetime Based on Noncommutative Geometry. *Phys. Rev. Lett.*, 111:101301, 2013.

[149] Li-Hua Wang and Meng-Sen Ma. Barrow black holes and the minimal length. *Phys. Lett. B*, 831:137181, 2022.

[150] S. Jalalzadeh, F. Rodrigues da Silva, and P. V. Moniz. Prospecting black hole thermodynamics with fractional quantum mechanics. *Eur. Phys. J. C*, 81(7):632, 2021.

[151] P. F. da Silva Junior, E. W. de Oliveira Costa, and S. Jalalzadeh. Emergence of fractal cosmic space from fractional quantum gravity. *Eur. Phys. J. Plus*, 138(9):862, 2023.

[152] Emanuel Wallison de Oliveira Costa, Raheleh Jalalzadeh, Pedro Felix da Silva, Junior., Seyed Meraj Mousavi Rasouli, and Shahram Jalalzadeh. Estimated Age of the Universe in Fractional Cosmology. *Fractal Fract.*, 7:854, 2023.

[153] I. P. Lobo and G. B. Santos. Thermal dimensional reduction and black hole evaporation. *Phys. Lett. B*, 817:136272, 2021.

[154] J. Feder. *Fractals*. Physics of solids and liquids. Plenum Press, 1988.

[155] Shilong Liu, Yingwen Zhang, Boris A. Malomed, and Ebrahim Karimi. Experimental realisations of the fractional Schrödinger equation in the temporal domain. *Nature Commun.*, 14(1):222, 2023.

[156] Boris A. Malomed. Basic fractional nonlinear-wave models and solitons. *Chaos*, 34(2):022102, February 2024.

[157] Luciano Petruzziello and Fabrizio Illuminati. Quantum gravitational decoherence from fluctuating minimal length and deformation parameter at the Planck scale. *Nature Commun.*, 12(1):4449, 2021.

[158] Iarley P. Lobo, Kelvin Sampaio, Gislaine Varão, Moises Rojas, and Valdir B. Bezerra. Liv-decoherence on gravitational cat states. *Physics Letters B*, 870:139923, 2025.

[159] Sandro Donadi and Matteo Fadel. Quantum gravitational decoherence of a mechanical oscillator from spacetime fluctuations. *Phys. Rev. D*, 111(2):026009, 2025.

[160] N. G. Van Kampen. A cumulant expansion for stochastic linear differential equations. I. *Physica*, 74(2):215–238, June 1974.

[161] Michele Arzano, Vittorio D'Esposito, and Giulia Gubitosi. Fundamental decoherence from quantum spacetime. *Commun. Phys.*, 6(1):242, 2023.

[162] H. P. Breuer, E. Goklu, and C. Lammerzahl. Metric fluctuations and decoherence. *Class. Quant. Grav.*, 26:105012, 2009.

[163] John R. Ellis, Subhendra Mohanty, and Dimitri V. Nanopoulos. Quantum Gravity and the Collapse of the Wave Function. *Phys. Lett. B*, 221:113–119, 1989.

[164] Charis Anastopoulos and Bei-Lok Hu. Quantum Superposition of Two Gravitational Cat States. *Class. Quant. Grav.*, 37(23):235012, 2020.

[165] William K. Wootters. Entanglement of formation of an arbitrary state of two qubits. *Phys. Rev. Lett.*, 80:2245–2248, 1998.

[166] G. J. Milburn, J. Corney, E. M. Wright, and D. F. Walls. Quantum dynamics of an atomic bose-einstein condensate in a double-well potential. *Phys. Rev. A*, 55:4318–4324, Jun 1997.

[167] I.V. Lukin, A.G. Sotnikov, and Yu.V. Slyusarenko. Aspects of bose-einstein condensation in a charged boson system over the dielectric surface. *Physics Letters A*, 417:127695, November 2021.

[168] Simone Rijavec, Matteo Carlesso, Angelo Bassi, Vlatko Vedral, and Chiara Marletto. Decoherence effects in non-classicality tests of gravity. *New J. Phys.*, 23(4):043040, 2021.

[169] Tanjung Krisnanda, Guo Yao Tham, Mauro Paternostro, and Tomasz Paterek. Observable quantum entanglement due to gravity. *npj Quantum Inf.*, 6:12, 2020.

[170] Giovanni Amelino-Camelia, Claus Laemmerzahl, Flavio Mercati, and Guglielmo M. Tino. Constraining the Energy-Momentum Dispersion Relation with Planck-Scale Sensitivity Using Cold Atoms. *Phys. Rev. Lett.*, 103:171302, 2009.

[171] Michele Arzano. Purity is not eternal in theories with Planck-scale deformed symmetries. *Phys. Rev. D*, 90(2):024016, 2014.

[172] Andrzej Borowiec and Aleksander Pachol. Classical Basis for $\kappa$-Poincaré Algebra and Doubly Special Relativity Theories. *J. Phys. A*, 43:045203, 2010.

[173] Hector L. Carrion, Onofre Rojas, Cleverson Filgueiras, and Moises Rojas. Decoherence Effects on Local Quantum Fisher Information and Quantum Coherence in a Spin-1/2 Ising-XYZ Chain. *Annalen Phys.*, 537(1):2400200, 2025.

[174] A. Einstein, B. Podolsky, and N. Rosen. Can Quantum-Mechanical Description of Physical Reality Be Considered Complete? *Phys. Rev.*, 47:777–780, 1935.

[175] Reinhard F. Werner. Quantum States with Einstein-Podolsky-Rosen Correlations Admitting a Hidden-Variable Model. *Phys. Rev. A*, 40:4277–4281, 1989.

[176] Artur K. Ekert. Quantum Cryptography Based on Bell's Theorem. *Phys. Rev. Lett.*, 67:661–663, 1991.

[177] Charles H. Bennett and Stephen J. Wiesner. Communication via One- and Two-Particle Operators on Einstein-Podolsky-Rosen States. *Phys. Rev. Lett.*, 69:2881–2884, 1992.

[178] Charles H. Bennett, Gilles Brassard, Claude Crépeau, Richard Jozsa, Asher Peres, and William K. Wootters. Teleporting an Unknown Quantum State via Dual Classical and Einstein-Podolsky-Rosen Channels. *Phys. Rev. Lett.*, 70:1895–1899, 1993.

[179] Scott Hill and William K. Wootters. Entanglement of a Pair of Quantum Bits. *Phys. Rev. Lett.*, 78:5022–5025, 1997.

[180] Vasileios Fragkos, Michael Kopp, and Igor Pikovski. On inference of quantization from gravitationally induced entanglement. *AVS Quantum Sci.*, 4:045601, 2022.

[181] Sabine Hossenfelder. Bounds on an energy-dependent and observer-independent speed of light from violations of locality. *Phys. Rev. Lett.*, 104:140402, 2010.

[182] I-Sheng Yang. Entanglement Timescale. *Phys. Rev. D*, 97(6):066008, 2018.

[183] V. Krutyanskiy et al. Entanglement of Trapped-Ion Qubits Separated by 230 Meters. *Phys. Rev. Lett.*, 130(5):050803, 2023.

[184] Pengfei Wang, Chun-Yang Luan, Mu Qiao, Mark Um, Junhua Zhang, Ye Wang, Xiao Yuan, Mile Gu, Jingning Zhang, and Kihwan Kim. Single ion-qubit exceeding one hour coherence time, 2020.

[185] Che-Ming Li, Neill Lambert, Yueh-Nan Chen, Guang-Yin Chen, and Franco Nori. Witnessing Quantum Coherence: From Solid-State to Biological Systems. *Sci. Rep.*, 2:885, 2012.

[186] Johan Aberg. Quantifying Superposition, 2006.

[187] Alexander Streltsov, Gerardo Adesso, and Martin B. Plenio. Quantum Coherence as a Resource. *Rev. Mod. Phys.*, 89:041003, 2017.

[188] T. Baumgratz, M. Cramer, and M. B. Plenio. Quantifying Coherence. *Phys. Rev. Lett.*, 113(14):140401, 2014.

[189] Alexander Streltsov. *Quantum Discord in Quantum Information Theory*, pages 17–22. Springer International Publishing, 2015.

[190] Harold Ollivier and Wojciech H. Zurek. Quantum Discord: A Measure of the Quantumness of Correlations. *Phys. Rev. Lett.*, 88:017901, 2001.

[191] Jonas Maziero. Computing Partial Traces and Reduced Density Matrices. *Int. J. Mod. Phys. C*, 28(1):1750005, 2017.

[192] John Watrous. *The Theory of Quantum Information*. Cambridge University Press, 2018.

[193] Michael A. Nielsen and Isaac L. Chuang. *Quantum Computation and Quantum Information*. Cambridge University Press, 2012.

[194] Anindita Bera, Tamoghna Das, Debasis Sadhukhan, Sudipto Singha Roy, Aditi Sen De, and Ujjwal Sen. Quantum discord and its allies: a review of recent progress. *Reports on Progress in Physics*, 81(2):024001, 2018.

[195] Qing Chen, Chengjie Zhang, Sixia Yu, XX Yi, and CH Oh. Quantum discord of two-qubit x states. *Physical Review A—Atomic, Molecular, and Optical Physics*, 84(4):042313, 2011.

[196] Mazhar Ali, A. R. P. Rau, and G. Alber. Quantum discord for two-qubit x states. *Physical Review A*, 81(4):042105, 2010.

[197] Davide Girolami and Gerardo Adesso. Quantum discord for general two-qubit states: Analytical progress. *Physical Review A*, 83(5):052108, 2011.

[198] A Slaoui, L Bakmou, M Daoud, and R Ahl Laamara. A comparative study of local quantum fisher information and local quantum uncertainty in heisenberg xy model. *Physics Letters A*, 383(19):2241–2247, 2019.

[199] Saulo L. L. Silva and Moises Rojas. Enhancement of thermal quantum coherence and teleportation in an Ising-XXZ diamond chain through impurity-induced effects. *Eur. Phys. J. Plus*, 140(1):31, 2025.

[200] Sunho Kim, Longsuo Li, Asutosh Kumar, and Junde Wu. Characterizing nonclassical correlations via local quantum fisher information. *Physical Review A*, 97(3):032326, 2018.

[201] Zakaria Dahbi, Atta Ur Rahman, and Mostafa Mansour. Skew information correlations and local quantum fisher information in two gravitational cat states. *Physica A*, 609:128333, 2023.

[202] Yi-Jun Lian and Jin-Ming Liu. Quantum Fisher information of a qubit-qutrit system in Garfinkle–Horowitz–Strominger dilation space–time. *Commun. Theor. Phys.*, 73(8):085102, 2021.

[203] Mikhail A. Yurischev and Saeed Haddadi. Local quantum fisher information and local quantum uncertainty for general x states. *Phys. Lett. A*, 476:128868, 2023.

[204] Géza Tóth and Iagoba Apellaniz. Quantum metrology from a quantum information science perspective. *Journal of Physics A Mathematical General*, 47(42):424006, October 2014.

[205] Carl W. Helstrom. *Quantum Detection and Estimation Theory.* Mathematics in Science and Engineering. Academic Press, 1976.

[206] A.S. Holevo. *Probabilistic and Statistical Aspects of Quantum Theory.* Publications of the Scuola Normale Superiore. Scuola Normale Superiore, 2011.

[207] Shu-Min Wu, Hao-Sheng Zeng, and Hui-Min Cao. Quantum coherence and distribution of N-partite bosonic fields in noninertial frame. *Class. Quant. Grav.*, 38(18):185007, 2021.

[208] C. Quesne and V. M. Tkachuk. Composite system in deformed space with minimal length. *Phys. Rev. A*, 81:012106, 2010.

[209] V. M. Tkachuk. Deformed Heisenberg algebra with minimal length and equivalence principle. *Phys. Rev. A*, 86:62112, jan 2013.

# APPENDIX A

## Deformed macroscopic dynamics

The dynamics implied by Eq. (3.43) applies solely at the microscopic level, i.e. , to elementary particles, and has to be amended to account for macroscopic objects. To elucidate this point, in this appendix we study its classical counterpart in the absence of external fields and curvature, and with aligning Lorentz-violation ($\mathcal{A}_i = 0$). The resulting Hamiltonian reads

$$H = \frac{1}{2M}\left(k^2 - \ell\sum_{n=1}^{3}\xi_n (Mc)^{3-n}k^n\right), \tag{A.1}$$

where $k^2 = \delta^{ij}k_ik_j$. Applying the Legendre transform, we obtain the Lagrangian

$$L = \frac{Mv^2}{2}\left[1 + \ell Mc\left(\xi_1\frac{c}{v} + \xi_2 + \xi_3\frac{v}{c}\right)\right], \tag{A.2}$$

with the velocity $v$. In order to study the kinematics of macroscopic objects, we consider $\mathcal{N}$ particles of equal mass,such that

$$L = \sum_{I=1}^{\mathcal{N}}\frac{Mv_I^2}{2}\left[1 + \ell Mc\left(\xi_1\frac{c}{v_I} + \xi_2 + \xi_3\frac{v_I}{c}\right)\right]. \tag{A.3}$$

In this context, the velocity of a single particle can be expressed as a sum of the macroscopic center-of-mass velocity $v_{\text{mac}}$ and the relative velocity of the particle.For simplicity, we assume the relative motion to be negligible. We are, thus, describing a macroscopic solid in motion. As a result, on the macroscopic level the Lagrangian becomes

$$\begin{aligned} L &= \sum_{I=1}^{\mathcal{N}}\frac{Mv_{\text{mac}}^2}{2}\left[1 + \ell Mc\left(\xi_1\frac{c}{v_{\text{mac}}} + \xi_2 + \xi_3\frac{v_{\text{mac}}}{c}\right)\right] \\ &= \frac{M_{\text{mac}}v_{\text{mac}}^2}{2}\left[1 + \frac{\ell M_{\text{mac}}c}{\mathcal{N}}\left(\xi_1\frac{c}{v_{\text{mac}}} + \xi_2 + \xi_3\frac{v_{\text{mac}}}{c}\right)\right]. \end{aligned} \tag{A.4}$$

where, in the last step, we introduced the mass of the macroscopic object $M_{\text{mac}} = \mathcal{N}M$. Hence, expressed in terms of the relevant variables for macroscopic objects, the quantum-gravity corrections deteriorate with the number of fundamental constituents, thereby avoiding a possible soccer-ball problem [80, 44, 81, 82].[1] As regards phenomenology, we effectively have to shift the relevant length scale as $\ell \to \ell/\mathcal{N}$. As we generally compare this diluted minimal-length scale to the macroscopic mass, this comes down to comparing the mass of the fundamental constituents to the Planck scale. As this mass is generally dominated by protons and the neutrons (both of which only encompass three elementary particles), it is generically the proton mass that is compared to the Planck mass. This fact which is compatible with other findings in the context of minimal-length models [208, 209, 148, 67] and has to be accounted for, when considering macroscopic objects.

[1] Note that a resolution of the soccer-ball problem of this kind creates a new "inverse" soccer-ball problem, for details see [67].

# APPENDIX B

## Analytic solution of the Lindblad equation

### B.1 Analytic solution of the Lindblad equation and asymptotic behavior of the density matrix

The Lindblad equation is

$$\begin{pmatrix} A_{11} & 0 & 0 & A_{14} \\ 0 & A_{22} & A_{23} & 0 \\ 0 & A_{32} & A_{33} & 0 \\ A_{41} & 0 & 0 & A_{44} \end{pmatrix} = 0,$$

where

$$A_{11} = 2\alpha\ell m\Big[(1-i)\rho_{14} - \rho_{23} - \rho_{32} + (1+i)\rho_{41}\Big] + 4\ell m\epsilon\Big(2\rho_{11} - \rho_{22} - \rho_{33}\Big) + 4\rho'_{11}, \tag{B.1}$$

$$A_{44} = 2\alpha\ell m\Big[(1+i)\rho_{14} - \rho_{23} - \rho_{32} + (1-i)\rho_{41}\Big] + 4\ell m\epsilon\Big(2\rho_{44} - \rho_{22} - \rho_{33}\Big) + 4\rho'_{44}, \tag{B.2}$$

$$A_{14} = 2\alpha\ell m\Big[(1-i)\rho_{11} - \rho_{22} - \rho_{33} + (1+i)\rho_{44}\Big] + 4\ell m\epsilon\Big(2\rho_{14} - \rho_{23} - \rho_{32}\Big) + 4\rho'_{14}, \tag{B.3}$$

$$A_{41} = 2\alpha\ell m\Big[(1+i)\rho_{11} - \rho_{22} - \rho_{33} + (1-i)\rho_{44}\Big] + 4\ell m\epsilon\Big(2\rho_{41} - \rho_{23} - \rho_{32}\Big) + 4\rho'_{41}, \tag{B.4}$$

$$A_{22} = 2\alpha\ell m\Big[-\rho_{14} + (1-i)\rho_{23} + (1+i)\rho_{32} - \rho_{41}\Big] + 4\ell m\epsilon\Big(-\rho_{11} + 2\rho_{22} - \rho_{44}\Big) + 4\rho'_{22}, \tag{B.5}$$

$$A_{23} = 2\alpha\ell m\Big[-\rho_{11} + (1-i)\rho_{22} + (1+i)\rho_{33} - \rho_{44}\Big] + 4\ell m\epsilon\Big(-\rho_{14} + 2\rho_{23} - \rho_{41}\Big) + 4\rho'_{23}, \tag{B.6}$$

$$A_{32} = 2\alpha\ell m\Big[-\rho_{11} + (1+i)\rho_{22} + (1-i)\rho_{33} - \rho_{44}\Big] + 4\ell m\epsilon\Big(-\rho_{14} + 2\rho_{32} - \rho_{41}\Big) + 4\rho'_{32}, \tag{B.7}$$

$$A_{33} = 2\alpha\ell m\Big[-\rho_{14} + (1+i)\rho_{23} + (1-i)\rho_{32} - \rho_{41}\Big] + 4\ell m\epsilon\Big(-\rho_{11} + 2\rho_{33} - \rho_{44}\Big) + 4\rho'_{33}. \tag{B.8}$$

and $\alpha = \sqrt{\epsilon^2 - \omega^2} + \epsilon$.

Subtracting the equations for $A_{11}$ and $A_{44}$, we find

$$i\alpha\ell m(\rho_{41} - \rho_{14}) + 2\ell m\epsilon(\rho_{11} - \rho_{44}) + (\rho'_{11} - \rho'_{44}) = 0 \tag{B.9}$$

Subtracting the equations for $A_{14}$ and $A_{41}$, we find

$$i\alpha\ell m(\rho_{44} - \rho_{11}) + 2\ell m\epsilon(\rho_{14} - \rho_{41}) + (\rho'_{14} - \rho'_{41}) = 0 \tag{B.10}$$

Let us call $\rho_{11} - \rho_{44} = A$ and $\rho_{14} - \rho_{41} = B$, where $B$ is two times the imaginary part of $\rho_{14}$. We then have

$$- i\alpha\ell m B(t) + 2\ell m\epsilon A(t) + A'(t) = 0 \tag{B.11}$$

$$- i\alpha\ell m A(t) + 2\ell m\epsilon B(t) + B'(t) = 0 \tag{B.12}$$

With initial conditions $A(0) = 0 = B(0)$, the solution is $A(t) = 0 = B(t)$. This proves that $\rho_{11} = \rho_{44}$ and that $\rho_{14} = \rho_{41} = \mathrm{Re}(\rho_{14})$ is a real function. We shall call $\rho_{11}(t) = a(t)$ and $\rho_{14}(t) = b(t)$.

Subtracting the equations for $A_{22}$ and $A_{33}$, we find

$$i\alpha\ell m(\rho_{32} - \rho_{23}) + 2\ell m\epsilon(\rho_{22} - \rho_{33}) + (\rho'_{22} - \rho'_{33}) = 0 \tag{B.13}$$

Subtracting the equations for $A_{23}$ and $A_{32}$, we find

$$i\alpha\,\ell m\,(\rho_{33} - \rho_{22}) + 2\ell m\epsilon\,(\rho_{23} - \rho_{32}) + (\rho'_{23} - \rho'_{32}) = 0 \tag{B.14}$$

Let us call $\rho_{22} - \rho_{33} = C$ and $\rho_{23} - \rho_{32} = D$, where $D$ is two times the imaginary part of $\rho_{23}$. We then have

$$- i\alpha\ell m D(t) + 2\ell m\epsilon C(t) + C'(t) = 0 \tag{B.15}$$

$$- i\alpha\ell m C(t) + 2\ell m\epsilon D(t) + D'(t) = 0 \tag{B.16}$$

With initial conditions $C(0) = \cos(2\theta)$ and $D(0) = 0$, the solution is

$$C(t) = \rho_{22}(t) - \rho_{33}(t) = \cos(2\theta)e^{-2\ell mt\epsilon}\cos(\alpha\ell mt), \tag{B.17}$$

$$D(t) = 2\mathrm{Im}(\rho_{23}(t)) = \rho_{23}(t) - \rho_{32}(t) = i\cos(2\theta)e^{-2\ell mt\epsilon}\sin(\alpha\ell mt). \tag{B.18}$$

Now, let us sum up the terms from $A_{23}$ and $A_{32}$:

$$\alpha\,\ell m\Big[(\rho_{22} + \rho_{33}) - (\rho_{11} + \rho_{44})\Big] + 2\ell m\epsilon\Big[(\rho_{23} + \rho_{32}) - (\rho_{14} + \rho_{41})\Big] + \Big(\rho'_{23} + \rho'_{32}\Big) = 0 \tag{B.19}$$

Let us call $\rho_{23}(t) + \rho_{32}(t) = F(t)$. Also, we notice that due to the property $\mathrm{Tr}(\rho) = 1$, we have $\rho_{22}+\rho_{33}=1-2a(t)$. This means that we can simplify the above equation to

$$-2\alpha\ell ma-4\ell m\epsilon b+\alpha\ell m(\rho_{22}+\rho_{33})+2\ell m\epsilon(\rho_{23}+\rho_{32})+\rho_{23}'+\rho_{32}'=0. \tag{B.20}$$

Expanding and grouping:

$$F'(t)-4\alpha\ell ma(t)-4\ell m\epsilon b(t)+2\ell m\epsilon F(t)+\alpha\ell m=0. \tag{B.21}$$

Also, the equations from $A_{11}$ and $A_{14}$ can be written as

$$a'(t)+4\ell m\epsilon a(t)+\alpha\ell mb(t)-\frac{1}{2}\alpha\ell mF(t)-\ell m\epsilon=0, \tag{B.22}$$

$$b'(t)+2\alpha\ell ma(t)+2\ell m\epsilon b(t)-\ell m\epsilon F(t)-\frac{1}{2}\alpha\ell m=0. \tag{B.23}$$

The solution of equations (B.22), (B.23) and (B.21) is for the initial conditions $a(0)=0=b(0)$ and $F(0)=\sin(2\theta)$ is

$$\begin{aligned}a(t)=&\rho_{11}(t)=\rho_{44}(t)=\frac{1}{4}-\frac{1}{8}e^{-2\ell mt(\sqrt{\epsilon^2-\omega^2}+3\epsilon)}(1+\sin(2\theta))\\&-\frac{1}{8}e^{-2\ell mt(\epsilon-\sqrt{\epsilon^2-\omega^2})}(1-\sin(2\theta)),\end{aligned} \tag{B.24}$$

$$\begin{aligned}b(t)=&\rho_{14}(t)=\frac{1}{4}\sin(2\theta)-\frac{1}{8}e^{-2\ell mt(\sqrt{\epsilon^2-\omega^2}+3\epsilon)}(1+\sin(2\theta))\\&+\frac{1}{8}e^{-2\ell mt(\epsilon-\sqrt{\epsilon^2-\omega^2})}(1-\sin(2\theta)),\end{aligned} \tag{B.25}$$

$$\begin{aligned}F(t)=2\mathrm{Re}(\rho_{23}(t))=&\frac{1}{2}\sin(2\theta)+\frac{1}{4}e^{-2\ell mt(\sqrt{\epsilon^2-\omega^2}+3\epsilon)}(1+\sin(2\theta))\\&-\frac{1}{4}e^{-2\ell mt(\epsilon-\sqrt{\epsilon^2-\omega^2})}(1-\sin(2\theta)).\end{aligned} \tag{B.26}$$

This implies that

$$\begin{aligned}\rho_{23}(t)=&\frac{1}{4}\sin(2\theta)+\frac{1}{8}e^{-2\ell mt(\sqrt{\epsilon^2-\omega^2}+3\epsilon)}(1+\sin(2\theta))-\frac{1}{8}e^{-2\ell mt(\epsilon-\sqrt{\epsilon^2-\omega^2})}(1-\sin(2\theta))\\&+\frac{i}{2}\cos(2\theta)e^{-2\ell mt\epsilon}\sin(\alpha\ell mt).\end{aligned} \tag{B.27}$$

From (B.17) and $\rho_{22}+\rho_{33}=1-2a(t)$, we derive the following solutions

$$\begin{aligned}\rho_{22}(t)=&\frac{1}{4}+\frac{1}{8}e^{-2\ell mt(\sqrt{\epsilon^2-\omega^2}+3\epsilon)}(1+\sin(2\theta))+\frac{1}{8}e^{-2\ell mt(\epsilon-\sqrt{\epsilon^2-\omega^2})}(1-\sin(2\theta))\\&+\frac{1}{2}\cos(2\theta)e^{-2\ell mt\epsilon}\cos(\alpha\ell mt),\end{aligned} \tag{B.28}$$

$$\rho_{33}(t) = \frac{1}{4} + \frac{1}{8}e^{-2\ell mt(\sqrt{\epsilon^2-\omega^2}+3\epsilon)}(1+\sin(2\theta)) + \frac{1}{8}e^{-2\ell mt(\epsilon-\sqrt{\epsilon^2-\omega^2})}(1-\sin(2\theta)) - \frac{1}{2}\cos(2\theta)e^{-2\ell mt\epsilon}\cos(\alpha\ell mt). \tag{B.29}$$

From these expressions, we can derive the asymptotic behavior of the density matrix when $t \to \infty$:

$$\lim_{t\to\infty} \rho_{11} = \lim_{t\to\infty} \rho_{22} = \lim_{t\to\infty} \rho_{33} = \lim_{t\to\infty} \rho_{44} = \frac{1}{4}, \tag{B.30}$$

$$\lim_{t\to\infty} \rho_{14} = \lim_{t\to\infty} \rho_{23} = \frac{\sin(\theta)\cos(\theta)}{2}. \tag{B.31}$$

This means that asymptotically, the off-diagonal elements of the density matrix are non-zero for an initially entangled (or partially entangled) state.

## B.2 Quantum Mutual Information of an $X$-state

Following the steps described in Section 6.3.3, the quantum mutual information for a bipartite system of $X$-shape (represented by a $4 \times 4$ density matrix):

$$\begin{aligned} I = \frac{1}{2\ln 2}\Bigg[ & -2(\rho_{11}+\rho_{22})\ln(\rho_{11}+\rho_{22}) - 2(\rho_{11}+\rho_{33})\ln(\rho_{11}+\rho_{33}) \\ & + \left(\rho_{22}+\rho_{33}-\sqrt{(\rho_{22}-\rho_{33})^2+4|\rho_{23}|^2}\right)\ln\left(\frac{1}{2}\left(\rho_{22}+\rho_{33}-\sqrt{(\rho_{22}-\rho_{33})^2+4|\rho_{23}|^2}\right)\right) \\ & + \left(\rho_{22}+\rho_{33}+\sqrt{(\rho_{22}-\rho_{33})^2+4|\rho_{23}|^2}\right)\ln\left(\frac{1}{2}\left(\rho_{22}+\rho_{33}+\sqrt{(\rho_{22}-\rho_{33})^2+4|\rho_{23}|^2}\right)\right) \\ & - 2(\rho_{22}+\rho_{44})\ln(\rho_{22}+\rho_{44}) - 2(\rho_{33}+\rho_{44})\ln(\rho_{33}+\rho_{44}) \\ & + \left(\rho_{11}+\rho_{44}-\sqrt{(\rho_{11}-\rho_{44})^2+4|\rho_{14}|^2}\right)\ln\left(\frac{1}{2}\left(\rho_{11}+\rho_{44}-\sqrt{(\rho_{11}-\rho_{44})^2+4|\rho_{14}|^2}\right)\right) \\ & + \left(\rho_{11}+\rho_{44}+\sqrt{(\rho_{11}-\rho_{44})^2+4|\rho_{14}|^2}\right)\ln\left(\frac{1}{2}\left(\rho_{11}+\rho_{44}+\sqrt{(\rho_{11}-\rho_{44})^2+4|\rho_{14}|^2}\right)\right)\Bigg]. \end{aligned} \tag{B.32}$$